SLAC-302
UC 34D
(T)

VARIATIONAL METHODS FOR FIELD THEORIES*

Shahar Ben-Menahem
Stanford Linear Accelerator Center
Stanford University
Stanford, California 94305

September 1986

Prepared for the Department of Energy
under contract number DE-AC03-76SF00515

Printed in the United States of America. Available from National Technical Information Service, U.S. Department of Commerce, 5285 Port Royal Road, Springfield, VA 22161. Price: Printed Copy—A13; Microfiche—A01.

*Ph.D. dissertation

TABLE OF CONTENTS

Part IV: Transfer Matrix Methods for the Ising Chain in a Transverse Magnetic Field

Acknowledgments

I would like to thank my advisor, Sidney D. Drell, who supervised the work reported here, for his valuable advise and encouragement; and members of the SLAC theory group for useful discussions—especially Marvin Weinstein, who suggested the idea for the second part of the thesis. Many thanks to Jacqueline A. Hahn, who typed the first manuscript.

Finally, special thanks are due to my family, and in particular to my father, mother and sister for their loving support from the very earliest stages of my unusual education to the present day.

ABSTRACT

The thesis has four parts, dealing with four field theory models: Periodic Quantum Electrodynamics (PQED) in (2 + 1) dimensions, free scalar field theory in (1 + 1) dimensions, the Quantum XY model in (1 + 1) dimensions, and the (1 + 1) dimensional Ising model in a transverse magnetic field. The last three parts deal exclusively with variational methods; the PQED part involves mainly the path-integral approach.

The PQED calculation results in a better understanding of the connection between electric confinement through monopole screening, and confinement through tunneling between degenerate vacua. This includes a better quantitative agreement for the string tensions in the two approaches.

In the second part, we use free field theory as a laboratory for a new variational blocking-truncation approximation, in which the high-frequency modes in a block are truncated to wave functions that depend on the slower background modes (Born-Oppenheimer approximation). This "adiabatic truncation" method gives very accurate results for ground-state energy density and correlation functions. Without the adiabatic method, a much larger number of states per block must be kept to get comparable results. Various adiabatic schemes, with one variable kept per site and then two variables per site, are used.

For the XY model, several trial wave functions for the ground state are explored, with an emphasis on the periodic Gaussian. A connection is established with the vortex Coulomb gas of the Euclidean path integral approach. The approximations used are taken from the realms of

statistical mechanics (mean field approximation, transfer-matrix methods) and of quantum mechanics (iterative blocking schemes).

In developing blocking schemes based on continuous variables, problems due to the periodicity of the model were solved. Our results exhibit an order-disorder phase transition. This transition is a rudimentary version of the actual transition known to occur in the XY model, and is systematically improvable.

In the fourth and final part of the thesis, the transfer-matrix method is used to find a good (non-blocking) trial ground state for the Ising model in a transverse magnetic field in $(1+1)$ dimensions, thereby improving upon results by Pearson.

General Introduction

This work is concerned with trial wave functions of the ground state for lattice models. Using variational methods, simple trial states incorporating little beyond the main symmetries of a model can give remarkably good results, for correlation functions as well as energies. This success is measured in comparison with Euclidean path-integral results, or the exact solution where that is known.

In the first model, periodic QED in (2 + 1) dimensions (PQED), the trial vacuum is chosen as a periodic Gaussian in the magnetic fields with long-range correlations; this incorporates all the symmetries of the model, reduces to the free-field vacuum in the zero-coupling limit, and succeeds in reproducing the Polyakov confinement mechanism for a pair of static (external) charges at low couplings. This mechanism was originally discovered in the path-integral formulation. The correspondence between quantum interference among degenerate vacua and semiclassical monopole configurations is made more exact. Our main results here are that

A) The quantitative differences, e.g., in the string tension, between the real-space and Euclidean results are due to the different treatments of the time direction, and

B) It is the compactness of the U(1) group, rather than the mere existence of semiclassical monopole solutions, that causes confinement.

In the second model we introduce some new techniques that drastically improve the agreement of both ground-state energy and, more significantly, correlation functions computed in the trial ground state, with their exact counterparts. The test case studied is scalar free field

theory in (1 + 1) dimensions. The trial state is obtained by a blocking-truncation scheme, and the methods we develop are of interest for non-soluble interaction models, as well. In this case we go beyond the symmetries of the model to incorporate an adiabatic (Born-Oppenheimer) approximation for the effect of lower-frequency modes upon the fast-mode wave function. A class of such adiabatic renormalization-group schemes is compared with standard blocking schemes, and it is found that better results are obtained while keeping fewer states per site and sites per block.

The third model treated is the planar quantum XY model, where an infinite-order phase transition is known to occur. This transition is named after Kosterlitz and Thouless, who discovered it. Apart from perturbative calculations augmented by Padé approximants, most of the body of knowledge about this phenomenon is derived from the Euclidean path integral approach. The transition is known to be caused by the unbinding of pairs of semiclassical configurations (vortices). Our aim was to develop variational trial wave-functions allowing us to find real-space approximations to this physics. Our starting point was the periodic Gaussian wave function, employed successfully for PQED (part I, ref. 3). Physical quantities are then expressed as averages in a classical statistical-mechanics ensemble. Two methods are used to evaluate these averages: a transfer-matrix method, that works only for finite-range propagators, and a self-consistent dielectric-medium approximation applicable for arbitrary ranges. The latter is an adaptation of the original Kosterlitz-Thouless calculation to the real-space

variational approach. In the real-space computation, the statistical mechanics problem is that of a one-, rather than two-dimensional, Coulomb gas.

Briefly, the results of the statistical-mechanics approach are as follows. The dialectric-medium approximation yields a transition, which differs in some subtle respects from the Euclidean one; this will be discussed. The transfer-matrix method gives an abrupt change of behavior, that becomes a phase transition in the infinite-range limit.

Next, we examine real-space renormalization-group approaches to the problem, based on continuous variables. It was found that naive truncation schemes lead either to spurious (first-order) phase transitions or to a trivial evolution of the Hamiltonian. The problem is caused by the need for any realistic truncation scheme to obey the periodicity of the model. A formalism is developed to solve this problem. The main result here is, again, a periodic Gaussian wave function; its propagator is naively blocked. The resulting truncation scheme, which we call NBPG (naively blocked periodic Gaussian), is shown to be a special case of the formalism. It is studied analytically in the two extreme regions $\lambda << 1$, $\lambda >> 1$ and numerically for the entire coupling-constant range.

The NBPG wave-function gives a realistic model of an infinite-order transition. It is an order-disorder transition, but beyond that it does not correspond to the Kosterlitz-Thouless transition. This is due to the incorrect long-range correlation functions. However, our results are only an example of what can be done using the formalism that we developed. Several avenues will lead to better results; these are discussed.

The last model we consider is the (1 + 1) dimensional Ising chain in a transverse magnetic field. We apply the transfer-matrix approach to this model, again in the context of a simple trial ground-state. The results show improvement in both ground-state energy and magnetization as the propagator range is increased.

The work reported in Part I was published in Phys. Rev. D20, 1923 (1979), and that reported in Part II was published in Phys. Rev. D26, 455 (1982). The computation in Part IV is connected with a collaborative work at SLAC.

Finally, a word about organization. Each of the four parts is self-contained, despite some cross-references, and has its own introduction, references, figures and tables.

PART I

CONFINEMENT IN PERIODIC QUANTUM ELECTRODYNAMICS FOR LOW COUPLINGS

1. Introduction

There have been several approaches to the problem of confinement in (2+1)-dimensional compact QED, for small coupling constant. All approaches yield a static potential energy $E(D) \simeq \gamma D$ between a $q\bar{q}$ pair a distance D apart, where γ vanishes nonanalytically with the coupling. This means there is confinement (but there are differences in the results). Since the approaches and the models themselves differ widely, we think it is worthwhile to try answering the following questions: How are the confinement mechanisms related? How much of the difference between the various results is caused by making different approximations in each case? There is also the question of periodicity. In one approach,[3] heavy use is made of the periodicity of the Hamiltonian as a function of magnetic field, whereas in the path integral approach of Ref. 1, the apparent cause of confinement is the presence of multipseudo-particle solutions, and these exist for nonperiodic field potentials as well (those possesing degenerate minima). One would like to know whether periodicity is really necessary for confinement.

What follows is an investigation of these points. We will begin by describing the main features of the approaches we will be referring to, but first a word about notation: our convention for electric and magnetic fields varies in different parts of the paper. To prevent confusion we will give their definitions in terms of the vector potentials A_i, whenever necessary. A_i are always normalized to satisfy canonical commutation relations with $\dot{A}_i$. We will always be working in the temporal $A_0 = 0$ gauge. Other conventions used are

(1) The latin indices i,j run over 1,2.

(2) Greek indices μ, ν, etc., run over 1,2,3.

(3) The 3 direction is the time direction (real or imaginary).

(4) Summation over like indices is sometimes implicitly used.

(5) Δ_μ, Δ_i are lattice difference operators.

(6) $\hat{\mu}$, $\hat{\imath}$ are unit vectors in the directions μ, i, respectively.

1.a. The path-integral method

This approach was implemented in two different ways which converge at a certain point.[1,2] Polyakov used a Georgi-Glashow QED, which we call model I. The Euclidean action is

$$\int d^3x \left[\frac{1}{4e^2} \vec{F}_{\mu\nu}^2 + \frac{1}{2} \left(D_\mu \vec{\phi} \right)^2 + \frac{1}{4} \lambda \left(\vec{\phi}^2 - \eta^2 \right)^2 \right] \quad , \tag{1.a.1}$$

$$\vec{F}_{\mu\nu} = e\left(\partial_\mu \vec{A}_\nu - \partial_\nu \vec{A}_\mu \right) + e^2 \vec{A}_\mu \times \vec{A}_\nu \quad ,$$

where $\vec{\phi}$ is the isovector Higgs field, and $\vec{F}_{\mu\nu}$ are the non-Abelian gauge fields for the SU(2) gauge group. $F^a_{\mu\nu}$ are derived from vector potentials A^a_μ, where a is the isospin index. η,λ are constants; e is the gauge coupling, and has dimension $(\text{length})^{-\frac{1}{2}}$; D_μ are covariant derivatives.

Model I contains a pseudoparticle solution, the 't Hooft-Polyakov monopole. By a suitable gauge transformation, $A^{1,2}_\mu$ are gauged away far from a monopole, and one is left with the vector potential $A_\mu = A^3_\mu$. Only a U(1) subgroup of the original SU(2) symmetry remains. Polyakov computes the correlation function

$$F(C) = \left\langle \exp\left\{ ie \oint_C A_\mu \, dx_\mu \right\} \right\rangle$$

for small e. C is the Wilson loop. He considers only the multimonopole contributions to the path integral. F(C) is thus expressed as a correlation function in a magnetic monopole gas, in the dilute-gas approximation. The monopoles have a long-range Coulomb interaction, but a screening occurs that makes the Green's function of the gas short range. In fact, the $k^2 = 0$ pole in the correlation function

$$\int e^{ik\,x} \langle T(B(0)\,B(x))\rangle\, d^3x \quad ,$$

where B is the magnetic field, disappears when an infinite set of Feynman graphs is summed. Instead of the massless vector boson A_μ, one gets a pole corresponding to a massive scalar field ϕ. F(C) is expressed as a path-integral over this field:

$$F(C) = \int [d\phi]\, \exp\left\{-\frac{1}{2}\,\pi e^2 \int d^3x \left([\nabla(\phi - \eta)]^2 - 2M^2 \cos\phi \right) \right\} ,$$

where

$$\eta(x) = \frac{1}{2} \int_S d\vec{\sigma} \cdot \frac{\vec{x} - \vec{y}}{|\vec{x} - \vec{y}|^3} \quad . \qquad (1.a.2)$$

S is the area bounded by the contour C. It is unambiguous if one chooses a planar C.

This path integral is computed using a stationary point in function space. The result is an area-law decrease,

$$F(C) \propto e^{-\gamma A} \quad , \qquad (1.a.3)$$

where A is the area of S and γ is a constant.[1]

The second model in which the path integral approach was used is compact QED on a spacetime lattice.[2] The Euclidean action is

$$\beta \sum_{r,\mu,\nu} \left[1 - \cos\theta_{\mu\nu}(r)\right] \qquad (1.a.4)$$

where $\theta_{\mu\nu}$ is a dimensionless multiple of the electromagnetic field tensor. We call this model II. The $\beta \to \infty$ limit is considered. Using a Villain approximation, a monopole partition sum is derived, and the results are a lattice version of those in Ref. 1. The discreteness of spacetime in this model eliminates short distance problems; in particular, the self-action of a monopole is computable. But the long distance behavior is not affected by discreteness, so (1.a.3.) is still true. β corresponds to $1/e^2a$, where e is the coupling in Ref. 1 and a is the lattice spacing. In both models I and II the static energy of a quark-antiquark pair at large separation Da is read off (1.a.3) and is

$$E(D) \simeq \gamma D \quad ,$$

where γ vanishes nonanalytically with the coupling. The treatments in Refs. 1 and 2 are valid for small couplings e; we further know compact QED confines for large e.[4] Hence these models cannot have a phase transition (at least not a single transition).

1.b. The variational approach

This approach to the problem is a Hamiltonian formulation on the two-dimensional lattice of compact QED. Here one examines the energy of a string connecting a static quark-antiquark pair.[3] As is well known, this approach is equivalent to the Wilson loop criterion. The compact QED Hamiltonian is

$$H = \frac{1}{2}\left\{ g^2 \sum_{\vec{p},i} E^2_{\vec{p},i} + \frac{2}{g^2} \sum_{\vec{p}} \left(1 - \cos B_{\vec{p}}\right)\right\} \qquad (1.b.1)$$

where $E_{\vec{p},i}$ is the <u>electric</u> field on a link $\vec{p} \to \vec{p} + \hat{i}$, $B_{\vec{p}}$ is the magnetic field on a plaquette, and we have set the lattice spacing a to be 1 for convenience. g corresponds to e in Ref. 1. In terms of the vector potentials we define (in the temporal gauge)

$$E_{\vec{p},i} = \frac{1}{g}\ \partial_3\ A_{\vec{p},i} \quad , \qquad (1.b.1)'$$

$$B_{\vec{p}} = g\ \varepsilon_{ij}\ \Delta_i\ A_{\vec{p},j} \quad .$$

We name this model III.

The separation energy E(D) is computed variationally in a special sector of Hilbert space. Let $|\{B_{\vec{p}}\}\rangle$ be a state with a well-defined magnetic field configuration, $B_{\vec{p}}$ at site p. Working in this basis, the wave function is

$$\chi\left(\left\{B_{\vec{p}}\right\}\right) = \left\langle \left\{B_{\vec{p}}\right\} \middle| \psi \right\rangle \qquad (1.b.2)$$

where $|\psi\rangle$ is that part of the $q\bar{q}$ state belonging to the photon sector. The Hamiltonian is periodic in each $B_{\vec{p}}$ with a period 2π. An operator $L_{\vec{p}}$ conjugate to $B_{\vec{p}}$ is defined as follows:

$$E_{\vec{p},i} = \varepsilon_{ij}\ \Delta_j\ L_{\vec{p}} + E^{\parallel}_{\vec{p},i} \quad .$$

$E^{\parallel}_{\vec{p},i}$ is the Coulomb static field and we choose it to be that generated by a static $q\bar{q}$ pair a distance D apart. Δ_j are lattice difference operators. The above-mentioned periodicity then means that

$$\left[\exp\left\{ 2\pi i \, L_{\vec{p}} \right\}, H \right] = 0 \quad .$$

Therefore $G_{\vec{p}} = \exp\{2\pi i \, L_{\vec{p}}\}$ are good quantum numbers, and so are $L_{\vec{p}}$ up to integral fluctuations. By choosing a sector in which

$$G_{\vec{p}} = \exp\left\{2\pi i \, \varepsilon_{\vec{p}}\right\}, \; L_{\vec{p}} = \varepsilon_{\vec{p}} + \text{integer} \quad , \tag{1.b.3}$$

we can label the trial wave function as

$$\chi\left(\left\{B_{\vec{p}}; \varepsilon_{\vec{p}}\right\}\right) \quad .$$

This is a Bloch-type wave function, with "wave numbers" $\varepsilon_{\vec{p}}$. The natural choice for $\varepsilon_{\vec{p}}$ is that which will screen the Coulomb field and squeeze the electric flux links into a string which runs in a straight line between the quark and antiquark. Then the question of confinement translates itself into the question: Will the string be stable?

Having made this choice of $\varepsilon_{\vec{p}}$, one must now determine the shape of χ inside a single potential well. χ is chosen to he a sum of Gaussians[3]

$$\chi_{\text{trial}}\left(\left\{B_{\vec{p}}; \varepsilon_{\vec{p}}\right\}\right) = \prod_{\vec{p}} \left(\sum_{n_{\vec{p}}=-\infty}^{\infty} \right) \exp\left\{ 2\pi i \sum_{\vec{p}} n_{\vec{p}} \, \varepsilon_{\vec{p}} \right\}$$

$$\times \exp\left\{ -\frac{1}{2g^2} \sum_{\vec{p}\vec{p}'} \left(B_{\vec{p}} - 2\pi n_{\vec{p}}\right) \Delta_{\vec{p}\vec{p}'} \left(B_{\vec{p}'} - 2\pi n_{\vec{p}'}\right) \right\} \delta\left(\sum_{\vec{p}} B_{\vec{p}} \right) \tag{1.b.4}$$

and $\Delta_{\vec{p}\vec{p}'}$ is a Green's function, determined variationally to be

$$\Delta_{\vec{p}\vec{p}'} = \frac{1}{V}\sum_{\vec{k}\neq 0} e^{i\vec{k}\cdot(\vec{p}'-\vec{p})}\left(4 - 2\cos k_x - 2\cos k_y\right)^{-1/2} \qquad (1.b.5)$$

up to corrections of orders g^2 and $e^{-\text{const}/g^2}$. $\vec{k}$ is the discrete lattice momentum. The variational computation then gives for E(D) an expression, derived from a partition sum

$$Z\left(\{\varepsilon_{\vec{p}}\}\right) = \prod_{\vec{p}}\left(\sum_{N_{\vec{p}}=-\infty}^{\infty}\right)\exp\left[-\frac{\pi^2}{g^2}\sum_{\vec{p}\vec{p}'} N_{\vec{p}}\Delta_{\vec{p}\vec{p}'}N_{\vec{p}'} + 2\pi i\sum_{\vec{p}} N_{\vec{p}}\varepsilon_{\vec{p}}\right]\delta\left(\sum_{\vec{p}} N_{\vec{p}}\right). \qquad (1.b.6)$$

This is a partition sum of a 2-dimensional Coulomb gas on the lattice, interacting with an imaginary external field. The charges of the gas have the interpretation of being tunnelings between the different B-vacua, i.e., they appear in the sum as a result of overlap integrals between different terms in (1.b.4). If one wants to push the tunneling interpretation further, one can say that the magnetic charges are electric vortices; a tunneling means a change of B with time, which causes an electric field circulation by virtue of Faraday's law. In Sections 2 and 3, we will examine the relation between these tunnelings and the monopoles of the other approach.

1.c. Plan for this part of thesis

In what follows, we will compare the various aspects of the different procedures — the "variational" (or "tunneling") approach and the "path integral" (or "monopole") approach. Our plan is as follows. In Section 2 we discuss classical monopoles in a certain continuum model, in order to gain a better understanding of the relation between model I and the other two models — in which no exact monopole solutions are known.

In Section 3 the mechanisms for screening and confinement are explained and compared in the two approaches. In Section 4 we explore the importance of compactness for screening and confinement. In Section 5, a numerical comparison is made between the results of Refs. 2 and 3, and an attempt is made to explain the different long-distance behavior of the Green's functions. In Section 6, the treatment of Ref. 2 (namely a space-time discretization) is applied to model III, and comparisons are made with both Refs. 2 and 3. In Section 7 we present concluding remarks.

2. Monopoles in Self-Interacting QED

To better understand the connection between the approaches, and also between models I and II, we will demonstrate how classical monopole solutions arise in certain self-interacting QED models. Models II and III are such models. Consider a generalization of model III with Euclidean time:

$$\text{Action} = \int dt \, \frac{1}{2g^2} \sum_{\vec{p}i} B^2_{\vec{p}i} + \frac{1}{g^2} \int dt \sum_{\vec{p}} V\left(B_{\vec{p}}\right) \quad . \tag{2.1}$$

Again we have set a = 1 for convenience, so the problem is now devoid of dimensional quantities. The convention for the fields is now as follows:

$$\begin{aligned} B_{\vec{p},i} &= g \, \epsilon_{ij} \, \partial_3 \, A_{\vec{p},j} \\ B_{\vec{p}} = B_{\vec{p},3} &= g \, \epsilon_{ij} \, \Delta_i \, A_{\vec{p},j} \quad . \end{aligned} \tag{2.1}'$$

Note that we have passed from a (2 + 1)-dimensional notation, in which there are two electric-field components and one magnetic component, to a three-dimensional notation where there are three magnetic field components. We choose a field potential V having two degenerate minima:

$$V(B) = \frac{1}{2} B^2 - 2\pi(B - \pi)\ \theta(B - \pi) \tag{2.2}$$

(see Fig. 1). This is a piecewise quadratic function. To find a classical solution of the equations of motion, we should solve a set of difference-differential equations. However, in order to make our point as simply as possible, we will replace the spatial lattice by a continuum for the remainder of this section. The action is now

$$\text{Action} = \frac{1}{2g^2} \int d^3x \sum_i \left[B_i(x)\right]^2 + \frac{1}{g^2} \int d^3x\ V(B) \quad , \tag{2.3}$$

where

$$\partial_\mu B_\mu = 0 \quad .$$

The last follows from (2.1)'. The equations of motion obtained from this action are

$$\partial_3^2 B + \sum_i \partial_i^2\ V'(B) = 0 \tag{2.4}$$

$$\sum_{ij} \epsilon_{ij}\ \partial_i\ B_j = 0 \quad , \quad \partial_\mu\ B_\mu = 0 \quad . \tag{2.5}$$

We seek a monopole solution. From (2.2) and (2.4)

$$\partial_3^2 B + \sum_i \partial_i^2 \left[B - 2\pi\theta(B - \pi)\right] = 0 \quad ,$$

$$\vec{\nabla}^2 B = 2\pi\left(\partial_1^2 + \partial_2^2\right)\theta(B - \pi) \quad . \tag{2.6}$$

Imagine a configuration $B^{(0)}$ in which $B = 2\pi$ in an infinitely long tube, $B = \pi$ on some surface K+T enveloping the tube, and $B = 0$ everywhere outside this tube (Fig. 2). Obviously, the R.H.S. in (2.6) is nonzero only on K and T, and singular there. It is equivalent to an infinite

current-solenoid terminating near the point P, which will generate another configuration, $B^{(1)}$, similar to the first. It will have the same T but a different K. Thus we can find an approximate monopole solution to (2.6) by iteration, which presumably will converge. From the first iteration $B^{(0)}$ onward, B behaves like a monopole field far from the tube, and from (2.5), all three components will behave like $\vec{r}/r^3$. We have used a singular field potential; for a potential V(B) that varies smoothly near $B = \pi$, like a cosine potential, the current-solenoid may develop a thickness.

Note that the equation (2.6) has no length scale, so the width of the monopole tube is arbitrary. The monopole point P is also arbitrary, but the tube must be along the $\hat{3}$ direction.

One can presumably find such monopole solutions for any potential V(B) possessing degenerate minima. This condition is satisfied in particular for periodic potentials, but periodicity is not required. This leads to the question raised in Section 1, of whether periodicity* is necessary for confinement. We will investigate this point in Section 4.

3. Screening and confinement mechanisms

In both approaches confinement is achieved by screening. The monopole picture in (2+1) dimensions is as follows:

The Wilson quark loop is an (imaginary) current loop C, producing a magnetic field. This field is the same as that of a narrow magnetic dipole sheet on the area S bounded by C, except on S itself. On the lattice, this sheet is one spacing thick. The energy of the loop increases only as the loop perimeter. However, the loop is immersed

---

*That is, compactness of the underlying group manifold.

in a magnetic monopole gas, which interacts directly with the dipole sheet, thus adding to the action a term proportional to the area of S. The gas becomes polarized, and monopoles of opposite polarity accumulate on the two sides of the sheet, screening both the magnetic field away from the sheet and the monopole-monopole interaction (Fig. 3). This gives the correlation function a finite range, whose inverse is interpreted as a mass of a scalar field. The mass vanishes nonanalytically with g. This effect causes the action to increase by an amount proportional to S. Thus

$$\left\langle \exp\left\{ ie \oint_C A_\mu \, dx_\mu \right\} \right\rangle$$

decreases according to an area law.

This picture can be projected into a static one in the two space dimensions. Here the current loop becomes a quark-antiquark pair a distance D apart, creating a Coulomb electric field. The electric field in this picture is simply related to the loop magnetic field by

$$E_i = \varepsilon_{ij} B_j \quad , \tag{3.1}$$

where $B_3 = B$ remains magnetic. Unlike in Section 2, E now includes a longitudinal part. The Coulomb field is purely longitudinal; a monopole adds an electric vortex in this picture. Vortices of opposite circulations accumulate on both sides of the $q\bar{q}$ line, focusing the electric flux to a narrow tube, which causes confinement (Fig. 4). This same spatial picture of confinement in the monopole approach can be seen in the mechanism of Ref. 3. There one has vacuum tunnelings rather than monopoles, but these are known to be related. Specifically, we saw such

a relation in Section 2. The sense in which electric vortices are present in Ref. 3 is the following one: if we isolate a single-gas-particle term in the partition sum (1.b.6), i.e., a configuration $N_{\vec{q}} = \delta_{\vec{p}\vec{q}}$, its contribution to $\langle L_{\vec{q}} \rangle$ is $i(\pi/g^2)\Delta_{\vec{q}\vec{p}}$. This shows that in the Hamiltonian approach, too, the "gas particles" are associated with electrical vortices. The i results from the fact that in the Hamiltonian formalism one has real, rather than imaginary time. In both approaches, screening makes the correlation function of the gas well behave at large spatial separations. But in the monopole approach the screened propagator decreases exponentially with distance (it developes a mass), whereas in Ref. 3 the decrease is a power law. In Section 5 we will discuss this discrepancy, and show how it might be an artifact of certain unjustified approximations made in Ref. 3.

4. Compactness

4.a. The case of a nonperiodic potential

In all three models, I, II and III, the action is compact in some way. In model I it is compact through the non-Abelian group in which U(1) is embedded; in model II, it is periodic in all three nonvanishing components of $\theta_{\mu\nu}$. In model III, the action is periodic only in B. If the action were not compact, the theory would not necessarily confine for large g. What happens to the small-g arguments for confinement in such a case? If V(B) is nonperiodic, $\{\varepsilon_{\vec{p}}\}$ are no longer well defined quantum numbers, since $G_{\vec{p}}$ (defined in 1.b) no longer commute with the Hamiltonian. To put it another way, the fluctuations of $L_{\vec{p}}$ around $\varepsilon_{\vec{p}}$ are no longer discrete. Therefore, even if V(B) has a (finite) number

of degenerate minima, (1.b.4) is no longer a reasonable trial wave function. Since no set $\{\varepsilon_{\vec{p}}\}$ is favored now, one should take the one leading to lowest energy, i.e., the vacuum assignment, and confinement is lost. Formulating this in the Wilson loop language, where the loop C is the rectangle shown in Fig. 5, one has for Euclidean time of duration T,

$$F(C) = \left\langle 0 \left| \exp\left\{-ig \sum_{\vec{p}=0}^{(D-1)\hat{1}} A_1(\vec{p})\right\} e^{-HT} \exp\left\{ig \sum_{\vec{p}=0}^{(D-1)\hat{1}} A_1(\vec{p})\right\} \right| 0 \right\rangle$$

and as $T \to \infty$, $F(C) \to 1$ unless $\langle 0|\exp\{ig \sum_{\vec{p}=0}^{(D-1)\hat{1}} A_1(\vec{p})\}|0\rangle = 0$. The latter is true for any quark positions only if the vacuum function is periodic, which in turn means V(B) must be periodic. Thus there is no area-law and no confinement for nonperiodic V(B). But consider a potential with a finite number > 1 of degenerate minima. There are still tunneling and monopoles in the theory, and one can argue that in a path integral calculation of F(C) these will cause screening and confinement, for $g \ll 1$, as described in Section 3. We will now demonstrate, for a particular double-well potential, how the screening mechanism breaks down, thus affirming that for small g, too, periodicity is needed for confinement as can be deduced from the general argument above.

4.b. An example

Let us choose a particular nonperiodic potential, and demonstrate how screening breaks down, even though V(B) has two degenerate minima and therefore tunneling and monopoles.

The breakdown will appear in a different way than in 4.a. Working on a space-time lattice, one cannot have two tunnelings of the same signature at the same spatial point and two consecutive times. This is because the potential we have chosen has only two minima. One does obtain a monopole gas as in Ref. 2, but the monopole charges m(r) do not vary independently, and we show how that ruins confinement.

We employ here the following convention for the fields:

$$E_i = \partial_3 A_i$$

$$B = \varepsilon_{ij} \Delta_i A_j \quad . \tag{4.b.1}$$

The potential we choose is (Fig. 6)

$$V(B) = -a^{-3} \ln\left(\exp\left\{-\frac{1}{2} a^3 B^2\right\} + \exp\left\{-\frac{1}{2} a^3 (B - B_0)^2\right\}\right), \quad a = \text{lattice spacing} \tag{4.b.2}$$

for large B_0. It has two minima, and is nonperiodic. It corresponds to a free photon in two limits: $B_0 \to 0$ and $B_0 \to \infty$. For small B, V(B) can be expanded around $1/2\ B^2$ and gives, for example, a 3-photon coupling proportional to

$$B_0^3 \exp\left\{-\frac{1}{2} B_0^2 a^3\right\} \quad .$$

Thus this potential has no strong coupling limit. But we choose it because a monopole gas can be derived exactly from the path-integral. In that monopole gas, B_0 corresponds to $1/g$ in Ref. 2.

Setting a = 1 for convenience, the correlation function is

$$F(C) = \left\langle \exp\left\{ ie \sum_{\mu,r} A_\mu(r)\, J_\mu(r) \right\} \right\rangle \qquad (4.b.3)$$

$$\propto \int [dA] \exp\left\{ ie \sum_{r\mu} A_\mu(r)\, J_\mu(r) - \frac{1}{2} \sum_{r,i} E_i^2(r) - \sum_r V(B(r)) \right\},$$

where r is the lattice site, and J_μ is[2]

$$J_\mu(r) = \begin{cases} 1 & \text{if the link } r \to r + \hat{\mu} \text{ is on C} \\ -1 & \text{if the link } r + \hat{\mu} \to r \text{ is on C} \\ 0 & \text{otherwise} \end{cases} .$$

For the potential (4.b.2),

$$\exp\left\{ - \sum_r V(B(r)) \right\} = \left(\prod_r \sum_{n_r=0}^{1} \right) \prod_r \exp\left\{ - \frac{1}{2} \left[B(r) - n_r \right]^2 \right\}$$

Therefore the integrand in (4.b.3) is Gaussian, and the path integration can be performed exactly. The result is, up to perimeter-law factors,

$$F(C) \propto \left(\prod_r \sum_{n_r=0}^{1} \sum_{N_r=-1}^{1} \right) \exp\left\{ \sum_{rr'} \frac{B_0^2}{2} N_r \left(\frac{1}{\Delta^2} \right)_{rr'} N_{r'} \right.$$

$$\left. - i(eB_0) \sum_r N_r \frac{\Delta_2}{\Delta^2} \left[\delta_{y,0}\, \theta_S(x,t) \right] \right\} \cdot \prod_r \delta_{N_r, n_{r+\hat{3}} - n_r} \qquad (4.b.4)$$

If we choose the curve C as in Fig. 5. $\theta_S(x,t)$ is 1 on S and 0 outside. The interpretation of (4.b.4) is a (dilute) monopole gas, where N_r are the monopole charges. They arise from tunnelings between vacua which have $B(r) = B_0 n_r$, $n_r = 0$ or 1. This implies a constraint on the

monopole charges, which is the Kronecker delta. It is this constraint that ruins the screening, as we will show. The external source coupled to N_r in (4.b.4) is the same as in Refs. 2 and 3. Defining

$$\eta_r = \frac{\Delta_2}{\Delta^2} \left[\delta_{y,0}\, \theta_S(x,t) \quad eB_0 \right] \quad , \tag{4.b.5}$$

We get by the usual resummation techniques,

$$\begin{aligned} F(C) \propto & \left(\prod_r \sum_{n_r} \sum_{N_r} \int_{-\infty}^{\infty} d\phi_r \right) \prod_r \delta_{N_r, n_{r+\hat{3}} - n_r} \\ & \times \exp\left\{ i \sum_r (\phi_r - \eta_r) N_r \right\} \exp\left\{ - \frac{1}{2B_0^2} \sum_{r,\mu} (\Delta_\mu \phi_r)^2 \right\} \quad . \end{aligned} \tag{4.b.6}$$

Without the constraint, this would give $(\cos\phi_r)$ factors, whose normal ordering in a diagram expansion give the Green's function a mass, similar to the mechanism in Ref. 3. However, due to the constraint,

$$\prod_r \sum_{n_r} \sum_{N_r} \prod_r \delta_{N_r, n_{r+\hat{3}} - n_r} \exp\left\{ i \sum_r (\phi_r - \eta_r) N_r \right\}$$

$$= \prod_r \sum_{n_r} \exp\left\{ i \sum_r (\phi_r - \eta_r)\left(n_{r+\hat{3}} - n_r \right) \right\}$$

$$= \prod_r \sum_{n_r} \exp\left\{ - i \sum_r n_r \left(\phi_r - \phi_{r-\hat{3}} + \eta_{r-\hat{3}} - \eta_r \right) \right\}$$

$$= \prod_r \left[1 + \exp\left\{ i \left(\phi_{r-\hat{3}} - \phi_r + \eta_r - \eta_{r-\hat{3}} \right) \right\} \right] \quad .$$

This introduces a derivative coupling of the ϕ_r field, and the self-energy will vanish as momentum $\to 0$. Thus, screening breaks down.

5. A Detailed Comparison: Models II and III

Models II and III differ in two respects: time is continuous in III while discrete in II, and the action in III is periodic only in B, not in the electric fields. In addition, the approximations used in Refs. 2 and 3 are different, although similar in nature. The strength γ of the linear confining potential comes out different in the two papers; in Section 6 we will show this is mainly an artifact of the differnt treatments of time. In 5.a we will compute the numerical coefficients in γ, based on Refs. 2 and 3.

A major qualitative difference in the results concerns the nature of screening: in Refs. 1 and 2, the screened Green's function of the monopole gas drops exponentially at large distance, whereas in Ref. 3 it drops as a power. In 5.b we will demonstrate how the approximations made in Ref. 3 may be responsible for this.

5.a. Numerical comparison for the linear potential

In both approaches, the separation energy for a $q\bar{q}$ pair a distance Da apart (a is the spatial lattice spacing) is

$$E(D) \simeq \gamma D \tag{5.a.1}$$

γ behaves for small g as

$$\gamma \simeq \delta \exp\left\{-d \frac{1}{g^2 a}\right\} \left(g^2 a\right)^c a^{-2} \tag{5.a.2}$$

where c, d, δ are numbers. We will compare them for the two approaches.

From Ref. 2 we found*

$$\gamma = \frac{2g^2M}{\pi^2} = \frac{4g\sqrt{2}}{\pi a^{3/2}} \exp\left\{-\frac{\pi^2 v_0}{g^2 a}\right\} \qquad (5.a.3)$$

where M is the screening mass, and v_0 is quoted as being

$$v_0 \simeq 0.253 \quad .$$

Thus,

$$c_2 = \frac{1}{2}$$

$$d_2 = 2.50$$

$$\delta_2 = 1.80$$

where the subscript refers to Ref. 2. In Ref. 3,

$$\gamma \simeq \frac{\pi^2 - 4}{\pi} a^{-2} \exp\left\{-\frac{\pi^2 J}{g^2 a}\right\}$$

where

$$J = \lim_{L\to\infty} \frac{1}{4L^2} \sum_{n_1=-L}^{L} \sum_{n_2=-L}^{L} \left(4 - 2\cos\frac{\pi n_1}{L} - 2\cos\frac{\pi n_2}{L}\right)^{-1/2}$$

$$= \frac{1}{4\pi^2} \int_{\pi}^{\pi} \int_{\pi}^{\pi} dk_1\, dk_2 \left(4 - 2\cos k_1 - 2\cos k_2\right)^{-1/2} \simeq 0.64$$

Thus,

---

*There are some wrong factors of π and 2 in Ref. 2. In Ref. 1, the formula (V.24) for γ is unclear; we have obtained there $\gamma = 8\pi e^2 M$. Banks *et al.*,[2] rely on Polyakov for γ.

$$c_3 = 0$$

$$d_3 = \pi^2 J \simeq 6.33$$

$$\delta_3 = 1.87 \quad .$$

5.b. The long-distance behavior of the Green's function

The Green's function of the gas has different long-distance behavior in Refs. 2 and 3. In Ref. 3, $\Delta_{\vec{p}\vec{p}'}$ is that given by (1.b.5) and normal-ordering the diagram expansion modifies it to

$$\Delta^{\mu^2}_{\vec{p}\vec{p}'} = \frac{1}{V}\sum_{\vec{k}} e^{i\vec{k}\cdot(\vec{p}'-\vec{p})}\left[\left(4 - 2\cos k_x - 2\cos k_y\right)^{1/2} + \frac{\mu^2}{g^2}\right]^{-1} \qquad (5.b.1)$$

where $\mu^2 = e^{-\pi^2\Delta_0/g^2}$. The latter is actually an equation for μ^2. $\Delta^{\mu^2}_{\vec{p}\vec{p}'}$ behaves as $1/|\vec{p}'-\vec{p}|^3$ at large distances, which is enough to eliminate volume divergences. However, this behavior differs from an exponential falloff. One would expect such a falloff when the 3-dimensional monopole gas of Ref. 2 is projected onto the two spatial dimensions, as described in Section 3.

The trial wave function χ is chosen to have a Gaussian form in Ref. 3. Actually, for a smooth field potential V(B), a Gaussian would only be accurate near the bottom of the potential wells; But it would be difficult to compute the integrals with a non-Gaussian wave function. However, an approximation is made in Ref. 3 even in deriving the $\Delta_{\vec{p}\vec{p}'}$ that extremizes $\langle\chi|H|\chi\rangle$.

We have found that changing this approximation can make $\Delta_{\vec{p}\vec{p}'}$ well behaved to begin with at large distances. We suggest that such effects

may combine to make the photon propagator drop exponentially, as in Ref. 2, but cannot prove it.

Defining as in Ref. 3

$$\Delta_{\vec{p}\vec{p}'} = \frac{1}{V} \sum_{\vec{k}} e^{ik\cdot(\vec{p}' - \vec{p})} \gamma_{\vec{k}}$$

We start by assuming that γ_0 is finite, and seek to show that this leads to self-consistent results. Thus, there is no need to freeze out the degree of freedom $\sum_{\vec{p}} B_{\vec{p}}$ as done in (1.b.4), so we remove the δ-function from χ_{trial}. Also, since $\Delta_{\vec{p}\vec{p}'}$ is well behaved at large distance, we can use the cluster expansion. This consists of expanding the exponential factor in (1.b.6) around $\exp\left\{-(\pi^2/g^2)\ \Delta_0 \sum_{\vec{p}} N_{\vec{p}}^2\right\}$, where $\Delta_0 = \Delta_{\vec{p}\vec{p}}$. For no external sources $\varepsilon_{\vec{p}} = 0$; one must minimize $\langle\chi|H|\chi\rangle = E(\{\gamma_{\vec{k}}\})$ as a function of the $\gamma_{\vec{k}}$-s. In the first approximation to the cluster expansion, this gives the equation

$$\frac{1}{4}\gamma_0^{-2} + \frac{4\pi^2}{g^2} \exp\left\{-\frac{\pi^2\Delta_0}{g^2}\right\} = 0$$

at $k^2 = 0$, which has no solution. In the second approximation the equation becomes

$$\frac{1}{4}\gamma_0^{-2} + \frac{4\pi^2}{g^2} \exp\left\{-\frac{\pi^2\Delta_0}{g^2}\right\} = \frac{32\pi^4}{g^4} \exp\left\{-\frac{2\pi^2\Delta_0}{g^2}\right\}\gamma_0 \quad , \qquad (5.b.2)$$

which admits the solution

$$\gamma_0 = \frac{g^2}{8\pi^2} \exp\left\{\frac{\pi^2\Delta_0}{g^2}\right\} + O(1) \quad .$$

Had we neglected all $e^{-\text{const}/g2}$ terms in (5.b.2) we would obtain $\gamma_0^{-2} = 0$ as in Ref. 3; it is this approximation that we have changed. Furthermore, for $\vec{k}^2$ small compared to γ_0^{-1} we can expand

$$\gamma_{\vec{k}} = \frac{g^2}{8\pi^2} \exp\left\{\frac{\pi^2\Delta_0}{g^2}\right\} + \frac{g^4}{1024\pi^4} \exp\left\{\frac{2\pi^2\Delta_0}{g^2}\right\}\vec{k}^2 + O(1)$$

and at finite $\vec{k}$, we obtain as in Ref. 3

$$\gamma_{\vec{k}} = \left(4 - 2\cos k_x - 2\cos k_y\right)^{-1/2} + O(g^2) + O\left(\exp\left\{-\frac{\pi^2\Delta_0}{g^2}\right\}\right).$$

Inclusion of higher-order terms in the cluster expansion will change (5.b.2), but to all orders we still have, at least formally,

$$\gamma_0 \sim \exp\left\{\frac{\pi^2\Delta_0}{g^2}\right\} .$$

6. A Modified Comparison

We will now refine the comparison between the path-integral and variational approaches by making the models, used as inputs for the two procedures, identical. That is, we will apply a path-integral method to model III. As a first step, we will put this model on a lattice in time as well as space, but with lattice spacing b in time and a in space. For b finite, we obtain results similar to those of Ref. 2; for b = a they coincide. This is done by employing approximations similar to those used in Ref. 2. We then take the continuum limit $b \to 0$. There our results are less accurate, since the approximation that all monopole charges are ± 1 breaks down. However, we are able to argue that the

crucial numerical coefficient d, governing the nonanalytic behavior of confinement near g = 0, is the same as obtained in the variational treatment of Ref. 3.

Model III for continuous time has the following action:

$$\int dt\ a^2 \sum_{\vec{p}} \left(\frac{1}{2} \sum_{i=1}^{2} \left[E_i(\vec{p},t) \right]^2 + \frac{1}{g^2 a^4} \left\{ 1 - \cos\left[g a^2 B(\vec{p},t) \right] \right\} \right) \quad , \quad (6.1)$$

where g is the coupling constant, a is the spatial lattice spacing, and $\vec{p}$ denotes a lattice site. g has dimension $(\text{length})^{-1/2}$.

We now make time discrete, with spacing b, and make space-time Euclidean. The action becomes

$$S = ba^2 \sum_{r} \left(\frac{1}{2} \sum_{i} \left[E_i(r) \right]^2 + \frac{1}{g^2 a^4} \left\{ 1 - \cos\left[g a^2 B(r) \right] \right\} \right) \quad , \quad (6.2)$$

where r now denotes a three-dimensional lattice site. In terms of the vector potentials, the electric and magnetic fields are

$$\begin{aligned} B &= \frac{1}{a} \left(\Delta_1 A_2 - \Delta_2 A_1 \right) \quad , \\ E_i &= \frac{1}{a} \Delta_j A_3 - \frac{1}{b} \Delta_3 A_j \quad . \end{aligned} \qquad (6.3)$$

Δ_μ are the difference operators in the three directions. We will rescale the A_μ,

$$\theta_i = ga\ A_i \quad ,$$

$$\theta_3 = gb\ A_3 \quad ,$$

and define

$$\theta_{\mu\nu} = \Delta_\mu \theta_\nu - \Delta_\nu \theta_\mu \quad , \tag{6.4}$$

so that

$$S = \frac{b}{g^2 a^2} \sum_r \left[1 - \cos\theta_{12}(r)\right] + \frac{1}{2g^2 b} \sum_{r,i} \left[\theta_{3i}(r)\right]^2 \quad , \tag{6.5}$$

and our aim is to compute

$$Z = \prod_r \int \left[d\theta_\mu(r)\right] \exp\left\{ -S - i \sum_{r,\mu} j_\mu(r)\ \theta_\mu(r) \right\} \quad , \tag{6.6}$$

where j_μ is the external source associated with the Wilson loop. To find j for a given contour C, we note that

$$\sum_{r,\mu} j_\mu(r)\ \theta_\mu(r) = g \sum_{r,i} aA_i(r)\ j_i(r) + g \sum_r bA_3(r)\ j_3(r) \quad .$$

We therefore choose,

$$j_\mu(r) = \begin{cases} 1 & \text{if the link } r \to r + \hat{\mu} \text{ is on C} \\ -1 & \text{if the link } r + \hat{\mu} \to r \text{ is on C} \\ 0 & \text{otherwise} \quad , \end{cases} \tag{6.7}$$

and this current is conserved: $\Delta_\mu\ j_\mu(r) = 0$.

What is the range of integration over $\theta_\mu(r)$ in (6.1)? The action is periodical neither in θ_3 nor in θ_i, so we let $\theta_\mu(r)$ vary over the entire real axis.

Separating θ_i into longitudinal and transverse parts,

$$\theta_i(r) = \Delta_i \lambda(r) - \varepsilon_{ij}\ \Delta_j \frac{1}{\Delta_1^2 + \Delta_2^2}\ \theta(r) \ ;$$

$$\theta_{12}(r) = \theta(r) \quad ,$$

We get the following exponent in (6.6):

$$S + i \sum_{r,\mu} j_\mu \theta_\mu = \frac{b}{g^2 a^2} \sum_r \left[1 - \cos\theta(r)\right]$$

$$+ \frac{1}{2g^2 b} \sum_r \left(\lambda \Delta_3^2 \Delta_i^2 \lambda + \theta \frac{\Delta_3^2}{\Delta_i^2} \theta - \theta_3 \Delta_i^2 \theta_3 - 2 \Delta_3 \theta_3 \Delta_i^2 \lambda \right)$$

$$+ i \sum_r j_3 (\theta_3 - \Delta_3 \lambda) - i \sum_r j_i \varepsilon_{ij} \frac{1}{\Delta_k^2} \Delta_j \theta \quad , \qquad (6.8)$$

with $\Delta_i^2 = \Delta_i \Delta_i = \Delta_1^2 + \Delta_2^2$. This expression is quadratic in θ_3 and λ, so integration over these variables can be easily performed, leaving only a path integral over the magnetic field $\theta(r)$. The result is

$$Z \propto \prod_r \int_{-\infty}^{\infty} d\theta(r) \exp \left\{ - \frac{b}{g^2 a^2} \sum_r \left[1 - \cos\theta(r)\right] \right.$$

$$\left. + \frac{1}{2g^2 b} \sum_r (\Delta_3 \theta) \frac{1}{\Delta_i^2} (\Delta_3 \theta) + i \sum_r (\Delta_1 j_2 - \Delta_2 j_1) \frac{1}{\Delta_i^2} \theta \right\} . \qquad (6.9)$$

The proportionality is up to a factor resulting from the self-interaction of the current loop j. Such factors contribute only a perimeter law and will be subsequently ignored. To compute Z we replace the cosine potential by its Villain version,*

$$\exp\left[-\beta(1-\cos\theta)\right] \to \sum_{\ell=-\infty}^{\infty} e^{i\ell\theta} \frac{1}{\sqrt{2\pi\beta}} e^{-\ell^2/2\beta} \qquad (6.10)$$

*This step is comparable to the approximation of choosing the trial wave function used in Ref. 3.

and perform the θ integration, which is now Gaussian:

$$Z \propto \prod_r \sum_{\ell(r)=-\infty} \exp\left\{ -\frac{g^2 a}{2} \sum_r \ell(r) \left[\frac{a}{b} + \frac{b}{a} \frac{\Delta_i^2}{\Delta_3^2} \right] \ell(r) \right.$$
$$\left. - g^2 b \sum_r \ell(r) \frac{1}{\Delta_3^2} \left(\Delta_1 j_2 - \Delta_2 j_1 \right) \right\} . \tag{6.11}$$

Substituting $\ell(r) = \Delta_3 L(r)$ and using the Poisson resumation technique gives

$$Z \propto \prod_r \sum_{m(r)=-\infty} \exp\left\{ \frac{2\pi^2}{b a^2 g^2} \sum_r m(r) \frac{1}{\left(\partial_3^2 + \frac{1}{a^2} \Delta_i^2 \right)} m(r) \right.$$
$$\left. + \frac{2\pi i}{a^2} \sum_r m(r) \frac{1}{\left(\partial_3^2 + \frac{1}{a^2} \Delta_i^2 \right)} \frac{1}{\Delta_3} \left(\Delta_1 j_2 - \Delta_2 j_1 \right) \right\}, \tag{6.12}$$

where $\partial_3 = (1/b)\Delta_3$. This is, once again, the partition sum for a monopole gas interacting with a current loop. We now consider two cases.

I. $\underline{b = a}$. In this case (6.12) coincides precisely with (A.2) of Ref. 2. This is interesting, since model III is not symmetric in space and time, and yet yields a symmetrical monopole gas.

II. $\underline{b << a}$. Let us characterize a configuration of $\{m(r)\}$ as

$$m(r) = \sum_k M_{xy}(k) \, \delta_{t, t_{xy}(k)} , \tag{6.13}$$

where $r = (x,y,t)$ and $\{M\}$ are restricted to be integers $\neq 0$. Now a configuration is characterized by a set $\{M_{xy}(k)\}$ of monopole strengths, and a set $\{t_{xy}(k)\}$ giving their times for every spatial site.

In the continuous time limit, $b \ll a$, ∂_3 becomes a true derivative, and $1 / [\partial_3^2 + (1/a^2)\ \Delta_i^2\ ]$ becomes a mixed matrix-integral operator. The external source

$$\eta_{xy}(t) = \frac{1}{\Delta_3}\ \left(\Delta_1 j_2 - \Delta_2 j_1\right) \tag{6.14}$$

is a finite, discontinuous function of t for a given x,y. Finally, we can replace

$$b \sum_r \ \rightarrow \int dt \sum_{xy} \quad ,$$

$$\frac{1}{b}\ \delta_{t,t_{xy}(k)} \rightarrow \delta\left[t - t_{xy}(k)\right] \quad ,$$

and all of the above gives:

$$Z \propto \sum_{\{t_{xy}(k)\}} \sum_{\{M_{xy}(k)\}} \exp\left\{ \frac{2\pi^2}{g^2 a^2} \sum_{xyk,x'y'k'} M_{xy}(k)\ B_{xyk,x'y'k'}\ M_{x'y'}(k') \right.$$

$$\left. + \frac{2\pi i}{a^2} \sum_{xyk} M_{xy}(k) \left(\frac{1}{\partial_t^2 + \frac{1}{a^2}\ \Delta_i^2}\ \eta_{xy}(t) \right)_{t = t_{xy}(k)} \right\} \quad ,$$

$$B_{xyk,x_0'y_0'k'} = \left(\frac{1}{\partial_t^2 + \frac{1}{a^2}\ \Delta_i^2}\ \delta\left[t - t_{x_0'y_0'}(k')\right]\ \delta_{x,x_0'}\ \delta_{y,y_0'} \right)_{t = t_{xy}(k)} \quad . \tag{6.15}$$

The summation over $\{t_{xy}(k)\}$ includes summation over the number of monopoles at the point xy. The numbers $B_{xyk,x'y'k'}$ are finite, and proportional to a. According to the procedure employed in Refs. 1, 2 and 3, one should at this point neglect all monopoles with charges not ± 1, since a monopole with a higher charge gets extra powers of $\exp\{-1/g^2 a\}$.

But since $b \ll a$, these configurations are no longer suppressed, since two big and opposite charges can come close to within a few b on the time axis and have a small action. We do not know how to compute Z in the limit $b \to 0$, but we now make the following assumption: along the time axis, monopoles will cluster into segments. These segments are of length $\sim a$, since this is the scale of the Green's function B. For two such segments, separated by a time interval $\gtrsim a$, the interaction B between them is less important than their self-action, so we can apply the approximation $M_{xy}(k) = \pm 1$ to the total charge of a segment. According to this mechanism, (6.15) effectively becomes the gas of Ref. 2, where "segments" replace monopoles. The main difference is in $D_0 = B_{xyk,\, xyk}$, which is derived from a continuous-time, rather than a discrete-time, Green's function. The d coefficient, defined in Section 5, is therefore

$$d = \frac{2\pi^2}{a} D_0 = \frac{2\pi^2}{a} \left(\frac{1}{\partial_t^2 + \frac{1}{a^2} \Delta_i^2} \; \delta(t) \; \delta_{x,0} \; \delta_{y,0} \right)_{t=x=y=0} . \quad (6.16)$$

The less important coefficients, c and δ, presumably depend on the details of the clustering phenomenon. Going to momentum base, (6.16) gives

$$d = \frac{a}{4\pi} \int_{-\infty}^{\infty} d\omega \int_{-\pi/a}^{\pi/a} \int_{-\pi/a}^{\pi/a} dk_1 \, dk_2 \left\{ \omega^2 + \frac{1}{a^2} \left[4 - 2\cos(k_1 a) - 2\cos(k_2 a) \right] \right\}^{-1}$$

$$= \frac{1}{4\pi} \int_{-\infty}^{\infty} d\omega \int_{-\pi}^{\pi} \int_{-\pi}^{\pi} dk_1 \, dk_2 \left[\omega^2 + 4 - 2\cos k_1 - 2\cos k_2 \right]^{-1}$$

$$= \frac{1}{4} \int_{-\pi}^{\pi} \int_{-\pi}^{\pi} \left(4 - 2\cos k_1 - 2\cos k_2 \right)^{-1/2} dk_1 \, dk_2 \quad , \quad (6.17)$$

which is exactly d_3, the result in Ref. 3, as written in Section 5.

7. Conclusions

We have compared the monopole and variational approaches to the problem of confinement in compact QED in 2+1 dimensions. We saw that the mechanisms for screening and confinement are qualitatively the same, and that the crucial coefficient d comes out the same if one takes care to treat time in the same way in the two approaches. The main remaining discrepancy is the nature of screening, which is only a power-law in Ref. 3 but is exponential in Refs. 1 and 2. However, we have seen that this might be an artifact of certain approximations made in Ref. 3. We have also demonstrated that the confinement mechanism breaks down for nonperiodic potentials.

REFERENCES

1. A. M. Polyakov, Nucl. Phys. B120, 429 (1977).

2. T. Banks et al., Nucl. Phys. B129, 493 (1977).

3. S. D. Drell et al., Phys. Rev. D19, 619 (1979).

4. K. Wilson, Phys. Rev. D10, 2445 (1974).

FIGURE CAPTIONS

Fig. 1. A piecewise-quadratic field potential.

Fig. 2. A monopole. B becomes π on surfaces T, K.

Fig. 3. The Wilson current loop, immersed in a monopole gas.

Fig. 4. A quark-antiquark pair. The lines are Coulomb field lines, the circles denote electric vortices.

Fig. 5. The Wilson Contour.

Fig. 6. A double-well field potential which does not confine.

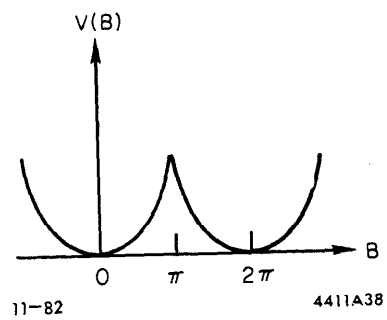

Fig. 1

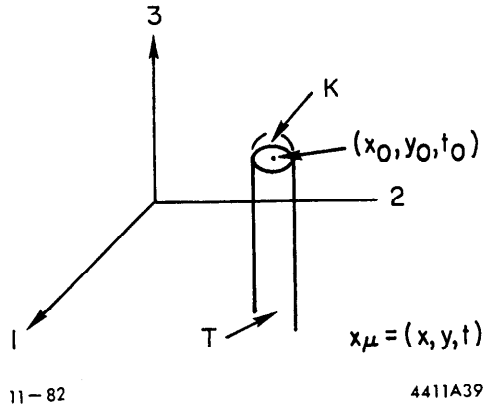

Fig. 2

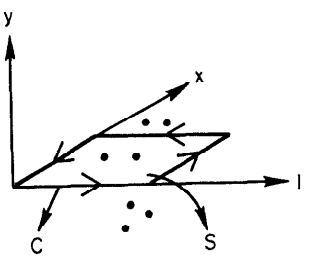

Fig. 3

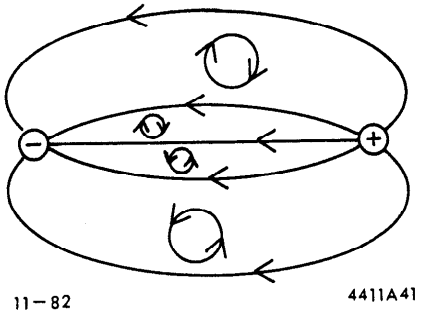

Fig. 4

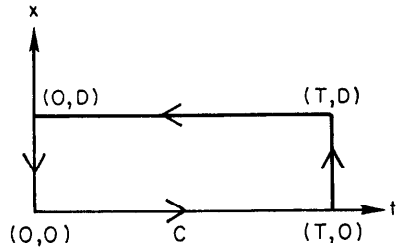

Fig. 5

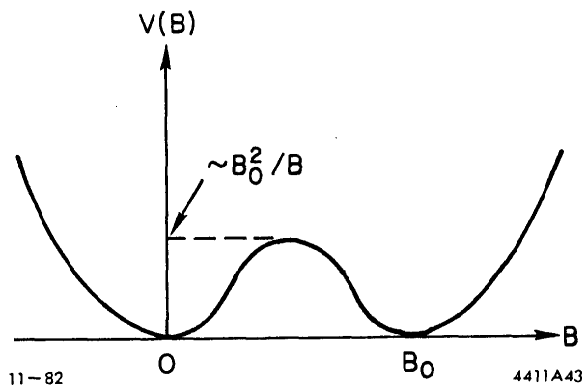

Fig 6

PART II

ADIABATIC TRUNCATION: A FREE FIELD EXERCISE

1. Introduction

The method of lattice Hamiltonian blocking, or the real space renormalization group, has been successful in a variety of models, yielding results for ground-state energies, mass gaps, and correlation functions. When applied to soluble 1 + 1 dimensional models, where it can be compared with exact solutions, it succeeds in giving fairly accurate results. Improving upon these results, however, usually necessitates complicated refinements of the procedure, and even so the spatial structure of correlation functions computed in such schemes is never very accurate.

Stated simply, a blocking scheme is a systematic way to compute scale transformations in a lattice model, from one ultraviolet cutoff Λ_1 to a smaller one, Λ_2. This is done by solving approximately for those modes that have frequencies $\Lambda_2 < \omega < \Lambda_1$, and removing them from the theory.

In Part II, we report a new method of treating these higher-frequency modes using an adiabatic (Born-Oppenheimer) approximation. The usefulness of the method is explained in general, and demonstrated in the framework of a very simple model: a free Bose scalar field theory in one space dimension. We examine in detail several schemes employing the method. For the most part, we concentrate on the massless case, which is the hardest to attack by blocking techniques due to its long-range correlations. The results of the adiabatic approach are compared with those of conventional blocking schemes.

For each scheme we treat, the ground-state energy and various equal-time Green's functions are computed for the trial ground-state.[1] We find excellent agreement with the exact results; using previous

methods, one must keep many more states per site and sites per block to attain accuracies that we can get using our adiabatic approach.

Our adiabatic method is closely related to, and grew out of, the recently developed Shadow Hamiltonian technique by Quinn and Weinstein[2] (QW). It is, however, more suited for treating Bose field theories. The QW technique was developed for a spin model, where one cannot define classically meaningful "fast" and "slow" modes. The distinction between these modes is, however, the cornerstone of our method. Both techniques can be applied to more complicated models than those they were tested for.

The plan of Part II is as follows: in Section 2 the adiabatic method is explained. In Section 3 our model is introduced and solved, and its relevant symmetries pointed out. In Section 4 we apply the new method to the model, keeping one "slow" variable per two-site block. In Section 5 we apply it keeping two variables, again with two-site blocks. In Section 6 we summarize our conclusions. We find it useful to work in the momentum basis, due to long-range effects.

2. Iterative Blocking-Truncation Methods

In a blocking scheme, one begins from a theory defined on a spatial lattice, and groups the lattice into blocks of two or more sites each. One then truncates away some block states or degrees of freedom. The choice of these states is based on energy: one would like to reject the (in some sense) "higher" excited states. The assumption underlying the truncation procedure is that the higher excitations will not affect the ground state by much.

Let us consider a Bose field theory. One can talk of field variables rather than states, and the problems of choosing low-lying

block states becomes that of identifying "slow" and "fast" (low- and high-frequency) variables.

In the "simple-blocking" schemes,[3] the Hamiltonian is split into terms involving a single block and terms coupling the blocks. This decomposition is obviously not unique, creating a certain ambiguity in the procedure. This ambiguity will disappear when we introduce our improved blocking method; but let us proceed with the description of the conventional method. The single-block Hamiltonian is solved, exactly or approximately, and the block modes are identified. One defines "slow" and "fast" modes; the latter are frozen in their approximate ground state. All operators are next truncated by computing their expectation values with respect to these fast modes. These modes thus drop out of the theory, leaving an effective Hamiltonian in the remaining variables. This Hamiltonian is defined on a new lattice, with the blocks serving as the new sites. The new theory has a larger lattice spacing, and correspondingly a smaller ultraviolet cutoff, than the old one. Hence the theory undergoes a scale transformation. This is called a renormalization-group transformation.[4]

By truncating operators, we may express their trial ground-state expectation values, or Green's functions, in terms of their counterparts in the rescaled theory. We refer to these relations as "mappings," or renormalization-group equations. The ground-state energy, for example, is computed by repeated mappings of the Hamiltonian. One repeats the mapping until the physics of $H_{effective}$ becomes either trivial, or so soft it does not affect the results any more.[5]

The difference in our new method is in its truncation prescription. Instead of using only the single-block terms in H to determine the fast-variable wave function, we allow the block-block terms to influence it. This is done by letting the fast variables in a block oscillate about mean values that change adiabatically with the slow modes in the surrounding blocks.

It is easy to understand how this can economize on the number of states we need to keep, since the adiabatic state of the fast modes is a superposition of many nonadiabatic (isolated-block) states.

The adiabatic state is a "wave packet" in the fast variables. We determine its center and shape variationally by combining the blocking with a mean-field approach. Namely, at each step we "look ahead" a certain number n_ℓ of iterations, after which some parametrized mean field trial state,

$$\prod_{\text{sites } j} |\varphi\rangle_j \quad ,$$

is used. $|\varphi\rangle$ is the same state for all j. Then the parameters of $|\varphi\rangle$, and of all previous n_ℓ wave packets, are varied to minimize the trial energy $\langle t|H|t\rangle$. $|t\rangle$ is now a completely specified trial state, in the modes of the last $H_{\text{effective}}$ and in all higher-frequency modes previously frozen. But having thus determined the variational parameters, we discard the mean field state and the last $(n_\ell - 1)$ look-ahead iterations, and use only the wave-packet parameters needed for a <u>single</u> mapping. The mapping thus proceeds one step at a time.

The intermediate trial states, $|t\rangle$, are never used to compute the final physical quantities; these are computed in the final trial state,

which we denote |trial>. It is obtained in the limit of an infinite number of blockings (for an infinite-volume lattice).

3. The Model

The model we treat has a scalar field x_r defined on each site r of the one-dimensional lattice, together with its canonically-conjugate variable p_r. The Hamiltonian is (for a system of volume L sites)

$$H = \sum_{r=0}^{L-1} \frac{1}{2} p_r^2 + \sum_{r,s=0}^{L-1} d(r-s)\, x_r x_s \quad , \qquad (3.1)$$

where $d(r-s)$ is some form of the lattice Laplacian. We work in units in which the lattice spacing is unity, and use periodic boundary-conditions.

Since we shall be working in the momentum basis, we rewrite H in that basis:[6]

$$H = \sum_k \left\{ \frac{1}{2} p(k)\, p^*(k) + d(k)\, x(k)\, x^*(k) \right\} \quad . \qquad (3.2)$$

d(k) can be made a symmetric function of k. In particular, for a field of mass μ and a nearest-neighbor definition of the gradient, we have

$$d(k) = \frac{1}{2} \mu^2 + (1 - \cos k) \quad . \qquad (3.3)$$

H has the following three symmetries which will concern us:

a) Parity invariance

$$P: \begin{cases} x(k) \to x(-k) \\ \\ p(k) \to p(-k) \end{cases} \quad . \qquad (3.4)$$

b) Field-translation invariance: this is the continuous symmetry

$$G(\tau): \begin{cases} x(k) \to x(k) + \tau\delta_{k,0} \\ p(k) \to p(k) \end{cases} \tag{3.5}$$

for arbitrary real τ. This symmetry is equivalent to the statement that the field is massless, and is valid only if $d(0) = 0$. [7]

c) Site-translation invariance: this is the invariance under the lattice symmetry of relabeling the j-th site as the j + m-th, or in momentum basis

$$T_m: \begin{cases} x(k) \to x(k)\ e^{ikm} \\ p(k) \to p(k)\ e^{ikm} \end{cases} \tag{3.6}$$

for any integer m. This symmetry can, in fact, be generalized to translations by a noninteger number of lattice spacings.

Throughout our blocking treatment of the model, we will demand that P and $G(\tau)$ be conserved by the truncation. The breaking of T_m is inherent in the blocking approach, and we will encounter in in various forms.

The solution of (3.2) is trivial: the ground-state wave function is

$$\langle\{x\}|g.s.\rangle = \exp\left\{-\sum_k \sqrt{\frac{d(k)}{2}}\ x(k)\ x^*(k)\right\}, \tag{3.7}$$

and the ground-state energy density is

$$\rho_{g.s.} = \frac{1}{2\pi\sqrt{2}} \int_0^{2\pi} dk \sqrt{d(k)} \tag{3.8}$$

in the large-volume limit. The equal-time, two-point Green's functions we shall study are

$$G(k) = \langle x(k)\ x^*(k)\rangle_{g.s.} = \frac{1}{2\sqrt{2d(k)}}$$
$$R(k) = \langle p(k)\ p^*(k)\rangle_{g.s.} = \sqrt{\frac{d(k)}{2}} \quad . \tag{3.9}$$

4. A One-Variable Adiabatic Scheme

Let us group the lattice sites into blocks, so that the j-th block contains the sites 2j and 2j + 1. We define sum and difference block variables,

$$\begin{aligned} x_+(j) &= \frac{1}{2}\left(x_{2j} + x_{2j+1}\right) \quad , \\ x_-(j) &= \frac{1}{\sqrt{2}}\left(x_{2j} - x_{2j+1}\right) \quad , \\ p_+(j) &= p_{2j} + p_{2j+1} \quad , \\ p_-(j) &= \frac{1}{\sqrt{2}}\left(p_{2j} - p_{2j+1}\right) \quad . \end{aligned} \tag{4.1}$$

To get an effective Hamiltonian with one variable per site, one of the two block modes must be frozen; in the simple blocking schemes that mode is $x_-(j)$ (essentially because it has a higher wave-number).[8]

In the momentum basis, Eqs. (4.1) assume the form [Eq. (A.3)]

$$\begin{aligned} e^{-ik/2}\, x(k) &= \sqrt{2}\cos(k/2)\, x_+(2k) - i\sin(k/2)\, x_-(2k) \quad , \\ e^{-ik/2}\, p(k) &= \frac{1}{\sqrt{2}}\cos(k/2)\, p_+(2k) - i\sin(k/2)\, p_-(2k) \quad . \end{aligned} \tag{A.3}$$

The fast modes $\{x_-\}$ will be frozen to a product of Gaussians over the blocks, with a Gaussian "wave-packet" at each block having as its center a function of the slow modes:

$$\langle\{x\}|\text{trial}\rangle = \prod_j \exp\left\{-\frac{1}{2}(\gamma_-)_j\left[x_-(j) - F_j(\{x_+\})\right]^2\right\}\psi_{\text{res}} \quad , \quad (4.2)$$

where ψ_{res} depends on the residual (slow) modes. As explained in Section 1, renormalization-group calculations are concerned with unraveling step-by-step, the physics of the various length-scales in the problem; the physics that is of concern right now is that which is interior to a block, i.e., that of the fast variables. Therefore, ψ_{res} need not be specified at this point. Nevertheless, some crude guess-form of ψ_{res} will have to be used for the purpose of variationally determining the wave-packet parameters — this is the essence of the look-ahead method (see Section 2). We shall come back to the look-ahead aspects of ψ_{res} at the end of this section.

Let us now further specify the fast-variable wave-function appearing in (4.2). F_j may, in general, be a nonlinear function, and $(\gamma_-)_j$; F_j may depend explicitly on j, but we will use a linear form without such dependence:

$$F_j(\{x_+\}) = \sum_{j'} i\,\rho(j - j')\,x_+(j') \quad (4.3)$$

and a j-independent[9] $(\gamma_-)_j = \gamma_-$. ρ is an n-dependent function, and when we wish to emphasize this dependence we will write ρ_n. We may then rewrite Eq. (4.2) in the momentum basis

$$\langle\{x\}|\text{trial}\rangle = \prod_k \exp\left\{-\frac{1}{2}\,\gamma_-\,\hat{x}_-(k)\,\hat{x}_-^*(k)\right\}\psi_{\text{res}} \quad , \quad (4.4)$$

where we have gone over to shifted variables via the canonical transformation

$$\begin{aligned} x_-(k) &= \hat{x}_-(k) + i\,\rho(k)\,\hat{x}_+(k) \quad , \\ x_+(k) &= \hat{x}_+(k) \quad , \\ p_-(k) &= \hat{p}_-(k) \quad , \\ p_+(k) &= \hat{p}_+(k) + i\,\rho(k)\,\hat{p}_-(k) \quad . \end{aligned} \tag{4.5}$$

From parity and hermiticity, $\rho(k)$ must obey

$$\rho^*(k) = -\rho(-k) = \rho(k) \quad . \tag{4.6}$$

For later convenience, we choose to rescale the slow modes,

$$\begin{aligned} \hat{x}_+(k) &= 2^{-1/4}\ \tilde{x}(k) \quad , \\ \hat{p}_+(k) &= 2^{1/4}\ \tilde{p}(k) \quad . \end{aligned} \tag{4.7}$$

The shift, rescaling and truncation together define the mapping of operators. We will only be interested here in mapping bilinear operators: xx^* and pp^*. Hence we only need the following rules:

$$\begin{aligned} \left[\hat{x}_-(k)\right]_{tru} &= \left[\hat{p}_-(k)\right]_{tru} = 0 \quad , \\ \left[\hat{x}_-(k)\ \hat{x}_-^*(k')\right]_{tru} &= \delta_{kk'}\ \frac{1}{2\gamma_-} \\ \left[\hat{p}_-(k)\ \hat{p}_-^*(k')\right]_{tru} &= \delta_{kk'}\ \frac{\gamma_-}{2} \quad , \end{aligned} \tag{4.8}$$

where the subscript denotes "truncated." The following mapping results:

$$\left[x(k)\ x^*(k)\right]_{tru} = \frac{1}{\sqrt{2}}\left[\sqrt{2}\cos(k/2) + \rho(2k)\sin(k/2)\right]^2 \times \tilde{x}(2k)\ \tilde{x}^*(2k) + \frac{1}{4\gamma_-}(1-\cos k) \quad ,$$

$$\left[p(k)\ p^*(k)\right]_{tru} = \frac{1}{2\sqrt{2}}(1+\cos k)\ \tilde{p}(2k)\ \tilde{p}^*(2k) + \frac{\gamma_-}{2}\left[\frac{1}{\sqrt{2}}\cos(k/2)\ \rho(2k) - \sin(k/2)\right]^2 \quad . \tag{4.9}$$

Note that a pair of momenta k, $k+\pi$, correspond to the same wave number $2k$ of the new lattice; this is an umklap phenomenon, related to the artificially imposed block boundaries. We introduce a notation for sums of contributions from such an umklap pair: for any function $f(k)$ denote

$$[f(k/2)]_u = f(k/2) + f(k/2+\pi) \quad . \tag{4.10}$$

Then from Eqs. (3.2) and (4.9) we obtain the mapping of the Hamiltonian

$$(H)_{tru} = \frac{L}{2}\ c_- + \frac{1}{\sqrt{2}}\ \tilde{H} \quad . \tag{4.11}$$

Here c_- is the zero-point energy per block of the frozen fast modes, L is the volume,[10] and $\tilde{H}$ is the mapped Hamiltonian:

$$8\pi c_- = \gamma_-^{(n)} \int_0^{2\pi} dk\left[1 + \frac{1}{2}\rho(k)^2\right] + \frac{1}{\gamma_-^{(n)}} \cdot \int_0^{2\pi}\left[\left(1-\cos\frac{k}{2}\right)\ d\left(\frac{k}{2}\right)\right]_u$$

$$\tilde{H} = \sum_k \left\{\frac{1}{2}\ \tilde{p}(k)\ \tilde{p}^*(k) + \tilde{d}(k)\ \tilde{x}(k)\ \tilde{x}^*(k)\right\} \tag{4.12}$$

$$\tilde{d}(k) = \left\{\left[\sqrt{2}\cos(k/4) + \rho(k)\sin(k/4)\right]^2\ d(k/2)\right\}_u \quad .$$

We have mapped the Hamiltonian, and we now want to determine the wave-packet parameters characterizing the renormalization group transformation. These parameters, $\gamma_-^{(n)}$ and $\rho(k)$, will be determined variationally via the look-ahead prescription.

First, we realize that due to the simplicity of the model under consideration, the task is easier than it could in general be. Namely, because $\tilde{H}$ does not depend on $\gamma_-^{(n)}$ but only on the shift ρ, we may ignore $\tilde{H}$ for the purpose of solving for γ_-, no matter what the look-ahead method used. (This is a feature unique to the free-field case). The point is, of course, that γ_- depends on $\rho(k)$, which <u>does</u> appear in $\tilde{H}$, and thus the fast and slow modes interact through ρ and the results are sensitive to the look-ahead scheme employed. We may, however, eliminate γ_- from our equations, and we proceed to do that. Minimizing c_- with respect to $\gamma_-^{(n)}$ gives from (4.12)

$$\gamma_-^{(n)} = \frac{\left(\int_0^{2\pi} \left\{ \left[1 - \cos(k/2) \right] d(k/2) \right\}_u dk \right)^{1/2}}{\left\{ \int_0^{2\pi} \left[1 + \frac{1}{2} \rho(k)^2 \right] dk \right\}^{1/2}} , \tag{4.13}$$

$$4\pi c_- = \left(\int_0^{2\pi} \left\{ \left[1 - \cos(k/2) \right] d(k/2) \right\}_u dk \right)^{1/2} \left\{ \int_0^{2\pi} \left[1 + \frac{1}{2} \rho(k)^2 \right] dk \right\}^{1/2} . \tag{4.14}$$

For a single look-ahead ($n_\ell = 1$ in the notation introduced in Section 2), we use the Gaussian mean-field guess for ψ_{res},

$$\psi_{res}\{\tilde{x}\} = \prod_j \exp\left\{ -\frac{1}{2} \gamma_n' (\tilde{x}_j)^2 \right\} = \prod_k \exp\left\{ -\frac{1}{2} \gamma_n' \tilde{x}(k) \tilde{x}^*(k) \right\} . \tag{4.15}$$

The intermediate trial state $|t\rangle$ for this scheme is obtained by substituting (4.15) in (4.2) or (4.4). The residual energy expectation value $\langle\tilde{H}\rangle$ in the state ψ_{res} is

$$\langle\psi_{res}|\tilde{H}|\psi_{res}\rangle = \left[\frac{\gamma_n'}{4} + \frac{1}{2\gamma_n'}\,\frac{1}{2\pi}\int_0^{2\pi}\tilde{d}(k)\,dk\right]\frac{L_n}{2} \tag{4.16}$$

Combining with (4.11) and (4.14) we find the total trial energy for this step (in the $n_\ell = 1$ scheme); it is

$$\langle t|H|t\rangle = \langle\psi_{res}|(H)_{tru}|\psi_{res}\rangle \tag{4.17}$$

$$= \frac{L_n}{2}\left\{\frac{1}{4\pi}A^{1/2}\int_0^{2\pi}\left[1+\frac{1}{2}\rho(k)^2\right]^{1/2}dk + \left[\frac{\gamma_n'}{4\sqrt{2}} + \frac{1}{2\sqrt{2}\,\gamma_n'\,2\pi}\int_0^{2\pi}\tilde{d}(k)\,dk\right]\right\}$$

where the dependence of $\tilde{d}$ on ρ is given in (4.12), and A is a constant in this variational problem:

$$A = \int_0^{2\pi}\left\{\left[1-\cos(k/2)\right]d(k/2)\right\}_u dk \tag{4.18}$$

Minimizing $\langle t|H|t\rangle$ with respect to γ_n' is trivial; the remaining minimization with respect to $\rho(k)$ depends on how long-range we wish to make the shift. Finally, if a number $n_\ell > 1$ of look-ahead steps is desired, the mapping should simply be carried out n_ℓ times before a mean-field Gaussian is used in the residual variables. All intermediate $\gamma_-^{(n)}$ values are given by (4.13), and one minimizes $\langle t|H|t\rangle$ with respect to all intermediate $\rho_n(k)$ - s.

From here on the variational problem is essentially numerical. We have solved it for various look-ahead schemes and various forms for the initial lattice-Laplacian, $d^{(0)}(k)$. Before reporting the results, we assume that the mapping parameters have been determined, and turn to the mapping of Green's functions.

The recursion relations for Green's functions follow from Eq. (4.9) by taking expectation values in the state $|\text{trial}\rangle$. Defining for the n-th iteration

$$G^{(n)}(k) = \left\langle x^{(n)}(k)\ x^{(n)*}(k)\right\rangle_{\text{trial}} ,$$
$$R^{(n)}(k) = \left\langle p^{(n)}(k)\ p^{(n)*}(k)\right\rangle_{\text{trial}} , \tag{4.19}$$

we get

$$G^{(n)}(k) = \frac{1}{\sqrt{2}}\left[\sqrt{2}\cos(k/2) + \rho^{(n)}(2k)\sin(k/2)\right]^2 \times G^{(n+1)}(2k) + \frac{1}{4\gamma_-^{(n)}}(1-\cos k) ,$$
$$R^{(n)}(k) = \frac{1}{2\sqrt{2}}(1+\cos k)\,R^{(n+1)}(2k) + \frac{\gamma_-^{(n)}}{2}\left[\frac{1}{\sqrt{2}}\cos(k/2)\,\rho^{(n)}(2k) - \sin(k/2)\right]^2 . \tag{4.20}$$

If these recursion relations are iterated ad infinitum, we get for $G^{(0)}$ and $R^{(0)}$ pathological functions of k that are nowhere smooth; this is just a reflection of the block umklap problem mentioned earlier.[11] What is happening is that an uncareful application of (4.20) causes the scaling behavior of G and R to be masked by these artificial umklap singularities; the way out of this problem is to consider $G^{(n)}(k)$, $R^{(n)}(k)$ only

at the discrete momenta values $k_r = \pi \cdot 2^{-r}$. The recursion relations (4.20) are then solved on this subset of the real axis. This is possible because they relate $G^{(n)}$ and $R^{(n)}$ at k_r to $G^{(n+1)}$ and $R^{(n+1)}$ at k_{r-1}, and moreover this trick causes the recursion to terminate when r reaches 0, $k_0 = \pi$. A demonstration of how we have solved recursion relations of this type is furnished in Appendix C.

Once the power laws for the Green's functions have been found at the discrete momentum values k_r, we can interpolate to all k values; this is a convenient way to smooth the nonanalytic benavior of G and R. Note that the discrete sequence $\{k_r\}$ has an accumulation point at $k = 0$, which is the region of interest (long-range). Physically, $\{k_r\}$ are the elementary harmonics quantized in the blocks of sizes[12] 2^r.

We next present the results of this one-variable adiabatic method for various forms of $\rho(k)$, $d(k)$ and look-ahead procedure.

The Results for One-Variable Schemes

The results of several one-variable schemes, of the type described above, are summarized in Tables I and II. In these tables, n_{shift} is the range of the shift in number of blocks; for a given range, the most general shift function compatible with parity is [see Eq. (4.6)],

$$\rho(k) = \sum_{j=1}^{n_{shift}} r_j \sin(jk) \quad . \tag{4.21}$$

For schemes with nearest-neighbor shifts, $n_{shift} = 1$, we recorded the limit

$$r_\infty = \lim_{n \to \infty} r_1^{(n)} \quad , \tag{4.22}$$

of the shift parameter as the number of iterations tends to infinity; it is a measure of the amount of adiabatic shifting in the large-scale limit. $\rho_{g.s.}$ is the ground-state energy density, while γ_G and γ_R are the asymptotic large-distance exponents as computed at the points $k_r = \pi \cdot 2^{-r}$ from (4.20):

$$G(k_r) \sim (k_r)^{\gamma_G} \quad ,$$

$$R(k_r) \sim (k_r)^{\gamma_R} \quad ,$$

as $r >> 1$. Since $\gamma_R = -\gamma_G$ for all the schemes we considered, we recorded only γ_G.

Both tables refer to a model with the nearest neighbor lattice derivative given in Eq. (3.3). Setting the shifts $\rho(k)$ to zero gives the simple-blocking scheme with mean field, i.e., with a one-step look-ahead; the no-mean-field scheme results when we determine the Gaussian parameters $\gamma_-^{(n)}$ by diagonalizing the block Hamiltonian. Both these schemes give[13] $\gamma_G = -1/2$, but the energy density is better with mean field than without it.

We see that allowing nearest-neighbor shifts improves both main physical quantities (energy and asymptotic exponent). Taking more look-ahead steps further improves them (except for $n_\ell = 2$), until beyond $n_\ell = 4$ the results change very little. Increasing the range of the shift improves them even more, but only when n_ℓ is at least 2.[14] The best scheme we have tried was that with a range-two shift and three look-ahead steps, giving $\gamma_G = -.998$.

Table II shows ratios of the trial energy density and Green's functions to their exact values, for various masses and momenta.

The nearest-neighbor gradient [Eq. (3.3)] was again used. For large masses, where simple blocking works well because the field is localized, the shift does not change the results much, but as the mass decreases the new method becomes superior both for $\rho_{g.s.}$ and Green's functions.[15]

Finally, we have checked the sensitivity of the above results to changes in the form of lattice gradient used (including the so-called "SLAC" derivative that is infinite-range and is designed to give a relativistic spectrum). Both the exact and trial energy densities changes, and the shift again improves the agreement, even though on the whole blocking is slightly less successful for longer-ranged derivatives. The asymptotic shifts and γ_G do not depend on the form of d(k). The fixed form of the gradient is given in Eq. (A.7); why this form is of range 4 lattice sites is also explained there.

5. Two-Variable Schemes

A. A two-variable formulation of the model

In the last section we saw how a nearest-neighbor adiabatic shift much improves on the simple Gaussian-truncation blocking scheme. The scheme can be made even more accurate by keeping more variables per site in the effective Hamiltonian, thus truncating away less of the dynamics. We will demonstrate this for a particular class of schemes in which two variables are kept per site. First we will cast the model in its two-variable form, by blocking once without truncation.

We start from Eq. (3.2), and decompose x(k), p(k) in terms of block variables according to Eq. (A.3). We redefine for convenience

$$y(k) = x_+(k) \ , \qquad z(k) = x_-(k)/\sqrt{2} \ ,$$
$$p_y(k) = p_+(k) \ , \qquad p_z(k) = \sqrt{2}\, p_-(k) \ . \tag{5.1}$$

H then assumes the form

$$H = \sum_k \left\{ \frac{1}{4} p_y p_y^* + \frac{1}{4} p_z p_z^* + (y \quad z) \begin{pmatrix} d_{yy} & id_{yz}/2 \\ id_{yz}/2 & d_{zz} \end{pmatrix} \begin{pmatrix} y^* \\ z^* \end{pmatrix} \right\} ; \tag{5.2}$$

here $d_{yy}(k)$, $d_{yz}(k)$ and $d_{zz}(k)$ are functions given in Eq. (A.4).

We now take Eq. (5.2) as our starting point. It is an effective Hamiltonian, but is equivalent to the original one. It is defined on a new lattice of volume L/2 and with a two-component scalar field at each site — a parity-even component y and a parity-odd component z. Under the symmetry $G(\tau)$ [Eq. (3.5)], we have

$$G(\tau): \begin{cases} y(k) \to y(k) + \tau\delta_{k,0} \ , \\ z(k) \to z(k) \ . \end{cases} \tag{5.3}$$

$$\left(p_y,\ p_z \text{ unchanged}\right)$$

Since z does not transform, it is allowed to have an effective mass term without violating any symmetry, and indeed there is such a term from the outset [Eq. (A.5)].

B. A two-variable adiabatic scheme

We group the sites in pairs to form blocks (which are 4-site "super-blocks" in the original sites), and define four block variables:

the sum and difference variables for y and z, denoted as $y_\pm$ and $z_\pm$ [see Eq. (A.6) for their exact definition]. y_-, z_+ and z_- are the three fast block modes, and y_+ is the slow mode (intuitively; since it corresponds to a k = 0 mode inside the superblock).

Within one block there can occur a mixing between the four modes. Parity invariance implies that the two even variables, y_+ and z_-, may only mix with each other, and so can the odd variables y_- and z_+. We will keep one even mode, and one odd mode which is a mixture of y_- and z_+. The other two modes will be truncated to adiabatic wave packets, with centers that are shifted to track the retained modes. Note that y_+ and z_- cannot actually mix (at least not orthogonally), because that would give a mass to y_+ and break the $G(\tau)$ invariance; hence we take the retained slow mode as simply y_+.

Let ζ be the mixing angle between the odd modes, defined such that the fast and slow mixed modes are, respectively,

$$z_+^M \equiv cz_+ - sy_- \quad ,$$

$$y_-^M \equiv sz_+ + cy_- \quad .$$

Here c and s are shorthand for $\cos\zeta$ and $\sin\zeta$, respectively. We now invoke the most general linear adiabatic shifts among the four modes y_+, y_-^M; z_+^M, z_- that are consistent with the symmetries of the model. The fast modes z_+^M, z_- each shift by a linear combination of the two slow modes y_+, y_-^M; as in the one-variable calculation, we work in momentum basis and the shift coefficients are k dependent. We thus define

$$\left.\begin{aligned} \hat{y}_+ &= y_+ \\ \hat{y}_- &= y_-^M \end{aligned}\right\} \text{ unshifted slow modes} \quad ,$$

$$\left.\begin{aligned} \hat{z}_+ &= z_+^M - i\rho_1 y_+ - \rho_2 y_-^M \\ \hat{z}_- &= z_- - \rho_3 y_+ - i\rho_4 y_-^M \end{aligned}\right\} \text{ shifted fast modes} \quad .$$

Disentangeling the original variables in terms of $\hat{y}_\pm$, $\hat{z}_\pm$ we find,

$$\begin{aligned} y_+ &= \hat{y}_+ \quad , \\ y_- &= (c - s\rho_2)\hat{y}_- - i\rho_1\, s\hat{y}_+ - s\hat{z}_+ \quad , \\ z_+ &= c\hat{z}_+ + i\rho_1\, c\hat{y}_+ + (s + \rho_2 c)\,\hat{y}_- \quad , \\ z_- &= \hat{z}_- + \rho_3\hat{y}_+ + i\rho_4\hat{y}_- \quad , \end{aligned} \tag{5.4}$$

where the shift coefficients ρ_i are functions of k. $\hat{z}_+$ and $\hat{z}_-$ are the fast modes that we truncate away.

If we assume that the shifts are all nearest-neighbor, then parity and $G(\tau)$ symmetries restrict them to the following forms, parametrized by five real numbers:

$$\begin{aligned} \rho_1(k) &= r_1 \sin k \quad , \\ \rho_2(k) &= r_2 + r_3 \cos k \quad , \\ \rho_3(k) &= r_4(1 - \cos k) \quad , \\ \rho_4(k) &= r_5 \sin k \quad . \end{aligned} \tag{5.5}$$

The six mix-shift parameters ζ, $\{r_i\}$, will be determined variationally.

The truncation is done with a product-Gaussian state:

$$\langle\{\hat{y},\hat{z}\}|\text{trial}\rangle = \left\{ \prod_k \left[e^{-\frac{1}{2}\gamma_1|\hat{z}_+(k)|^2} \; e^{-\frac{1}{2}\gamma_2|\hat{z}_-(k)|^2} \right] \right\} \psi_{\text{res}}(\{y_\pm\}), \quad (5.6)$$

where ψ_{res} is the wave function in the remaining variables, and γ_1,γ_2 are two more variational parameters. The guess-form we use for a one-step look-ahead is a product over single-site Gaussians, $\prod_k \exp\{-\frac{1}{2}\gamma_3|\hat{y}_+(k)|^2 - \frac{1}{2}\gamma_4|\hat{y}_-(k)|^2\}$. To complete the definition of the mapping we rescale,

$$\begin{aligned} \tilde{y} &= 2^{1/4}\,\hat{y}_+ \quad , \\ \tilde{z} &= 2^{-1/4}\,\hat{y}_- \quad , \\ \tilde{p}_y &= 2^{-1/4}\,\hat{p}_y^+ \quad , \\ \tilde{p}_z &= 2^{1/4}\,\hat{p}_y^- \quad . \end{aligned} \qquad (5.7)$$

We have studied three equal-time Green's functions,

$$\begin{aligned} G_1(k) &= \langle y(k)\; y^*(k)\rangle_{\text{trial}} \quad , \\ G_2(k) &= i\langle y(k)\; z^*(k)\rangle_{\text{trial}} \quad , \\ G_3(k) &= \langle z(k)\; z^*(k)\rangle_{\text{trial}} \quad , \end{aligned} \qquad (5.8)$$

which are arranged as a vector of rank 3, and their canonically conjugate counterparts, the vector $\vec{R}(k)$. The mapping of bilinear operators gives a tensor version of the renormalization group equations encountered in the one-variable case; e.g.,

$$\vec{G}^{(n)}(k) = \overleftrightarrow{\Gamma}^{(n)}(k) \cdot \vec{G}^{(n+1)}(2k) + \vec{\sigma}^{(n)}(k) \quad , \qquad (5.9)$$

where the matrix $\overleftrightarrow{\Gamma}^{(n)}$ and the vector $\vec{\sigma}^{(n)}$ depend on the mix-shift parameters. This equation is easily obtained from Eqs. (5.8), (A.6), (5.4) and (5.6) upon integrating out the fast "shift-mixed" variables, $\hat{z}_{\pm}$. We iterated these equations for the momenta $k = k_r$, using parameter values obtained variationally through a look-ahead procedure. The mapping of the Hamiltonian is of the form Eq. (4.11), with the new Hamiltonian being again of the form Eq. (5.2). The fixed form of H has functions d_{yy}, d_{yz}, d_{zz} of range four lattice spacings, for the same reason the range of $d^{(n)}$ was 4 in Section 4 [see Eq. (A.7)]. As in the one-variable calculations, this fixed form is independent of the exact form of the lattice gradient we start from, and so are the values of the Green's function exponents, defined as follows:

$$G_i(k_r) \sim (k_r)^{\gamma_G^i} \quad , \qquad R_i(k_r) \sim (k_r)^{\gamma_R^i} \quad , \tag{5.10}$$

where $1 \leq i \leq 3$ and $r \gg 1$.

Table III summarizes the results and compares them with the simple-blocking scheme: without mean field (Ref. 16) and with mean field. The adiabatic scheme is for $n_\ell = 2$, and we see that γ_G^1, γ_G^2 and γ_R^1 agree with the exact values up to ~ 1 part in 10^4. The other exponents are incorrect, as in the conventional schemes. We expect them to, because they involve the z mode, which is "faster" than y and so the truncation affects it more. This is again traceable to the lack of translational (T_m) invariance in blocking schemes; for in any trial state that obeys that invariance, one can prove that

$$\gamma_G^3 - 2 = \gamma_G^2 - 1 = \gamma_G^1 \quad ,$$
$$\gamma_R^3 - 2 = \gamma_R^2 - 1 = \gamma_R^1 \quad . \tag{5.11}$$

For the case of only one look-ahead step, an anomalous phenomenon occurs: the $\hat{z}_+$ mode, that in the no-shift schemes lies above $\hat{y}_-$, crosses below it. Therefore, choosing $\hat{y}_-$ repeatedly as a "slow mode" has a disastrous effect — it causes the $z^{(n)}$ oscillator to keep increasing its effective mass with n, and it eventually decouples from $y^{(n)}$. Thus, the $n_\ell = 1$ scheme reproduces, in effect, the results of the one-variable scheme. This could be avoided by allowing $\hat{y}_-$ to lower its frequency too, by shifting with the slowest mode $\hat{y}_+$. But for $n_\ell \geq 2$ the level ordering

$$E_{y_+} < E_{y_-} < E_{z_-} < E_{z_+} \tag{5.12}$$

remains intact throughout the iterations.

We also applied the scheme in which the three fast modes in a block are adiabatically shifted by the y_+ mode; that did not give a much better $\rho_{g.s.}$ than the one-variable schemes, and did not improve γ_G^i and γ_R^i.

C. Possible improvements

After having demonstrated that the results of the one-variable adiabatic scheme can be improved impressively by keeping two variables per site, we briefly discuss the generality of the procedure used in B. The two even modes in a block, y_+ and z_-, are not allowed to mix orthogonally if one of them (i.e., z_-) is then truncated by a Gaussian,

since that would give y_+ a fictitious mass. But y_+ could still shift by an amount proportional to z_- (i.e., a nonorthogonal mixing is allowed). One may also choose a different rescaling than Eq. (5.7).[17] A no-shift, several-look-ahead calculation we did indicates that in such an approach the $\hat{z}_-$ mode crosses below $\hat{y}_-$, suggesting that perhaps the two even modes should be kept per block. To avoid such breakdowns in a blocking scheme as this or what happens for $n_\ell = 1$, one should not predetermine at all which of the four modes are to be truncated. Their energies should be allowed to determine that anew at each step of the iteration. One should also allow for more general shifts, as discussed in Section B. But the calculations presented here suffice to make the point that systematic improvement wihin our approach is possible.

6. Conclusions

We have seen how the adiabatic truncation method can be used to improve the accuracy of real-space renormalization group techniques on the lattice for the case of a free scalar field. The improvement is especially noteworthy for large-distance behavior of trial Green's functions. The same method can be generalized to interacting field theories, and to any number of dimensions. We expect it to yield better results for phase transition locations, critical exponents, etc., than was possible with conventional methods.

APPENDIX A

In going from position to momentum basis we used the following relations:

$$\begin{aligned} d(r) &= \frac{1}{L} \sum_k e^{ikr}\, d(k) \quad , \\ x(r) &= \frac{1}{\sqrt{L}} \sum_k e^{-ikr}\, x(k) \quad , \\ p(r) &= \frac{1}{\sqrt{L}} \sum_k e^{-ikr}\, p(k) \quad , \end{aligned} \tag{A.1}$$

where L is the volume of the system in the current iteration, and k ranges over the values $2\pi\, m_k/L$, $0 \le m_k \le L - 1$. The canonical commutation relations are

$$\left[x(k),\, p^*(k)\right] = i\, \delta_{k,k'} \quad , \tag{A.2}$$

and since x is a real field, $x^*(k) = x(-k)$, and likewise for p.

To get the blocking relations in momentum basis, start from Eq. (4.1)。 Multiply both sides of each equation by e^{+2ijk} and sum over $0 \le j \le L/2-1$. Using for the block variables $x_\pm$, $p_\pm$ Fourier transformations similar to Eq. (A.1), but with L replaced by the decimated volume L/2, we find the relations

$$\begin{aligned} e^{-ik/2}\, x(k) &= \sqrt{2}\, \cos(k/2)\, x_+(2k) - i\, \sin(k/2)\, x_-(2k) \quad , \\ e^{-ik/2}\, p(k) &= \frac{1}{\sqrt{2}}\, \cos(k/2)\, p_+(2k) - i\, \sin(k/2)\, p_-(2k) \quad . \end{aligned} \tag{A.3}$$

For the two-variable schemes, the "Laplacian matrix" appearing in Eq. (5.2) has the components

$$\begin{aligned} d_{yy}(k) &= \left\{\left[1+\cos(k/2)\right] d(k/2)\right\}_u \quad , \\ d_{yz}(k) &= -2\left\{\sin(k/2)\, d(k/2)\right\}_u \quad , \\ d_{zz}(k) &= \left\{\left[1-\cos(k/2)\right] d(k/2)\right\}_u \quad , \end{aligned} \tag{A.4}$$

where we have used the definition (4.10) for the umklap sum. For the zero-mass nearest-neighbor gradient, $d(k) = 1 - \cos k$ and

$$\begin{aligned} d_{yy}(k) &= 1-\cos k \quad , \\ d_{yz}(k) &= 2\sin k \quad , \\ d_{zz}(k) &= 3+\cos k \quad . \end{aligned} \tag{A.5}$$

The definitions of the four block variables and their canonical momenta are

$$\begin{aligned} e^{-ik/2}\, y(k) &= \sqrt{2}\cos(k/2)\, y_+(2k) - i\sin(k/2)\, y_-(2k) \quad , \\ e^{-ik/2}\, z(k) &= \cos(k/2)\, z_+(2k) - i\sin(k/2)\, z_-(2k) \quad , \\ e^{-ik/2}\, p_y(k) &= \frac{1}{\sqrt{2}}\cos(k/2)\, p_y^+(2k) - i\sin(k/2)\, p_y^-(2k) \quad , \\ e^{-ik/2}\, p_z(k) &= \cos(k/2)\, p_z^+(2k) - i\sin(k/2)\, p_p^-(2k) \quad . \end{aligned} \tag{A.6}$$

Fixed forms: In the one-variable scheme with $n_{shift} = n_\ell = 1$, any model with a gradient of range four lattice spacings or less has the fixed-form gradient

$$d^{(n)}(k) \xrightarrow[n \uparrow \infty]{} C_0 \Big\{ (1 - \cos k) - .24\Big[1 - \cos(2k)\Big] + 0.35\Big[1 - \cos(3k)\Big] + .001\Big[1 - \cos(4k)\Big] \Big\} \quad , \tag{A.7}$$

where C_0 decreases exponentially with n. It is easy to prove that, starting with a lattice Lapalacian $d^{(0)}(k)$ of range ≤ 4, $d^{(n)}(k)$ reaches the maximal range of four. An interaction term of range r lattice sites becomes, upon blocking, of the range $[(r-2)/2]+1$, where $[x]$ is the largest integer smaller or equal to x; this range rapidly iterates to nearest-neighbor, 1. But with a nearest-neighbor adiabatic shift, $\tilde{x}_{j-1}$ "knows" about $\tilde{x}_{j+1}$ through $\hat{x}_-(j)$, so we must add 2 to the iterated range:

$$r_{it} = \left[\frac{r-1}{2} \right] + 3$$

which iterates to 4 for all $r_{initial} \leq 4$.

APPENDIX B

A QUALITATIVE EXPLANATION FOR THE ANOMALOUS MASS GAPS

Simple-blocking schemes tend to give the massless model fictitious mass-gaps, decreasing as the $-1/2$ power of the block volume; this is responsible for asymptotic exponents (γ_G in the one-variable schemes and γ_G^1 in the two-variable schemes) coming out to be $-1/2$. Why this occurs may be understood in a qualitative way as follows: consider a super-block, formed after n iterations, of volume $V = 2^n$ sites; we look at the part H_V of the original Hamiltonian that involves only fields inside this super-block, and add to it two symmetric surface terms to represent the effects of the rest of the system:[18]

$$H_V = \sum_{j=1}^{V} \frac{1}{2} p_j^2 + \sum_{j=1}^{V-1} \frac{1}{2}\left(x_{j+1} - x_j\right)^2 + \frac{\alpha^2}{2}\left(x_1^2 + x_V^2\right) \quad . \tag{B.1}$$

The freedom in choosing the surface terms stems from the arbitrary nature of the decomposition into "block energy" and "block-block interaction," pointed out in Section 2. The surface terms will cause the field x_j quantized in this volume to have an effective mass $\alpha\sqrt{2/V}$, which scales with the anomalous power $-1/2$ (α being of order unity). The particular choice $\alpha = 1$ corresponds to the choice of block Hamiltonian of Ref. 19.

APPENDIX C

We now demonstrate the method used to solve the recursion relations (4.20) for the values of Green's functions at $k = k_r$. The example to be worked out in detail is the no-shift, one look-ahead case, i.e., $\rho_n(k) \equiv 0$. For a nearest-neighbor gradient $d^{(0)}(k) = 1 - \cos k$ [Eq. (3.3) for $\mu = 0$], we find from (4.13)

$$\gamma_-^{(n)} \equiv \sqrt{3} \quad . \tag{C.1}$$

In this case, Eq. (4.20) simplifies to

$$\begin{aligned} G^{(n)}(k) &= \frac{1}{\sqrt{2}}(1+\cos k)\, G^{(n+1)}(2k) + \frac{1}{4\sqrt{3}}(1-\cos k) \quad , \\ R^{(n)}(k) &= \frac{1}{2\sqrt{2}}(1+\cos k)\, R^{(n+1)}(2k) + \frac{\sqrt{3}}{4}(1-\cos k) \quad . \end{aligned} \tag{C.2}$$

Using $1 + \cos k = 1/2\,[\sin^2 k/\sin^2(k/2)]$, we find upon iterating (C.2) ad infinitum

$$\begin{aligned} G(k) = G^{(0)}(k) &= \frac{1}{4\sqrt{3}}\left\{1-\cos k + \sum_{m=1}^{\infty}\left[1-\cos\left(2^m k\right)\right]\left(\frac{1}{2\sqrt{2}}\right)^m \frac{\sin^2\left(2^{m-1}k\right)}{\sin^2(k/2)}\right\} \\ &= \frac{1}{4\sqrt{3}}\left\{1-\cos k + \frac{4}{1-\cos k}\sum_{m=1}^{\infty}(8)^{-m/2}\sin^4\left(2^{m-1}k\right)\right\} \quad , \end{aligned} \tag{C.3}$$

$$R(k) = R^{(0)}(k) = \frac{\sqrt{3}}{4}\left\{1-\cos k + \frac{4}{1-\cos k}\sum_{m=1}^{\infty}(32)^{-m/2}\sin^4\left(2^{m-1}k\right)\right\} \quad .$$

These are nonanalytic functions, but at $k = k_r = \pi \times 2^{-r}$ the sums terminate and we obtain

$$G(k_r) = \frac{1}{4\sqrt{3}} \left\{ 1 - \cosk_r + \frac{4}{1 - \cosk_r} \sum_{m=1}^{r} (8)^{-m/2} \sin^4 \pi \times 2^{m-1-r} \right\},$$

$$R(k_r) = \frac{\sqrt{3}}{4} \left\{ 1 - \cosk_r + \frac{4}{1 - \cosk_r} \sum_{m=1}^{r} (32)^{-m/2} \sin^4 \pi \times 2^{m-1-r} \right\} . \qquad (C.4)$$

These are the types of sums that appear in all our truncation schemes. For large r, the first few terms (low m) behave approximately as a geometric series, with some ratio α. If $\alpha > 1$, the large-m part of the sum dominates, whereas if $\alpha < 1$ the low-m terms dominate. For the case at hand, $\alpha > 1$ for both sums (C.4), so they are dominated by m = r:

$$G(k_r) \sim \frac{1}{(k_r)^2} (8)^{-r/2} \sim (k_r)^{-1/2}$$

$$R(k_r) \sim \frac{1}{(k_r)^2} (32)^{-r/2} \sim (k_r)^{1/2}$$

(see Table I).

REFERENCES

1. This state is obtained by repeated application of the scale transformation; eventually all modes become "fast" and have their dynamics specified by the truncation.
2. H. R. Quinn and M. Weinstein, SLAC-PUB-2795, Phys. Rev. D25, 1661 (1982).
3. That is how we refer to the conventional blocking procedure.
4. The difference between it and its continuum counterpart is that there, the rescaled theory was equivalent to the original one, whereas here we discarded some of the physics by truncating away the fast modes.
5. In the massless theory in an infinite volume, one must block ad infinitum.
6. See Eq. (A.1).
7. It becomes a U(1) symmetry if the model is made compact, e.g., if it is made into an XY model.
8. To conserve the symmetries, this is the only block mode one can choose; x_+ and x_- have even and odd parities, respectively, so they cannot mix, and x_+ itself cannot be truncated since that would break $G(\tau)$.
9. In interaction models we expect the optimal F to be nonlinear; this may even be true for the free-field case. An explicit j dependence is desirable to study kinks.
10. We denote the volume at the n-th iteration, defined as the number of effective lattice sites, by L_n; $L_0 = L$ and due to the blocking of site pairs, $L_{n+1} = L_n/2$.

11. The umklaps also cause the breaking of the T_m symmetry, i.e., nonconservation of momentum. The nonsmoothness of G and R, inherent in blocking schemes, is evident in position-basis treatments as well [see for example Eq. (3.10) of J. Richardson and R. Blankenbecler, Phys. Rev. D20, 1351 (1979), where the mapping involves the binary digits of the position].
12. This is equivalent to the usual position basis practice of computing Green's functions at spatial separations equal to block sizes.
13. See Appendix B for a qualitative explanation of this anomaly.
14. It should be remembered that, unlike in a simple Rayleigh-Ritz variational approach, simply varying over more parameters in a look-ahead scheme is not guaranteed to improve even the energy, let alone the wave function. However, improvement in energy will occur if n_ℓ is sufficiently large.
15. For any finite mass μ, the trial Green's functions are exact at $k = 0$ for both shifted and nonshifted schemes; the real test is for $\mu \ll k \ll \pi$.
16. S. D. Drell and M. Weinstein, Phys. Rev. D17, 3203 (1978).
17. Unlike the one-variable case, that could change the results. It is equivalent to making the odd-mode mixing nonorthogonal. The re-scaling Eq. (5.7) is the optimal one in the case of the simple-blocking scheme in Ref. 16.
18. This argument is in the spirit of the Shadow Hamiltonian approach of Ref. 2, in which the parameter α would be varied over.
19. S. D. Drell, M. Weinstein, S. Yankielowicz, Phys. Rev. D16, 1769 (1977).

Table I. Results from one-variable schemes in the massless model

Scheme	n_ℓ	n_{shift}	$\rho_{g.s.}$	γ_G	r_∞
Simple-blocking without mean field	0	0	.773	- .5	0
Simple-blocking with mean field	1	0	.670	- .5	0
Adiabatic truncation schemes	1	1	.643435	- .984	- .384
	2	1	.643447	- .979	- .388
	3	1	.643425	- .987	- .380
	4	1	.643424	- .989	- .378
	5	1	.643424	- .989	- 3.78
	1	2	.643933	- .91	-
	1	∞	.643878	- .93	-
	2	2	.643399	- .997	-
	3	2	.643377	- .998	-
Exact values	-	-	.6366	-1	-

Table II. Ratios of trial to exact quantities for various masses and momenta $k_r = \pi 2^{-r}$: a) for the adiabatic truncation scheme with $n_{shift} = n_\ell = 1$, and b) for the no-shift scheme, i.e., simple blocking, with a mean-field look-ahead.

	$\frac{1}{2}\mu^2$	$\frac{\rho_{g.s.}(\text{trial})}{\rho_{g.s.}(\text{exact})}$	$\frac{G_{trial}(k_r)}{G_{exact}(k_r)}$	
			r = 5	r = 14
(a)	10	1.000095	.990	.99998
	10^{-6}	1.01	.518	.828
	10^{-9}	1.01	.518	.472
	$\frac{1}{2}\mu^2$	$\frac{\rho_{g.s.}(\text{trail})}{\rho_{g.s.}(\text{exact})}$	$\frac{G_{trial}(k_r)}{G_{trial}(k_r)}$	
			r = 5	r = 14
(b)	10	1.00025	.995	.99999
	10^{-6}	1.05	.249	.082
	10^{-9}	1.01	.249	.011

Table III. Results for the various two-variable schemes. The numbers in the first row are the ratios of trial to exact ground-state energy densities. ζ is the mixing angle of the two odd-parity modes within a block, and the γ parameters are the asymptotic exponents, defined in Eq. (5.10).

Scheme	Two-look-ahead shift-mix adiabatic truncation	No shift one-look-ahead mixing	Simple-blocking no look-aheads	Exact exponents
$\frac{\rho_{g.s.}(\text{trial})}{\rho_{g.s.}(\text{exact})}$	1.002	1.04	1.06	-
ζ	66.7°	17°	30°	-
γ_G^1	- 1.00022	- .5	- 1	- 1
γ_G^2	- .00022	1	0	0
γ_G^3	0	0	0	1
γ_R^1	.99991	.5	.5	1
γ_R^2	1	0	0	2
γ_R^3	0	0	0	3

PART III

REAL SPACE METHODS FOR THE XY MODEL

1. Introduction

We have developed several methods for treating the XY model in the Hamiltonian, or real-space, formulation. These methods fall into two (overlapping) categories.

(1) Periodic-Gaussian trial wave functions for the ground state, with variationally determined propagators.

These are similar to the wave functions used in Part I. Physical quantities are then expressed as averages in a classical, one-dimensional statistical-mechanics ensemble. The transfer matrix method, applicable for finite-range propagators, is used to evaluate the partition sums exactly; for infinite range propagators, a self-consistent mean-field method is used to approximate the sum. The transfer matrix results mimick the small-λ perturbative behavior of the exact ground state, and undergo an abrupt change at the coupling value expected from Padé approximants. This change falls short of a transition, and this is traced to the approximations made in converting the field theory to a finite-range classical ensemble.

The mean-field calculation is a dielectric-medium approximation; that is, the partition sum is interpreted as a Coulomb gas, and the screening effect taken into account via a self-consistent, separation-dependent dielectric constant. This approximation is based on the original Kosterlitz-Thouless treatment of the Euclidean XY model;[1] the differences are the lower dimensionality of the Coulomb gas (one- rather than two-dimensional), and the variational treatment of the 'force law' in the one-dimensional gas. The resulting transition, and a comparison between it and its Euclidean counterpart, furnish us with

insight into the way in which the vortex physics is reproduced in our simple trial state.

(2) Ground-state trial wave functions obtained via a real-space blocking-truncation iteration.

Here, the main challenge proved to be carrying out the renormalization-group evolution while preserving the periodicity of the global wave-function. The problem was solved by means of what we call the quasi-spin formalism. The bookkeeping of the periodicity properties, which becomes progressively more cumbersome with repeated iterations, is handled via effective spin-towers that grow in dimension as the block volume. In this formalism, iterated operators act both on continuous variables and on discrete indices, and the result is a cross between a field theory and a spin model.

Our main result in this approach is a renormalization-group scheme obtained by naive blocking of the propagator in the periodic Gaussian wave-function. This scheme, which we name for short NBPG (Naively Blocked Periodic Gaussian), is shown to be a special case of the quasi-spin formalism; thus the methods of (1) and (2) overlap. NBPG was chosen for its simplicity, and we shall see that it has several easily correctable flaws.

The scheme is studied analytically in the two perturbative regions, $\lambda << 1$ and $\lambda >> 1$, and numerically for all couplings. The result is an order-disorder phase transition, which appears to be infinite-order (in a restricted numerical sense). It is manifested as a change in the large-distance behavior of the correlation functions.

The NBPG scheme is the first real-space renormalization group we know of that gives a smooth (high-order) phase transition with nontrivial physics in both regimes. It is but one of a whole class of schemes allowed by our formalism. Its main drawback is that it is based on a naive blocking, which as seen in Part II leads to incorrect correlation functions. For the model at hand, we do not have the exact solution, but a comparison can still be made with the Euclidean path-integral transition, and also with real-space Padé results. Such a comparison shows that NBPG indeed gives the wrong correlations in both regimes. Simple ways now being studied, which will improve the situation and give a true Kosterlitz-Thouless transition, are discussed.

Part III is organized as follows: In Section 2.1, the Hamiltonian formulation of the model is presented. In Sections 2.2, 2.3 we discuss the physics in the $\lambda << 1$ and $\lambda >> 1$ regions, respectively.
In Section 3, a brief review of past work on the XY model is presented.

In Section 4 the periodic Gaussian trial wave-function is introduced, and the no-tunneling (pure-Gaussian) case is treated.
In Section 5 finite-range approximations are employed, using the transfer matrix method. In Section 6, the long-range case is treated in the dielectric medium approximation. Section 7 is devoted to iterative blocking-truncation schemes, leading up to NBPG.

2.1 The model

The model under investigation is the $(1+1)$-dimensional field theory with the Hamiltonian

$$H = \sum_{j=0}^{L-1} \frac{1}{2} p_j^2 - \lambda \sum_{j=0}^{L-1} \cos\left(x_j - x_{j+1}\right) \quad , \qquad (2.1.1)$$

where λ is the (positive) coupling, L is the volume, and the lattice spacing is set to unity. x_j is the field at the site j and p_j is the corresponding canonical momentum. We shall refer to this as the real-space XY model.

H possesses the following symmetries:

(1) The U(1) symmetry: $x_j \to x_j + \alpha$, $p_j \to p_j$, where α is a constant between 0 and 2π.

(2) Periodicity: $x_j \to x_j + 2\pi\delta_{jr}$, $p_j \to p_j$ for any given site r.

(3) Space-reflection: $x_j \to x_{-j}$, $p_j \to p_{-j}$.

(4) Field-reflection: $x_j \to -x_j$, $p_j \to -p_j$.

2.2 $\lambda \ll 1$ region

Here the field theory is best described as a spin model with infinite spin-towers. We proceed to formulate the model in this manner. Define

$$\left.\begin{aligned} J_+(j) &\equiv e^{ix_j} \quad \text{(raising operator)} \quad , \\ J_-(j) &\equiv e^{-ix_j} \quad \text{(lowering operator)} \quad , \\ J_3(j) &\equiv p_j \quad \text{(magnetic quantum-number)} \quad . \end{aligned}\right\} \qquad (2.2.1)$$

The canonical commutation relations then become

$$\left.\begin{aligned} \left[J_3(j), J_\pm(j')\right] &= \pm \delta_{jj'} J_\pm(j) \quad , \\ \left[J_\pm(j), J_\pm(j')\right] &= 0 \end{aligned}\right. \qquad (2.2.2)$$

and the Hamiltonian (2.1.1) becomes

$$H = \frac{1}{2} \sum_j J_3(j)^2 - \frac{\lambda}{2} \sum_j \left\{ J_+(j)\, J_-(j+1) + J_-(j)\, J_+(j+1) \right\} \quad . \tag{2.2.3}$$

The convenient basis of states for small λ is the discrete set of states $|\{m\}\rangle$, where m_j range over the integers. $J_3, J_\pm$ act in this basis as follows:

$$\begin{aligned} J_3(j)|\{m\}\rangle &= m_j|\{m\}\rangle \quad , \\ J_\pm(j)|\{m\}\rangle &= |\{m'\}\rangle, \quad m'_r = m_r \pm \delta_{rj} \quad . \end{aligned} \tag{2.2.4}$$

The ground state is $|\{m_j \equiv 0\}\rangle$, perturbed by massive spin-pair excitations created by the operators $J_\pm(j)\, J_\mp(j+1)$ Since exciting a spin $\pm m$ at a site requires at least m applications of the Hamiltonian, all but the lowest spins will remain inactive for small enough λ.

The main physical quantities in this region are the ground-state energy density and the mass gap. The latter is the slope of exponential falloff for the correlation function $\langle J_+(j)\, J_-(j+n)\rangle$ as $n \gg 1$. Perturbative calculations, carried out to the critical point using Padé approximants,[3] have been to date the main source of knowledge about the real-space XY model.

The correlation function,

$$C(n) \equiv \langle J_+(j)\, J_-(j+n)\rangle \tag{2.2.5}$$

is disordered in the small-λ regime, but the dual correlation,

$$\tilde{C}(n;\alpha) \equiv \left\langle \exp\left\{ i\alpha \sum_{r=j+1}^{j+n} J_3(r) \right\} \right\rangle, \text{ any } \alpha \ , \tag{2.2.6}$$

is ordered. We will concentrate for the most part on C(n), and by 'disorder' we shall generally mean 'decay of C(n) for n >> 1'.

2.3 $\lambda << 1$ region

The model in this region is a massless scalar field theory with weak quartic (and higher) self-couplings. The large coefficient λ in (2.1.1) forces the cosines to be close to 1, so $x_j \simeq 0$. It is thus convenient to rescale the fields via the cannonical transformation,

$$\begin{aligned} x_j \to x'_j &= \lambda^{+1/4}\, x_j \quad , \\ p_j \to p'_j &= \lambda^{-1/4}\, p_j \quad , \\ H \to H' &= \lambda^{-1/2}\, H \quad . \end{aligned} \tag{2.3.1}$$

The Hamiltonian becomes

$$H' = \frac{1}{2}\sum_j p_j'^2 + \frac{1}{2}\sum_j \left(x'_{j+1}-x'_j\right)^2 + \sum_j \sum_{n=2}^{\infty} \frac{(-)^{n+1}\lambda^{(1-n)/2}}{(2n)!}\left(x'_{j+1}-x'_j\right)^{2n} \tag{2.3.2}$$

We recognize the first two terms as the massless free-field theory of Part II. The third term is the self-interaction of the field, and can be treated perturbatively for $\lambda >> 1$. A demonstrative calculation to relative order $O(\lambda^{-1})$ is carried out in Appendix A. The results for ground-state energy density and long-range correlation function are, respectively,

$$\rho_{g.s.} \equiv \frac{1}{L}\langle H\rangle = \sqrt{\lambda}\left\{\frac{2}{\pi} - \frac{1}{2\pi^2}\ \lambda^{-1/2} + \lambda^{-1}\left(\frac{1}{3\pi^3} + I\right) + O\left(\lambda^{-3/2}\right)\right\}, \tag{2.3.3}$$

$$C(n) = \left\langle \cos\left(x_j - x_{j+n}\right)\right\rangle = \left(4\, e^{\gamma_E} n\right)^{-(1/2\pi)\lambda^{-1/2} - \left(1/8\pi^2\right)\lambda^{-1}} + O\left(\lambda^{-3/2}\right),$$

where γ_E is Euler's constant and I is a number given in (A.12).

The power falloff of the correlation is due to disordering caused by the fluctuations of the free field; complete order is forbidden by Coleman's theorem. As λ decreases, nonperturbative disordering will occur due to topological excitations (vortices) caused by the U(1) symmetry. Below $\lambda = \lambda_c$, the critical coupling, that disordering is sufficient to change the power-law into an exponential decay, as we saw in Section 2.2.

3. The Kosterlitz-Thouless Phase Transition: A Review of the Known

It was discovered,[1,2] in the Euclidean path-integral formulation, that the XY model undergoes a phase transition from the small-λ regime (disordered, spin-model-like) to the large-λ regime (massless field, power law correlations). We will now describe the mechanism for the transition, as a background to our real-space approach.

The Euclidean action of the planar XY model is

$$S = J \sum_{\langle ij\rangle} \cos\left(x_i - x_j\right) \tag{3.1}$$

where x_i is the classical rotor angle at site i on the square lattice, and the sum is over all nearest-neighbor pairs of sites. J corresponds

roughly to λ of the Hamiltonian model (although for an exact correspondence, H should be constructed as a transfer matrix.)

Kosterlitz and Thouless[1] noted the existence of topological vortex configurations of vorticity ± 1 (see Fig. 1), and approximated the partition integral

$$Z = \int [dx]\, e^{-\beta s} \tag{3.2}$$

by a sum over vortex configurations. The fluctuations (spin-waves) around these configurations are assumed to decouple. Namely, once the compact nature of the model was taken into account through the vortices, the cosine action was replaced by its free-field counterpart,

$$\cos(x_i - x_j) \to 1 - \frac{1}{2}(x_i - x_j)^2 \tag{3.3}$$

and x was decomposed into noninteracting vortex and spin-wave components.

The approximation (3.3) is reasonable in the strong-coupling regime, as we saw in Section 2.3.

Since the spin-waves decouple, what is left is a partition sum of a two-dimensional Coulomb gas of vortices,

$$Z \sim \sum_{\{q,r\}} \exp\left\{ -\frac{1}{2}\beta \sum_{\substack{i,j \\ (i\neq j)}} q_i q_j U(|r_i - r_j|) \right\} \tag{3.4}$$

Where $\{q,r\}$ denotes a configuration with vortices of charges q_i located at positions $\vec{r}_i$. U(r) is the interaction energy between two vortices: it is

$$U(r) = \begin{cases} -4\pi J \ln\left(\frac{r}{r_0}\right) + 2\mu & r > r_0 \\ 0 & r < r_0 \end{cases} \tag{3.5}$$

where μ plays the role of chemical potential. It is half the energy required to create a vortex pair of opposite charges at separation r_0 lattice sites. Both r_0 and μ depend on the details of the definition of a single vortex near its center; Kosterlitz and Thouless found

$$r_0 = \frac{e^{-\gamma_E}}{2\sqrt{2}} \quad (\gamma_E = \text{Euler's constant}) \ ,$$
$$\mu = 2\pi J \left(\gamma_E + \frac{3}{2} \ln 2\right) \ . \tag{3.6}$$

For low temperatures, or high couplings, the vortex gas is dilute. The energy of an isolated vortex diverges logarithmically with the volume, so only closely bound vortex pairs of opposite charges are created in the gas.

In a simple mean-field approximation, valid for large couplings, the interaction between different pairs is ignored. But as J decreases, the density of pairs increases and they become larger, so pairs overlap and screening occurs. The gas acquires a distance-dependent dielectric constant, for which a self-consistent equation can be written. Beneath a critical coupling, $J = J_c$, the vortex-vortex potential is completely screened at some distance — the correlation length (inversely related to the mass gap discussed in Section 2.2) In this regime, free vortices occur and the Coulomb gas becomes conducting. The transition is an infinite-order one, with an essential singularity at $J = J_c$. Kosterlitz and Thouless found (for $\beta = 1$)

$$J \simeq \frac{1}{\pi} 1.12 = .357 \ . \tag{3.7}$$

Jose *et al.*,[4] find, using a Villain model (that allows for spin-wave-vortex interaction), $K_c = 2/\pi = .637$; K is, however, an effective coupling and is an unknown function of J. $K(J)/J \to 1$ as $J \to \infty$.

Finally, for the real space version of the XY model, Elitzur *et al.*,[3] find* from high order strong-coupling perturbation theory with Padé approximants,

$$\lambda_{\text{critical}} \simeq .86 \tag{3.8}$$

4. The Periodic Gaussian Trial Wave Function

We have seen in Part I that for a field theory with a periodicity in the field, a periodic long-range Gaussian may serve as a reasonable trial ground-state wave function. Such a wave-function ψ combines two essential aspects of the field theory. One is the Gaussian shape of ψ near the bottoms of the degenerate potential wells, i.e., near the classical degenerate vacua. This shape describes the free-field fluctuations of the field. The other aspect is the tunneling between the degenerate vacua, which is related to semiclassical field configurations in the path-integral approach.

The two aspects couple in a nontrivial way if the Gaussian propagator is treated variationally.

From what is known about the XY model in the path integral formulation, semiclassical configurations (two-dimensional vortices) cause the phase transition. It is also known[4] that, unlike in the original dialectric-medium mean field calculation, the free-field fluctuations

*They treat the Z(N) model, but the results quoted for $n \geq 12$ may be approximately applied to the XY model, which is the $N \to \infty$ limit of Z(N).

(spin-waves) in the massless regime do couple to the vortex Coulomb gas. Thus, it is natural to use the Periodic Gaussian as a trial ground-state wave function in the real space XY model.

This trial wave function is, in the Villain form,

$$\psi\{x\} = \sum_{\substack{\{N\} \\ -\infty<N_j<\infty}} \exp\left\{-\frac{1}{2}\sum_{jj'}\left(x_j - 2\pi N_j\right)\Delta\left(j-j'\right)\left(x_{j'} - 2\pi N_{j'}\right)\right\} \quad , \qquad (4.1)$$

where the propagator components $\Delta(j)$ are variational parameters.

All operator expectation values in this state can be expressed as statistical-mechanics expectation values in a Coulomb gas, with the norm serving as the partition sum

$$\langle\psi|\psi\rangle = \text{const.}\sum_{N,N'} \exp\left\{-\pi^2\sum_{jj'}\left(N_j - N_j'\right)\Delta\left(j-j'\right)\left(N_{j'} - N_{j'}'\right)\right\} \quad . \qquad (4.2)$$

We may remove an infinite but irrelevant factor form this sum, since the expression inside the sum depends only on differences $N_j - N_j'$. We then get up to a constant

$$Z \equiv \langle\psi|\psi\rangle = \sum_{\{N\}} \exp\left\{-\pi^2\sum_{jj'} N_j\,\Delta\left(j-j'\right)N_{j'}\right\} \quad . \qquad (4.2)'$$

This is the partition sum for a Coulomb gas, with an interaction law $\Delta(j-j')$. The $N_j \neq 0$ contributions to the sum stem, quantum mechanically, from interference between two Gaussian terms in ψ with centers differing by $2\pi N_j$; this is the tunneling effect mentioned above. In order to preserve the space-reflection symmetry of the Hamiltonian, $x_j \to x_{-j}$, we must have

$$\Delta(j) = \Delta(-j) \quad . \qquad (4.3)$$

Then the wave function (4.1) respects all the symmetries of the Hamiltonian listed in Section 2.1. As we shall see, this is crucial since trial wave functions that do not obey the U(1) or periodicity symmetries give

spurious first- or second-order transitions. We next look at an example of this behavior, *the pure Gaussian case*. Consider the single (nonperiodic) Gaussian wave function,

$$\psi\{x\} = \exp\left\{-\frac{1}{2}\sum_{jj'} x_j\, \Delta(j-j')\, x_{j'}\right\} \quad . \tag{4.4}$$

This is an interesting choice because ψ becomes the exact wave function in the free field limit, $\lambda \to \infty$. We want to know how well it does for finite λ. The calculation is straightforward. Going to the momentum basis,

$$\Delta(j) = \frac{1}{L}\sum_{k} e^{ijk}\, \tilde{\Delta}(k) \quad , \tag{4.5}$$

where $k = 2\pi n_k/L$, $0 \le n_k \le L-1$. We have, in the infinite volume limit,

$$\begin{aligned} &\langle\psi|\frac{1}{2}\sum_{j} p_j^2\, |\psi\rangle = \frac{1}{4\pi}\int_0^{2\pi} dk\, \Delta(k) \quad , \\ &\langle\psi|\cos(x_j - x_{j+1})|\psi\rangle = e^{-p} \quad , \\ &p \equiv \frac{1}{8\pi}\int_0^{2\pi} dk\, (1-\cos k)\, \tilde{\Delta}^{-1}(k) \quad , \end{aligned} \tag{4.6}$$

And thus from (2.1.1),

$$\rho_{g.s.} = \frac{1}{L}\langle\psi|H|\psi\rangle = \frac{1}{4\pi}\int dk\, \tilde{\Delta}(k) - 2\, e^{-p} \quad . \tag{4.7}$$

Varying $\tilde{\Delta}(k)$ to minimize $\rho_{g.s.}$, we find the condition

$$\begin{aligned} \frac{\delta\rho_{g.s.}}{\delta\tilde{\Delta}(k)} &= \frac{1}{4\pi} - \lambda\, e^{-p}\, \frac{1}{8\pi}\, (1-\cos k)\, \tilde{\Delta}(k)^{-2} = 0 \quad , \\ \tilde{\Delta}(k) &= \sqrt{1-\cos k}\, \left(\frac{\lambda}{2}\, e^{-p}\right)^{1/2} \quad . \end{aligned} \tag{4.8}$$

Combining this with (4.6), we find a transcendental equation for the parameter p:

$$f(p) \equiv p\, e^{-p/2} = \frac{1}{\pi\sqrt{\lambda}} \quad . \tag{4.9}$$

Solutions of this equation are stationary points of $\rho_{g.s.}$, but we only want the absolute minimum of the energy density. From (4.7), (4.8),

$$\rho_{g.s.}(p;\lambda) = \frac{1}{\pi^2 p} - \lambda\, e^{-p} \quad . \tag{4.10}$$

f(p) is plotted in Fig. 2. It attains its maximal value at p = 2 where f(2) = 2/e, so (4.9) has no solutions for $\lambda < (e^2/4\pi^2) = .187$, and two solutions

$$\begin{aligned} p_1 &= p_1(\lambda) \leq 2 \quad , \\ p_2 &= p_2(\lambda) \geq 2 \quad , \end{aligned} \tag{4.11}$$

for $\lambda \geq (e^2/4\pi^2)$. From (4.9), (4.10) it is easy to prove that p_2 is a local maximum, and that the two regimes are as follows:

(1) for $\lambda < \lambda_c \equiv e/\pi^2 = .275$ the absolute minimum of $\rho_{g.s.}$ is at $p = \infty$, $\rho_{g.s.} = 0$ and $\tilde{\Delta}(k) \equiv 0$;

(2) for $\lambda > \lambda_c$ the absolute minimum is at $p = p_1(\lambda)$. $p_1(\lambda_c) = 1$, and the resulting (spurious) transition is first order.

From (4.9)-(4.10),

$$\rho_{g.s.}(\lambda) = \frac{p_1(\lambda) - 1}{\pi^2 p_1(\lambda)^2} \quad . \tag{4.12}$$

The energy density and 1/p are plotted versus λ in Figs. 3,4. Note that from (4.8), $\tilde{\Delta}(k)$ is proportional to the free-field propagator

but with a coupling-dependent coefficient. The correlation function is,

$$\begin{aligned} C(n) &\equiv \langle\psi|\cos\left(x_j - x_{j+n}\right)|\psi\rangle \\ &= \exp\left\{-\frac{1}{4}\left(\frac{\lambda}{2}\right)^{-1/2} e^{p_1(\lambda)} \int_0^{2\pi} \frac{dk}{2\pi} \frac{1-\cos(nk)}{\sqrt{1-\cos k}}\right\} \qquad (4.13) \\ &\to \text{const. } n^{\left[-(1/2\pi)\lambda^{-1/2} \exp\left\{p_1(\lambda)\right\}\right]} \text{ as } n \to \infty \quad ; \end{aligned}$$

In the $\lambda \to \infty$ limit,

$$\begin{aligned} p = p_1(\lambda) &= \frac{1}{\pi} \lambda^{-1/2} + O\left(\lambda^{-1}\right) \quad , \\ \tilde{\Delta}(k) &= \sqrt{\frac{\lambda}{2}} (1-\cos k)^{1/2} + O(1) \quad , \qquad (4.14) \\ \rho_{g.s.}(\lambda) &= -\lambda + \frac{2}{\pi} \sqrt{\lambda} + O(1) \quad . \end{aligned}$$

Comparing (4.13) with (2.3.3), we see that the power-law is the exact perturbative result to leading order in $\lambda^{-1/2}$, but not to the next order.

The spurious first order transition resulting from the use of the wave function (4.4) is due to the growing importance of inter-vacua tunneling, i.e., wave-function periodicity, as λ decreases. Below λ_c it is important enough to force ψ to be periodic, which it can only be at $\tilde{\Delta}(k) \equiv 0$; hence the sharp transition. As we shall see, this does not occur for the periodic Gaussian (4.1).

5. Transfer Matrix Method

Expectation values of operators in the trial state (4.1) are statistical-mechanics averages in a Coulomb gas, with the partition sum (4.2)'.

In this section, we will evaluate these averages for finite-range propagators using transfer matrices, and carry out a variational calculation to find the propagator that minimizes the ground-state energy. In addition to restricting the spatial range, we truncate the infinite spin-towers, in order to keep the size of the transfer matrix manageable. We go up to a range of two lattice spacings, and spin-tower dimension of seven.

Our main results are that in this approximation, the small-λ physics is qualitatively reproduced, and there is sharp change of behavior at roughly the critical coupling value expected from Padé calculations. It is not actually a phase transition, because of the spin truncation and the finite range. We will discuss methods that systematically improve upon this approximation.

The section is organized as follows. In 5.1 we employ a Poisson resummation and convert the partion sum to the basis {m}. In 5.2 we treat the zero-range (quantum-mean field) case, show that it exhibits a spurious second-order transition and find the cause of this in the violation of the U(1) symmetry by the trial state. We then switch to a new spin-basis, that is manifestly U(1)-invariant. In 5.3, we treat the zero-range mean-field case in the new basis; the spurious transition disappears. In 5.4, we improve the approximation by allowing a range of two lattice spacings, and set up the transfer-matrix formalism. We use the formalism to compute the ground-state energy, minimize it with respect to the propagator components and calculate the correlatin functions. These calculations are performed numerically. In 5.5 we

present the conclusions for this Section, and discuss mass gaps and systematic improvements of the trial ground-state.

5.1 Converting to {m} basis

Starting from (4.1), we apply a Poisson resummation by noting that for any function F,

$$\sum_{\{N\}} F\{2\pi N\} = \left(\prod_j \int_{-\infty}^{\infty} dy_j \right) \prod_j \left[\sum_{N_j=-\infty}^{\infty} \delta\left(y_j - 2\pi N_j\right) \right] F\{y\} \quad ,$$

$$2\pi \sum_{N=-\infty}^{\infty} \delta(y - 2\pi N) = \sum_{m=-\infty}^{\infty} e^{imy} \quad , \tag{5.1.1}$$

$$F\{2\pi N\} = \sum_{\{m\}} G\{m\}$$

where G is the Fourier transform of F:

$$G\{m\} = \left(\prod_j \int \frac{dy_j}{2\Pi} \exp\left\{ i m_j y_j \right\} \right) F\{y\} \tag{5.1.2}$$

We thus find a new form for ψ, the Periodic Gaussian wave-function:

$$\psi\{x\} = \sum_{\{m\}} \exp\left\{ i \sum_j m_j x_j \right\} \exp\left\{ -\frac{1}{2} \sum_{jj'} m_j \, \Delta^{-1}(j - j') \, m_{j'} \right\} , \tag{5.1.3}$$

Where Δ^{-1} is the inverse propagator. The partition sum defined by the norm of the state, (4.2)', becomes in this basis

$$Z \equiv \langle \psi | \psi \rangle = \sum_{\{m\}} \exp\left\{ - \sum m_j \, \Delta^{-1}(j - j') \, m_{j'} \right\} , \tag{5.14}$$

modulo irrelevant volume-dependent factors.

5.2 Quantum mean-field in the {m}-basis

Since in this part of the thesis we go back and forth between the quantum-mechanical formulation and the effective statistical-mechanics-problem generated by it, it is useful to point that there are two corresponding varieties of mean-field approximations.

We now restrict the inverse propagator to be zero-range:

$$\Delta^{-1}(j) = \frac{1}{\gamma} \gamma_{j0} \quad . \tag{5.2.1}$$

Then $\psi(x)$ is a product wave function,

$$\begin{aligned} \psi(x) &= \prod_j \psi_0(x_j) \quad , \\ \psi_0(x) &= \sum_{m=-\infty}^{\infty} \exp\left\{ -\frac{1}{2\gamma} m^2 \right\} \exp\left\{ imx \right\} \quad . \end{aligned} \tag{5.2.2}$$

This is a quantum mean-field trial state.

The Hamiltonian is, [(2.1.1)]

$$H = \sum_j \frac{1}{2} p_j^2 - \lambda \sum_j \cos(x_j - x_{j+1}) \quad , \tag{5.2.3}$$

and the energy density in ψ is

$$\rho_{g.s.} = \frac{1}{L} \langle \psi | H | \psi \rangle = \frac{1}{2} \frac{\langle \psi_0 | p^2 | \psi_0 \rangle}{\langle \psi_0 | \psi_0 \rangle} - \lambda \left(\frac{\langle \psi_0 | \cos x | \psi_0 \rangle}{\langle \psi_0 | \psi_0 \rangle} \right)^2 , \tag{5.2.4}$$

expressed in terms of single-site expectation values. Those can be written as sums,

$$\langle\psi|\psi\rangle = \sum_{m=-\infty}^{\infty} \exp\left\{-\frac{m^2}{\gamma}\right\} ,$$

$$\langle\psi_0|p^2|\psi_0\rangle = \sum_{m=-\infty}^{\infty} m^2 \exp\left\{-\frac{m^2}{\gamma}\right\} ,$$

$$\langle\psi_0|\cos x|\psi_0\rangle = \sum_{m=-\infty}^{\infty} \exp\left\{-\frac{m^2}{2\gamma} - \frac{(m+1)^2}{2\gamma}\right\} ,$$

$$= \exp\left\{-\frac{1}{4\gamma}\right\} \exp\left\{-\sum_{m=-\infty}^{\infty} \frac{\left(m+\frac{1}{2}\right)^2}{\gamma}\right\} , \qquad (5.2.5)$$

and (5.2.4) gives us:

$$\rho_{g.s.} = \frac{1}{2} \frac{\sum_{m=-\infty}^{\infty} m^2 \exp\left\{-\frac{m^2}{\gamma}\right\}}{\sum_{m=-\infty}^{\infty} \exp\left\{-\frac{m^2}{\gamma}\right\}} - \lambda \exp\left\{-\frac{1}{2\gamma}\right\} \left[\frac{\sum_{m=-\infty}^{\infty} \exp\left\{-\frac{\left(m+\frac{1}{2}\right)^2}{\gamma}\right\}}{\sum_{m=-\infty}^{\infty} \exp\left\{-\frac{m^2}{\gamma}\right\}}\right]^2 . \qquad (5.2.6)$$

This is to be minimized with respect to γ. The result for $z = \exp\{-1/\gamma\}$ and $\rho_{g.s.}$ as a function of λ is shown in Figs. 5,6. For $\lambda < \lambda_c = 1/4$, z vanishes and $\rho_{g.s.} = 0$. By expanding $\rho_{g.s.}$ in powers of z we find,

$$\rho_{g.s.}(z;\lambda) = (1-4\lambda)z + (16\lambda - 2)z^2 + O(z^3) \qquad (5.2.7)$$

and for $\lambda = (1/4) + \varepsilon$ this attains a minimum at

$$z = z_{min} = \varepsilon + O(\varepsilon^2) ,$$

$$\rho_{g.s.} = -2\varepsilon^2 + O(\varepsilon^3) \sim -2(\lambda - \lambda_c)^2 . \qquad (5.2.8)$$

Thus the mean-field state exhibits a sharp (second-order) transition at $\lambda_c = 1/4$ and a trivial behavior for $\lambda < \lambda_c$. It has neither the correct massive regime nor the infinite-order transition. In the $\lambda > \lambda_c$ regime, that should be massless, it does not give the correct physics either.

The above behavior does not depend on the particular wave-function form we use for ψ_0. As a demonstration of this, we chose

$$\psi_0(x) = 1 + 2z_1 \cos x + 2z_2 \cos(2x) \tag{5.2.9}$$

and solved for z_1, z_2 variationally. The results for z_1, z_2 are shown in Fig. 7.

The failure of the product trial state (5.2.2) to reproduce the spin-excitation physics in the small-coupling domain is due to the fact that ψ contains nonphysical excitations. For instance, the configuration

$$|\{m\}\rangle = |00 \ldots 010 \ldots 0\rangle \tag{5.2.10}$$

is not created by the Hamiltonian; as mentioned in Section 2.2, only configurations with total spin $\Sigma\, m_j = 0$ are created. The creation of 'good' configurations is accompanied by 'bad' ones, and for small enough λ this does not lower the energy and so the optimal $\psi_0(x)$ is a constant.

Another way to state the problem is that since $\sum_j m_j \neq 0$ the U(1) symmetry of the model is violated by ψ. We proceed to restore the invariance, by making m_j a gradient:

$$m_j = \ell_j - \ell_{j-1} \quad , \qquad -\infty < \ell_j < \infty \qquad . \tag{5.2.11}$$

The periodic Gaussian (5.1.3) now becomes

$$\psi\{x\} = \sum_{\{\ell\}} \exp\left\{ i \sum_j \ell_j (x_j - x_{j+1}) \right\} \exp\left\{ -\frac{1}{2} \sum_{jj'} \ell_j \Delta_1^{-1}(j-j') \ell_{j'} \right\} ,$$

$$\Delta_1^{-1}(j) = 2\Delta^{-1}(j) - \Delta^{-1}(j+1) - \Delta^{-1}(j-1) \quad . \tag{5.2.12}$$

It is now manifestly invariant under the global U(1) transformation,

$$x_j \to x_j + \alpha \quad . \tag{5.2.13}$$

5.3 Mean-field in $\{\ell\}$ basis

In this case we choose Δ_1^{-1} to be of zero range,

$$\Delta_1^{-1}(j) = \zeta \delta_{jo} \quad . \tag{5.3.1}$$

Then ψ is again a product [(5.2.12)]

$$\psi\{x\} = \prod_j \psi_0(x_j - x_{j+1}) \quad , \tag{5.3.2}$$

$$\psi_0(y) = \sum_{\ell=-\infty}^{\infty} \exp\left\{ i\ell y \right\} \exp\left\{ -\frac{1}{2} \zeta \ell^2 \right\} \quad .$$

We define new canonical variables

$$y_j = x_j - x_{j+1} \quad , \tag{5.3.3}$$

$$p_j = p_y(j) - p_y(j-1) \quad .$$

The Hamiltonian becomes

$$H = \frac{1}{2} \sum_j \left[p_y(j) - p_y(j-1) \right]^2 - \sum_j \cos y_j \quad . \tag{5.3.4}$$

The computation of the energy proceeds as in (5.2). We find from (5.3.2)-(5.3.4)

$$\rho_{g.s.}(\zeta;\lambda) = \frac{\sum_{\ell=-\infty}^{\infty} \ell^2 \exp\left\{-\zeta \ell^2\right\}}{\sum_{\ell=-\infty}^{\infty} \exp\left\{-\zeta \ell^2\right\}} - \lambda e^{-\zeta/4} \frac{\sum_{\ell=-\infty}^{\infty} \exp\left\{-\zeta\left(\ell+\frac{1}{2}\right)^2\right\}}{\sum_{\ell=-\infty}^{\infty} \exp\left\{-\zeta \ell^2\right\}} \tag{5.3.5}$$

And this should be minimized with respect to ζ. The results for $z = e^{-\zeta}$ and $\rho_{g.s.}$ are shown in Figs. 8,9; note that the spurious transition disappeared, and there is now no transition at all. The correlation function is:

$$\langle\psi|\cos\left(x_j - x_{j+n}\right)|\psi\rangle = \alpha^n \quad ,$$

$$\alpha = \frac{\langle\psi_0|\cos y|\psi_0\rangle}{\langle\psi_0|\psi_0\rangle} = z^{1/4} \frac{\sum_{\ell=-\infty}^{\infty} z^{[\ell+(1/2)]^2}}{\sum_{\ell=-\infty}^{\infty} z^{\ell^2}} \quad , \tag{5.3.6}$$

and α varies smoothly between 0 and 1 (Fig. 10); in order for the massless regime to exist, α must be 1 above some λ value.

5.4 Range 2: the transfer matrix

We next improve upon the mean-field approximation by allowing the inverse propagator to be of range two:

$$\Delta_1^{-1}(j) = 2\beta\delta_{j,0} + \frac{1}{2}\delta_1\delta_{j,\pm1} + \frac{1}{2}\delta_2\delta_{j,\pm2} \tag{5.4.1}$$

The partition sum in the $\{\ell\}$ basis is [(5.2.12)]

$$Z \equiv \langle\psi|\psi\rangle = \sum_{\{\ell\}} \exp\left\{-\sum_{jj'} \ell_j \, \Delta_1^{-1}(j-j') \, \ell_{j'}\right\}$$

$$= \sum_{\{\ell\}} \exp\left\{-2\beta \sum_j \ell_j^2 - \delta_1 \sum_j \ell_j \ell_{j+1} - \delta_2 \sum_j \ell_j \ell_{j+2}\right\} \quad . \tag{5.4.2}$$

We will truncate the ℓ-spin-towers, so that only those terms in the wave function with

$$-\ell_c \le \ell \le \ell_c \tag{5.4.3}$$

are left. We want to write the configuration sum (5.4.2) in a form where a transfer matrix may be defined, i.e., the exponent must contain only nearest-neighbor correlations. This can be done by grouping the sites into pairs; let sites $(2j, 2j+1)$ belong to the j-th block, and define some block spin variable L, that has a one-to-one correspondence with a pair of spins (ℓ_{2j},ℓ_{2j+1}); specifically, we choose

$$L_j = 1 + \ell_{2j} + \ell_c + \left(2\ell_c+1\right)\left(\ell_{2j+1} + \ell_c\right) \equiv L\left(\ell_{2j},\ell_{2j+1}\right) \quad ,$$

$$1 \le L_j \le \left(2\ell_c+1\right)^2 \quad . \tag{5.4.4}$$

The range-two site-site interaction in (5.4.2) now becomes a nearest neighbor block-block interaction:

$$Z = \sum_{\{L\}} \prod_j P\left(L_j, L_{j+1}\right) \quad , \tag{5.4.5}$$

where $P(L,L')$ are the elements of the $(2\ell_c+1)$-dimensional transfer matrix $\overleftrightarrow{P}$. It is defined as follows:

$$L = L(\ell_1, \ell_2)$$

$$L' = L(\ell_1', \ell_2')$$

$$P(L,L') = \exp\left\{-\beta\left(\ell_1^2 + \ell_2^2 + \ell_1'^2 + \ell_2'^2\right)\right. \tag{5.4.6}$$

$$\left. - \frac{1}{2}\,\delta_1\left(\ell_1\ell_2 + \ell_1'\ell_2' + 2\ell_2\ell_1'\right) - \delta_2\left(\ell_1\ell_1' + \ell_2\ell_2'\right)\right\}$$

The only aspects of $\overleftrightarrow{P}$ that will enter the equations are its dominant (highest in magnitude) eigenvalue, p_1, and its corresponding eigenvector $\vec{v}_1$. $\overleftrightarrow{P}$ is in general not symmetric, but it has the following property:

$$P(L,L') = P\left(L'^s, L^s\right) \quad , \tag{5.4.7}$$

where L^s is the spatial reflection of L:

$$L = L(\ell_1, \ell_2),\ L^s = L(\ell_2, \ell_1) \quad . \tag{5.4.8}$$

This property is due to the space-reflection symmetry of the model.

If we define for the vector $\vec{v}_1$ a corresponding vector,

$$v_1^s(L) = v_1\left(L^s\right) \quad , \tag{5.4.9}$$

then the dominant part of $\overleftrightarrow{P}$ is

$$\overleftrightarrow{P}_{\text{dominant}} = p_1 \vec{v}_1 \vec{v}_1^s \quad . \tag{5.4.10}$$

The normalization condition is

$$v_1^s \cdot v_1 = 1 \quad . \tag{5.4.11}$$

With these definitions, the partition sum is simply $(p_1)^{\text{volume}}$.

Next we calculate operator expectation values. For an operator $\exp\{i \sum_j q_j y_j\}$, where q_j are integers, we find

$$\left\langle \psi \middle| \exp\left\{ i \sum_j q_j y \right\} \middle| \psi \right\rangle = \sum_{\{\ell\}} \exp\left\{ -\frac{1}{2} \sum_{jj'} (\ell_j + q_j) \Delta_1^{-1}(j-j')(\ell_{j'} + q_{j'}) \right.$$

$$\left. - \frac{1}{2} \sum_{jj'} \ell_j \Delta_1^{-1}(j-j') \ell_{j'} \right\}$$

$$= \exp\left\{ -\frac{1}{2} \sum_{jj'} q_j \Delta_1^{-1}(j-j') q_{j'} \right\} \tag{5.4.12}$$

$$\times \sum_{\{\ell\}} \exp\left\{ -\sum_{jj'} \ell_j \Delta_1^{-1}(j-j') \ell_{j'} - \sum_j \varepsilon_j \ell_j \right\},$$

where

$$\varepsilon_j = \sum_{j'} \Delta_1^{-1}(j-j') q_{j'} \quad . \tag{5.4.13}$$

For the nearest-neighbor correlation, we find, by rewriting (5.4.12) in terms of block spin variables,

$$\left\langle \cos(x_j - x_{j+1}) \right\rangle = \frac{\langle \psi | \cos y_j | \psi \rangle}{\langle \psi | \psi \rangle} = e^{-\beta \frac{1}{p_1^2} \vec{v}_1^{\,s} \cdot \overleftrightarrow{A} \cdot \overleftrightarrow{B} \cdot \vec{v}_1} \quad , \tag{5.4.14}$$

where $\overleftrightarrow{A}$, $\overleftrightarrow{B}$ are defined in (B.1). Similarly,

$$\left\langle \frac{1}{2} \left[p_y(j) - p_y(j-1) \right]^2 \right\rangle = \vec{v}_1^{\,s} \cdot \overleftrightarrow{D} \cdot \vec{v}_1 \quad , \tag{5.4.15}$$

where

$$D(L,L') = \frac{1}{2} (\ell_1 - \ell_2)^2 \delta_{LL'} \quad . \tag{5.4.16}$$

Thus the trial energy is

$$\rho_{g.s.} = \vec{v}_1^{s} \cdot \overleftrightarrow{D} \cdot \vec{v}_1 - \lambda e^{-\beta \vec{v}_1^{s}} \overleftrightarrow{A} \cdot \overleftrightarrow{B} \cdot \vec{v}_1 \Big/ (p_1)^2 \qquad (5.4.17)$$

We have minimized $\rho_{g.s.}$ with respect to the propagator parameters β, δ_1 and δ_2, for spin cutoffs $\ell_c = 1$, 2 and 3. The results for these parameters and the energy are given in Figs. 11-14. As ℓ_c increases, a change of behavior develops for these quantities at $\lambda \simeq .8$. We refer to this as the 'turnover'.

We have computed the large-distance behavior of the correlation functions C and $\tilde{C}$ (see Section 2.2). For C(n), we use (5.4.12); the result in the transfer matrix language is

$$\left\langle \cos\left(x_j - x_{j+n}\right)\right\rangle \underset{n>>1}{\sim} \left[\left(\frac{p_E}{p_1}\right)^{1/2} \exp\left\{-\left(\beta + \frac{\delta_1}{2} + \frac{\delta_2}{2}\right)\right\}\right]^n \equiv \alpha^n \quad , \qquad (5.4.18)$$

where p_E is the leading eigenvalue of the matrix $\overleftrightarrow{E}$ [(B.7)]. The derivation of (5.4.18) is given in Appendix B. In Fig. 15, α is plotted versus λ for $\lambda_c = 2,3$. α undergoes a smooth, but rapid, increase at the turnover and reaches a constant value in the large λ limit; this value increases with ℓ_c and will tend toward unity as $\ell_c \to \infty$; the $\lambda > .8$ regime is thus the one where C(n) is more ordered, as expected.

For the dual correlation, we find for large n, (ε arbitrary)

$$\left\langle \exp\left\{ i\varepsilon \sum_{r=j+1}^{j+n} p_r \right\} \right\rangle = \left\langle \exp\left\{ i\varepsilon \left[p_y(j+n) - p_y(j) \right] \right\} \right\rangle \simeq \left[\eta(\varepsilon)\right]^2 , \qquad (5.4.19)$$

where

$$\eta(\varepsilon) = \left\langle \exp\left\{ i\varepsilon \cdot p_y(j) \right\} \right\rangle \quad .$$

α and η (π) are plotted against λ for $\ell_c = 2$ in Fig. 16. It drops sharply at the turnover, in accord with the fact that $\tilde{C}(\eta,\varepsilon)$ is more ordered in the small λ regime.

5.5 Possible Improvements

We have seen that a range-two inverse propagator in the ℓ-spin (or y_j) basis is sufficient to see a smooth but rapid turnover, associated with an increase of order in $C(n)$, and a decrease of order in the dual $\tilde{C}(n)$. This turnover, however, is not yet a phase transition; $C(n)$, for instance, decays exponentially for all λ. The calculations we have done indicate that as ℓ_c and the range r increase, the turnover becomes sharper, but it is unlikely there will be a transition as long as r is finite. In this the XY model differs from simpler models such as the one treated in Part IV; there the transition exists in the simplest approximations.

We regard our transfer-matrix exercise as a first approximation that can be improved upon systematically. These improvements are along two main lines.

(1) Within the Periodic Gaussian approximation. Here, we may add a range > 2 piece to $\Delta_1^{-1}(j)$ and treat it perturbatively. We can also increase the spin-tower size ℓ_c to infinity, without having to diagonalize the matrices of absurdly high dimensions, by means of the following approximation. The transfer matrix formulation is really a reduction of the one-dimensional statistical-mechanics problem to a zero-dimensional quantum-mechanical problem, with a Hamiltonian matrix,

$$\overleftrightarrow{h} = \ell n \overleftrightarrow{P}$$

acting on the ℓ-spin basis. We may therefore apply a Rayleigh-Ritz variational approximation, i.e., pick a trial form for $\vec{v}_1$, with a small number of parameters and vary them to maximize $\langle P \rangle$. Thus we can avoid diagonalizing P. Note, however, that this approximation will no longer yield an upper bound for the energy $\langle H \rangle$, only for the free energy of the statistical-mechanics problem; and the latter does not have a direct physical meaning for the XY model.

(2) Improvements outside the Periodic Gaussian (PG) approximation. These might include an expansion in spin and/or kink excitations around ψ_{PG}. A useful exercise in that direction would be a calculation of mass gaps of isolated plane wave excitations. A moving kink, for instance, has the wave function

$$|\{\theta\}\rangle \propto \sum_j \exp\left\{ i \sum_{n=0}^{n_1} \theta_{j+n} P_y(j) \right\} |\psi_{PG}\rangle \qquad (5.5.1)$$

where $\theta_j, 0 \le j \le n_1$, is some kink configuration of size n_1. A stationary kink always lies higher in energy than the trial ground-state (see Appendix). The mass gap of the moving kink may be negative for some coupling regions, thus signaling the inadequacy of the trial ground state.

6. Dielectric Medium Mean-Field

6.1 Counting vortices

It was pointed out in Section 4 that the {N} configuration in the partition sum (4.2)' correspond to semiclassical vortex configurations in the Euclidean formulation. In this Section, we will apply the self-consistent mean-field approximation, originally used in Ref. 4 for the two-dimensional vortex gas, to our one-dimensional gas. In order to do that, it is useful to make the correspondence between {N} and vortices more specific.

Consider a vortex-antivortex pair separated by a distance R in the spatial direction of the space-time plane at a common time $t = t_0$. Assume, along with Ref. 1, that the field configurations x_j of the two monopoles are additive. Then x is zero far from the vortices and is maximal (2π) along the line sigment AB between them. This corresponds to an $N_j \equiv 0$ vacuum before and after t_0, and a tunneling in and out of the degenerate vacuum,

$$N_j = \begin{cases} 1 & 1 \le j \le R \\ \\ 0 & \text{otherwise} \end{cases} , \qquad (6.1.1)$$

occuring at $t = t_0$. Thus, the gradient of N_j,

$$M_j \equiv N_j - N_{j+1} = \begin{cases} -1 & \text{at } j = 0 \\ +1 & \text{at } j = R \\ \\ 0 & \text{otherwise} \end{cases} \qquad (6.1.2)$$

reproduces the vortex charge distribution for the pair.

The above is no more than a heuristic argument, but it is justified *a posteriori* by the logarithmic behavior of the interaction law between M_j charges, as we now show.

The {N} partition sum is [(4.2)'],

$$Z = \sum_{\{N\}} \exp\left\{ - \pi^2 \sum_{jj'} N_j \, \Delta(j-j') \, N_{j'} \right\} \quad . \tag{6.1.3}$$

Let $\tilde{\Delta}(k)$ be the momentum-basis propagator defined by (4.5), and let us define a new propagator

$$\Delta_1(j) = \frac{1}{L} \sum_{k \neq 0} \frac{\tilde{\Delta}(k)}{2(1-\cos k)} \, e^{ikj} \tag{6.1.4}$$

then Z is rewritten in terms of the M_j charges as follows:

$$Z = \sum_{\substack{\{M\} \\ -\infty < M_j < \infty}} \exp\left\{ - \pi^2 \sum_{jj'} M_j \, \Delta_1(j-j') \, M_{j'} \right\} \tag{6.1.5}$$

Note that Δ_1 is the same as that defined in (5.2.12).

The propagator $\Delta(j)$ should be determined variationally; but if we use the pure-Gaussian result [(4.8)], valid for $\lambda >> \lambda_c$,

$$\tilde{\Delta}(k) \propto \sqrt{\lambda} \, \sqrt{1-\cos k} \quad , \tag{6.1.6}$$

we find

$$\begin{aligned} \tilde{\Delta}_1(k) &\propto \frac{\sqrt{\lambda}}{\sqrt{1-\cos k}} \quad , \\ \Delta_1(j) &\propto \sqrt{\lambda} \, \ell n \, (j) \quad . \end{aligned} \tag{6.1.7}$$

Thus the Coulomb gas of the M charges has a logarithmic interaction law, as the two-dimensional vortex gas does. We may think of the {M} configurations as one-dimensional time slices of the vortex gas. Due to the logarithmic interaction law, we may apply the approach of Ref. 1 to our one-dimensional gas.

6.2 Self-consistent mean-field

In this Section we will apply the method described in Section 2.4 to the partition sum (6.1.15). Following the discussion of Section 6.1, we shall refer to the M configurations as 'vortices'.[5] We truncate the allowed M_j values to be -1, 0 and 1:

$$-1 \leq M_j \leq 1 \quad . \tag{6.2.1}$$

For large coupling λ, the Coulomb-gas coupling constant J is [(6.1.7)]

$$J \propto \sqrt{\lambda} \quad , \quad \lambda >> 1 \quad . \tag{6.2.2}$$

There is a long-range logarithmic attraction between vortices, and they are created in pairs [since the energy of an isolated vortex diverges as log (L)]. The chemical potential per pair is proportional to J, so the gas is dilute for large λ.

The residual interaction between vortex pairs is small, so they may be treated in a mean field approximation. But as λ decreases, the pairs grow in size and density, and begin to overlap and screen each other. We separate the treatment of the screening phenomenon into three steps.

(1) Independent-pair approximation: The vortex-antivortex pairs are treated as independent, and their average density distribution is computed as a function of their size.

(2) Polarization: A vortex-antivortex pair, treated as external charges, polarizes the smaller pairs lying between them.

(3) Screening: The polarized pairs partially cancel the interaction energy of the external charges, thus modifying $\Delta_1(j)$ into an effective screened propagator, $\Delta_s(j)$.

Independent-pairs. The Boltzmann factor for vortex-antivortex pairs a distance j lattice sites apart is

$$Z(j) = \exp\left\{ - 2\pi^2 \left[\Delta_1(0) - \Delta_1(j)\right]\right\} \quad , \qquad (6.2.3)$$

and this is also the density of pairs of separation j; the latter follows from the Independent pair assumption, since the pairs then obey a Poisson distribution.

Polarization. Consider two charges, a vortex at site J and an antivortex at site J'.

$$M_J = +1, \quad M_{J'} = -1, \quad J < J' \quad . \qquad (6.2.4)$$

We will denote this pair as (J,J'), and treat it as external. Let us define as a 'small' pair (j, j+r) one lying between the two external charges,

$$J < j \ , \ (j+r) < J' \quad \text{where } r << (J' - J) \ . \qquad (6.2.5)$$

The small pair is polarized by the interaction energy,

$$\mathcal{E}(j,r) = 2\pi^2\left[\Delta_1(j-J) - \Delta_1(j-J') - \Delta_1(j'-J) + \Delta_1(j'-J')\right]$$
$$\simeq -2\pi^2 r \frac{\partial}{\partial j}\left[\Delta_1(j-J) - \Delta_1(j-J')\right] \quad , \tag{6.2.6}$$

between it and the external charges. Without the external charges there are equal numbers of pairs $(j-r, j)$ and $(j, j+r)$ with opposite orientations: with the external charges, the average densities of such pairs are

$$\rho_{\pm}(r;j) = \frac{2z(r)\exp\{\mp\varepsilon(r)\}}{\exp\{\varepsilon(r)\} + \exp\{-\varepsilon(r)\}} \text{ , for pairs } (j,\ j\pm r) \text{ .} \tag{6.2.7}$$

The average interaction energy per unit volume among 'small' pairs $(j,\ j\pm r)$ of all sizes r, and the external pair, is [(6.2.3)-(6.2.7)]

$$\langle E(j)\rangle = \sum_r \left[\ \varepsilon(r)\rho_+(r;j) - \varepsilon(r)\rho_-(r;j)\ \right]$$
$$= -2\sum_r z(r)\ \varepsilon(r)\ \tanh\varepsilon(r) \tag{6.2.8}$$
$$\simeq -8\left(\sum_{r=1}^{J'-J} r^2\, z(r)\right)\left(\frac{\partial}{\partial j}\left\{\pi^2\left[\Delta_1(j-J) - \Delta_1(j-J')\right]\right\}\right)^2 \quad .$$

The r sum is cut off at $r = J' - J$, since the strongest polarization is in the region between the two external charges. The total energy, summed over the position j of the small pair, is

$$\left\langle E_{\text{total}}\right\rangle \simeq -8\pi^4 \sum_{r=1}^{J'-J} r^2 z(r) \sum_{j=J}^{J'} \left\{\frac{\partial}{\partial j}\left[\Delta_1(j-J) - \Delta_1(j-J')\right]\right\}^2 \quad . \tag{6.2.9}$$

Screening. The interaction energy between the external charges and the small pairs lowers the energy of the external pair, $2\pi^2[\Delta_1(0) - \Delta_1(j)]$, to an effective $2\pi^2[\Delta_s(0) - \Delta_s(j)]$, where $\Delta_s(j)$ is a screened propagator. Since the 'small' pairs are in turn screened by yet smaller pairs, one should replace $\Delta_1(j)$ by $\Delta_s(j)$ in (6.2.9) to obtain a self-consistent approximation for the screening effect. Thus we find,

$$K_s(J'-J) = K_1(J'-J) - 4\left[\sum_{r=1}^{J'-J} r^2 z(r)\right] \sum_{j=1}^{J'-J} \left\{ \frac{\partial}{\partial j} \left[K_s(j-J) - K_s(j-J')\right] \right\}^2 ,$$

or, if we set $J = 0$ and rename some dummy indices:

$$K_s(j) = K_1(j) - 4\left[\sum_{r=1}^{j} r^2 \exp\left\{-2K_s(j)\right\}\right] \sum_{r=1}^{j} \left\{ \frac{\partial}{\partial r} \left[K_s(r) - K_s(j-r)\right] \right\}^2 , \tag{6.2.10}$$

We have defined for convenience the subtracted propagators,

$$\begin{aligned} K_1(j) &= \pi^2\left[\Delta_1(0) - \Delta_1(j)\right] \quad , \\ K_s(j) &= \pi^2\left[\Delta_s(0) - \Delta_s(j)\right] \quad . \end{aligned} \tag{6.2.11}$$

The equation (6.2.10) may be solved iteratively, starting from the initial condition $K_s(1) = K_1(1)$ and incrementing the vortex-antivortex separation, j, by one at each step. The input to the equation is the unscreened propagator $K_1(j)$, which is to be determined variationally. We next discuss the solution of the mathematical problem formulated heretofore.

6.3 Solution of the problem

The variational mean-field problem as formulated so far consists of the following steps:

A) the bare (unscreened) propagator, $K_1(j)$, is parameterized with a small number of variational parameters;

B) the self-consistency equation (6.2.10) is solved, and the screened propagator $K_s(j)$ is determined as a function of the variational parameter; and

C) the quantum mechanical ground-state energy and correlation functions are computed in the dialectric-medium approximation, and $\rho_{g.s.}$ minimized with respect to the variational parameters.

A. Parameterization. We parameterize $\tilde{\Delta}(k)$ to be a constant times the free-field propagator, following the pure-Gaussian form (4.8):

$$\tilde{\Delta}(k) = \sqrt{1-\cos k}\,\left(2\lambda\, e^{-p}\right)^{1/2} \quad , \tag{6.3.1}$$

but where $p = p(\lambda)$ is not necessarily the function determined in the pure-Gaussian computation. It is the propagator in the {N} (or {x}) basis, governing the partition sum (4.2)'. Thus the {M} (or {y})-basis propagator $\Delta_1(j)$ is [Eqs. (5.2.12), (6.1.5)]

$$\begin{aligned}\Delta_1(j) &= \frac{1}{2\pi}\int_0^{2\pi} dk\ \frac{\tilde{\Delta}(k)}{2(1-\cos k)}\ e^{ijk} \\ &= \left(\frac{\lambda e^{-p}}{2}\right)^{1/2}\ \frac{1}{2\pi}\ \int_0^{2\pi} dk\, \frac{e^{ikj}}{\sqrt{1-\cos k}} \quad .\end{aligned} \tag{6.3.2}$$

Therefore from the definition (6.2.11),

$$K_1(j) = -\frac{\pi}{4}\left(2\lambda\, e^{-p}\right)^{1/2} \int_0^{2\pi} dk\, \frac{1}{\sqrt{1-\cos k}}\left(e^{ikj}-1\right) \quad . \qquad (6.3.3)$$

It is straightforward to show that

$$\int_0^{2\pi} dk\, \frac{1}{\sqrt{1-\cos k}}\left(e^{ikj}-1\right) = -4\sqrt{2}\sum_{m=0}^{j-1}\frac{1}{2m+1} \quad , \qquad (6.3.4)$$

so the input (unscreened) propagator for Eq. (6.2.10) is

$$K_1(j) = 2\pi\left(\lambda\, e^{-p}\right)^{1/2}\sum_{m=0}^{j-1}\frac{1}{2m+1} \quad . \qquad (6.3.5)$$

The asymptotic behavior of this for large distances j is

$$K_1(j) \xrightarrow[j \gg 1]{} \pi\left(\lambda\, e^{-p}\right)^{1/2}\left[\ell n(j) + \gamma_{Euler} + 2\,\ell n\, 2\right] \quad . \qquad (6.3.6)$$

B. *Solution of self-consistency equation*. We have solved (6.2.10) numerically, and also found an approximate analytical solution; we used (6.3.5) for the bare propagator. We now discuss the behavior of the equation as a function of the effective coupling $\lambda' = \lambda e^{-p}$, without specifying λ' as a function of λ at this point. The following facts were found from a combination of analytical and numerical methods.

For large λ', the Boltzmann factor $z = \exp\{-2K_s(j)\}$ supresses the screening correction to the propagator as $\exp\{-\text{const}\sqrt{\lambda}\}$, so $K_s(j) \simeq K_1(j)$. For finite λ' above a critical value λ'_c, $K_s(j) \xrightarrow[j \gg 1]{} K_1(j) + c_0$, where c_0 is a negative constant. Therefore the screening is additive, rather than the multiplicative screening at large separations that one would expect in a dielectric medium.

The multiplicative screening does occur in the two-dimensional (Euclidean) screening equation (Ref. 1); this can be seen in the two-dimensional version of (6.2.10).[6] The question arises, how do we recover the multiplicative screening that exists in the Euclidean calculation, in our real-space calculation. The answer is that the variational parameter p, which as we saw in Section 4 is greater than one in the $\lambda > \lambda_c$ regime, causes the effective coupling λ' to be lower than λ, and so long-range screening in the massless regime is recovered through the variational parameter. The numerically determined $c_0(\lambda')$ is plotted in Fig. 17.

Below $\lambda' = \lambda_c' \simeq .24$, the screening is sufficiently strong to make $K_s(j)$ go negative above a certain distance $j = j_1(\lambda')$; j_1 may be thought of as inverse mass gap. Unlike in the Euclidean calculation, $j_1(\lambda')$ does not possess an essential singularity at $\lambda' = \lambda_c'$, but rather diverges as a (noninteger) inverse power:

$$j_1(\lambda') \simeq \left(\lambda' - \lambda_c'\right)^{-\eta} , \quad \eta \simeq 10 \quad .$$

$j_1(\lambda')$ up to $\lambda' = .1$ is shown in Fig. 18. Note that $j_1(\lambda')$ might have an essential singularity, depending on what the function $\lambda'(\lambda)$ is.

Figure 19 shows the bare and screened propagators for $\lambda' = .19$; note the precipitous drop of $K_s(j)$. The correlation function is approximately given by (4.13).

C. Minimization of energy. If we use the function $p(\lambda)$ determined in the pure-Gaussian variational calculation (Section 4), we get the effective coupling $\lambda'(\lambda)$ plotted in Fig. 20. At $\lambda = \lambda_c = .44$, $\lambda'(\lambda) = .24$, so λ_c is the critical point in this approximation.

Better results for both λ_c and the $(\lambda - \lambda_c)$ dependence of physical quantities near the transition would probably result, if $p(\lambda)$ were redetermined variationally in the framework of the dielectric-medium approximation. Our result for $\rho_{g.s.}(p;\lambda)$ is

$$\rho_{g.s.}(p;\lambda) = \frac{\sqrt{\lambda'}}{\pi} - 2\pi^2 \lambda' S - \lambda\{1 - 8S\} \exp\left\{ - \frac{1}{\pi\sqrt{\lambda'}} \right\} \quad ,$$

where S is the sum

$$S = \sum_{j=1}^{\infty} \exp\left\{-2K_s(j)\right\} \quad .$$

The minimization of $\rho_{g.s.}$ with respect to p has not yet been done.

7. Renormalization Group Approach

We have seen in Section 5 that increasing the range of the propagator improves the ground-state wave-function, and that an infinite range is probably needed to get an actual phase transition. In this section, we will study trial wave functions obtained by iterative blocking-truncation schemes. These wave functions have built into them infinite range effects, and so furnish a realistic picture of the transition.

One could block the model in the spin-model formulation of the model (Section 2.2) and keep a small number of spin-states per block; that would, however, not suit our purpose. We have sought an approach that makes the physics in both the massive and massless regimes equally transparent. As λ increases, more and more states in the spin-towers become active, and in order to gain insight into which states should be truncated, we need a continuous variable (Schrodinger) picture. In the

$\lambda \to \infty$ limit, infinite $\{\ell\}$- spin towers must be kept in order to get $\alpha \to 1$ (α is the correlation parameter; see Section 5).

However, ordinary continuous-variable blocking, or even the kind developed in Part II, must fail for the XY model, due to its periodicity symmetry; this is shown in Section 7.1. We were thus led to develop blocking schemes that use a hybrid spin variable-continuous variable basis; this is what we call the quasi-spin formalism. This formalism is developed in Section 7.2. In Sections 7.3-7.4 we return to the periodic-Gaussian wave function of Section 4 and show how, with a naively blocked propagator, it becomes a special case of the quasi-spin formalism. We refer to such schemes as naively-blocked periodic-Gaussian, or NBPG schemes for short. In Section 7.5 we report the results of solving the renormalization group equations for the NBPG scheme. The solution is performed analytically for the regions $\lambda << 1$ and $\lambda >> 1$, and numerically for all values of the coupling. The resulting model for the transition is discussed. In Section 7.6, we point out several ways to improve the NBPG scheme.

7.1 Inadequacy of standard truncation

We want a blocking scheme for the Hamiltonian [(2.2.1)]

$$H = \sum_j \frac{1}{2} p_j^2 - \lambda \sum_j \cos\left(x_j - x_{j+1}\right) \quad . \tag{7.1.1}$$

We will concentrate on two-site blocking. The sites 2j, 2j+1 are grouped to form the j-th block, for which we define the variables

$$\begin{aligned} \tilde{x}_j &= \frac{1}{2}\left(x_{2j} + x_{2j+1}\right) \quad \text{(slow block variables)} \quad , \\ x_-(j) &= x_{2j} - x_{2j+1} \quad \text{(fast block variables)} \quad . \end{aligned} \tag{7.1.2}$$

The "fast" modes are the ones to be truncated; for a detailed discussion of this concept, see Part II.

The cannonically conjugate variables are

$$\begin{aligned} p_j &= p_{2j} + p_{2j+1} \quad , \\ p_-(j) &= p_{2j} - p_{2j+1} \quad , \end{aligned} \tag{7.1.3}$$

and the Hamiltonian becomes

$$\begin{aligned} H &= \sum_j \tfrac{1}{4} \tilde{p}_j^2 + \sum_j \left[p_-(j)^2 - \lambda \cos\left(x_-(j)\right) \right] - \lambda \sum_j \cos\left(x_{2j+1} - x_{2j+2}\right) \\ &= \sum_j \left\{ \tfrac{1}{4} \tilde{p}_j^2 - \lambda \cos\left[\tilde{x}_j - \tilde{x}_{j+1} - \tfrac{1}{2} \left(x_-(j) + x_-(j+1) \right) \right] \right\} \\ &\quad + \sum_j \left[p_-(j)^2 - \lambda \cos\left(x_-(j)\right) \right] \quad . \end{aligned} \tag{7.1.4}$$

Standard continuous-variable truncation methods call for choosing a trial state in the $\{x_-\}$ (fast mode) sector of a block,

$$g\left[x_-(j)\right] \quad , \tag{7.1.5}$$

and truncating the $\{x_-\}$ dependence of the global trial state ψ as a product of the g functions,

$$\psi\{x\} = \prod_j g\left[x_-(j)\right] \psi_{res}\{\tilde{x}\} \quad . \tag{7.1.6}$$

Here ψ_{res} is the residual wave-function in the x_j (slow) block modes. (7.1.6) is not the most general truncation possible, as we saw in

Part II; larger blocks may be used, or more than one mode retained per block. But all such schemes share a common inadequacy when applied to the XY model. In order to point out that problem, and to build successful blocking schemes, we shall use the class of truncation schemes (7.1.6) as our departure point. We already saw in Section 4 that a pure-Gaussian trial wave-function fails to recover the small-λ and transition-region aspects of the model; it is therefore useless to choose $g(x_-)$ as a Gaussian. Since ψ should be periodic in x_j with period 2π, a natural choice seems a $g(x_-)$ periodic in x_- with the same period:

$$g(x_-) = 1 + a\sqrt{2}\cos x_- \quad (0 \le x_- \le 4\pi) \quad , \tag{7.1.7}$$

where the range of x_- follows from the fact that $0 \le x_j \le 2\pi$. After integrating out the x_- variables, the truncated Hamiltonian is [(7.1.4)],

$$(H)_{tru} = \left(\frac{a^2}{1+a^2} - \frac{2\lambda a}{\sqrt{2}\left(1+a^2\right)} \right) \frac{L}{2} + \frac{1}{4} \sum_j \tilde{p}_j^2 \quad . \tag{7.1.8}$$

Here L is the volume and the subscript 'tru' denotes 'truncated'. We see that the interaction terms have dropped out, leaving a trivial free-rotor model after a single iteration. This is due to the $\exp\{\pm i x_-/2\}$ dependence of the interaction in (7.1.4). Thus our choice for $g(x_-)$ was over-periodic.

Our next attempt is to choose g to be periodic with period 4π; e.g.,

$$g(x_-) = 1 + a\sqrt{2}\cos\left(\frac{x_-}{2}\right) \quad , \quad 0 \le x_- < 4\pi \quad . \tag{7.1.9}$$

This truncation causes $\psi\{x\}$ to be nonperiodic under $x_j \to x_j + 2\pi\,\delta_{jr}$; we will now show how this causes a spurious transition. By truncating

with this g, a nontrivial evolution for H results. From (7.1.4), the iterated Hamiltonian is

$$(H)_{tru} = \frac{L}{2}(1-2\lambda)\frac{a^2}{4(1+a^2)} + \sum_j \frac{1}{4}\tilde{p}_j^2 - 2\lambda\frac{a^2}{(1+a^2)^2}\sum_j \cos(\tilde{x}_j - \tilde{x}_{j+1}) . \tag{7.1.10}$$

We have carried out a single-look-ahead variational calculation (see Part II), that is, we used for the residual wave-function the trial form

$$\psi_{res}\{\tilde{x}\} = \prod_j \left[1 + b\sqrt{2}\cos(\tilde{x}_j - \tilde{x}_{j+1})\right] . \tag{7.1.11}$$

The reason we chose a product state in the $y_j = x_j - x_{j+1}$ basis is because we saw in Section 5 that this prevents a spurious transition caused by lack of U(1) invariance. We will now show that another spurious transition occurs in this renormalization-group scheme, this time caused by the lack of periodicity.

The look-ahead trial energy density is [(7.1.10), (7.1.11)]

$$\rho_{Look}(a,b;\lambda) = \frac{1}{L}\left\langle (H)_{tru}\right\rangle_{Look}$$

$$= (1-2\lambda)\frac{a^2}{8(1+a^2)} + \frac{b^2}{4(1+b^2)} + \lambda\frac{a^2 b\sqrt{2}}{(1+a^2)^2(1+b^2)} . \tag{7.1.12}$$

This should be minimized with respect to a and b. For $\lambda = 0$, the minimum is clearly $a = b = 0$. By Taylor expansions with respect to a and b, we get

$$\rho_{Look} = \frac{1}{8}(1-2\lambda)\,a^2(1-a^2) + \frac{1}{4}b^2 - \lambda\sqrt{2}\,a^2 b + O(b^4) + O(a^2b^3) + O(a^6) + O(a^4 b) . \tag{7.1.13}$$

From this expansion, it is easy to prove that for $\lambda < 1/2$, there is a local minimum at $a = b = 0$, whereas for $\lambda > 1/2$, there is not. In fact, numerical calculations show that the transition to a nonzero minimum occurs already at $\lambda = \lambda_c = .36$. ρ_{Look}, a and b are plotted in Fig. 27 as functions of λ. Once again, the physics of the trial wave-function is trivial for the small-λ regime. Further iterations of the renormalization group mapping (7.1.10) are useless, since the iterated Hamiltonian is trivial in that regime.

The first-order spurious transition obtained from the choice (7.1.9) for the fast-mode wave-function is due to the lack of periodicity of the total ground-state wave-function, and is similar to the transition encountered in Section 4 when we used a pure (long-range) Gaussian for ψ. Since both periodic truncation, such as (7.1.7), and nonperiodic truncations yield trivial physics for the massive regime of the model, it is clear that we must develop truncation schemes that respect the periodicity of the total wave-function. In the next Subsection we develop a class of such schemes.

7.2 The quasi-spin formalism

In order to develop a truncation scheme that respects the periodicity symmetry of ψ, we will truncate the x_- modes to <u>two</u> states, one periodic under $x_- \to x_- + 2\pi$ and one antiperiodic:

$$\begin{aligned} g_0(x_-) &= G_0(x_-) \quad , \\ g_1(x_-) &= \cos\left(\frac{x_-}{2}\right) G_1(x_-) \quad , \\ G_{0,1}(x_- + 2\pi) &= G_{0,1}(x_-) \quad . \end{aligned} \tag{7.2.1}$$

Both of these states are necessary pieces in the wave function of the small-λ regime, as the following simple consideration shows. ψ must include plane-wave spin-pair excitations of zero momentum,

$$\text{plane-wave} = \sum_j \cos\left(x_j - x_{j+1}\right) \quad ,$$

with an amplitude of order λ. These excitations arise in small-λ perturbation theory (see Section 2.2). But in terms of the block variables (7.1.2),

$$\text{plane wave} = \sum_j \cos\left(x_j - x_{j+1}\right) = \sum_j \left[\cos x_-(j) + \cos\left(x_{2j+1} - x_{2j+2}\right)\right] \tag{7.2.2}$$

$$= \sum_j \cos x_-(j) + \sum_j \cos\left\{\tilde{x}_j - \tilde{x}_{j+1} - \frac{1}{2}\left[x_-(j) + x_-(j+1)\right]\right\},$$

and thus contains both periodic and antiperiodic functions of x_-.

The total trial wave-function in the scheme (7.2.1) is

$$\psi\{x\} = \sum_{\substack{\{r_j\} \\ r_j=0,1}} \left\{ \prod_j g_{r_j}\left[x_-(j)\right] \right\} \psi_{res}\left\{\tilde{x}_j, r_j\right\} , \tag{7.2.3}$$

where ψ_{res} is the residual wave-function in the slow block modes, $\tilde{x}_j$. Operators truncated via (7.2.3) will act on both $\{\tilde{x}\}$ and $\{r\}$; thus the effective model that evolves in this renormalization-group scheme will be a hybrid field theory-spin model. We therefore call this approach the quasi-spin formalism, where r_j are the quasi-spin variables. These variables allow us to transform the periodicity constraint,

$$\left[\exp\left\{ 2\pi i p_j \right\} - 1\right] \psi\{x\} = 0 \quad , \tag{7.2.4}$$

into a constraint on the iterated (residual) wave function; by (7.2.1) and (7.2.4), this iterated constraint is

$$\left[\exp\left\{ \pi i \tilde{p}_j \right\} - \exp\left\{ \pi i r_j \right\}\right] \psi\{\tilde{x}, r\} = 0 \quad ; \tag{7.2.5}$$

where $x_-(j)$ range between 0 and 4π. The orthonormality condition

$$\left(g_{r'}, g_r\right) = \delta_{r'r} \quad \text{(internal product)}$$

therefore implies (7.2.6)

$$\int_0^{4\pi} dx_- \left[G_r(x_-)\right]^2 = 1 \quad .$$

We use the abbreviation:

$$\int G^2 \quad \text{for} \quad \int dx_- G(x_-)^2 \ , \quad \text{etc.}$$

Truncation of x_- of p_- dependent operators turn them into 2×2 matrices in the r basis. In order to truncate the Hamiltonian (7.1.4), we note that

$$\left(g_{r'}, p_-^2 g_r\right) = \left[\left(\int G_0'^2\right)\delta_{r0} + \left(\frac{1}{4} + \int G_1'^2\right)\delta_{r1}\right]\delta_{rr'} \quad ,$$

$$\left(g_{r'}, \cos x_- g_r\right) = \left\{\left(\int G_0^2 \cos x_-\right)\delta_{r0} + \frac{1}{2}\left[\int G_1^2 \overline{\cos}\, x_-\left(1 - \cos x_-\right)\right]\delta_{r1}\right\}\delta_{rr'} \ ,$$

$$\left(g_{r'}, e^{\pm i\left(x_-/2\right)} g_r\right) = \left(\delta_{r0}\,\delta_{r'1} + \delta_{r1}\,\delta_{r'0}\right)\frac{1}{2}\int G_0\, G_1\, \left(1 + \cos x_-\right) . \tag{7.2.6}'$$

The once-iterated Hamiltonian $H^{(1)} = H_{tru}$ already achieves the fixed form of $H^{(n)}$:

The once-iterated Hamiltonian $H^{(1)} = (H)_{tru}$ already achieves the fixed form of $H^{(n)}$:

$$H^{(n)} = 2^{-n-1} \sum_j p_j^2 + \sum_j \Big[\overleftrightarrow{\mathcal{O}}_1(j) - \tfrac{1}{2} \overleftrightarrow{\mathcal{O}}_2(j)\, \overleftrightarrow{\mathcal{O}}_2^{T}(j+1) \times \exp\Big\{-i\big(x_j - x_{j+1}\big)\Big\} - \tfrac{1}{2} \overleftrightarrow{\mathcal{O}}_2^{T}(j)\, \overleftrightarrow{\mathcal{O}}_2(j+1) \exp\Big\{i\big(x_j - x_{j+1}\big)\Big\}\Big] \quad , \tag{7.2.7}$$

where $\overleftrightarrow{\mathcal{O}}_1$, $\overleftrightarrow{\mathcal{O}}_2$ are matrices in the r basis, given in (C.3). The superscript T denotes "transpose."

We proceed to iterate $H^{(n)}$ for $n \geq 1$. We shall be making use of some facts that we later prove by induction for all n.

The periodicity constraint for the wave-function of the n-th iteration is

$$\Big[\exp\Big\{2\pi i\, 2^{-n} p_j\Big\} - \exp\Big\{2\pi i\, 2^{-n} r_j\Big\} \Big] \Big|\psi^{(n)}\Big\rangle = 0, \text{ for all } j \ . \tag{7.2.8}$$

There are thus 2^n distinct quasi-spin values:

$$0 \leq r_j \leq 2^n \quad . \tag{7.2.9}$$

The r_j will be understood from here on to be modulo 2^n.

As discussed at the beginning of Section 7, infinite spin-towers are needed to recover the correct high-λ physics, and so we must keep all those spin sectors; this will indeed be done in Section 7.3 when we treat the NBPG schemes. But in order to demonstrate the quasi-spin formalism, we treat the simplest case that leads to a nontrivial renormalization group; this turns out to be when r_j are truncated as follows,

$$-2 \le r_j \le 2 \qquad (n \le 2) \quad ; \tag{7.2.11}$$

Thus, the spin matrices in $H^{(n)}$ will be of rank 5 for $n \ge 2$.

Blocking for $n \ge 1$. When we block the model, not only x_- but the quasi-spins in a block must be truncated, since otherwise we would have to keep 4^n spin states per block, which is more than the 2^{n+1} sectors of $\psi^{(n+1)}$ defined by the constraint (7.2.8). By combining the constraints at sites 2j and 2j+1, we find

$$\left[\exp\left\{2\pi i\, 2^{-n}\ \tilde{p}_j\right\} - \exp\left\{2\pi i\, 2^{-n}\left(r_{2j}+r_{2j+1}\right)\right\}\right]\psi = 0 \quad . \tag{7.2.12}$$

To preserve the form of the constraint in the (n+1)-th iteration, we want a residual wave function $\psi_{res}\{\tilde{x}_j, R_j\}$ such that

$$\left[\exp\left\{2\pi i\, 2^{-n-1}\tilde{p}_j\right\} - \exp\left\{2\pi i\, 2^{-n-1}\, R_j\right\}\right]\psi_{res}\{\tilde{x},R\} = 0 \quad . \tag{7.2.12}'$$

From (7.2.12) we see that ψ contains two R_j components for every given (r_{2j}, r_{2j+1}); this is because $\{r\}$ are defined modulo 2^n. The addition rule for quasi-spins is thus

$$R_j = r_{2j} + r_{2j+1} + 2^n \eta_j \quad , \quad 0 \le \eta_j \le 1 \quad . \tag{7.2.13}$$

This variable is modulo 2^{n+1}. The n-th iteration wave function is expressed in terms of the (n+1)-th as follows:

$$\psi\left\{x_j, r_j\right\} = \sum_{\substack{\{\eta_j\} \\ \eta_j=0,1}} \left\{\prod_j g_{\eta_j}\left[x_-(j); r_{2j}, r_{2j+1}\right]\right\} \psi_{res}\left\{\tilde{x}_j, R_j\right\} \quad . \tag{7.2.14}$$

The function g specifies the truncation in both the quasi-spin and continuous variables. In addition to the total block spin R_j, we also define an internal spin,

$$S_j \equiv r_{2j} - r_{2j+1} - 2^n \eta_j = 2r_{2j} - R_j \quad ; \tag{7.2.15}$$

then by (7.2.8), (7.2.12)' and (7.2.14),

$$\left[\exp\left\{2\pi i\, 2^{-n}\, p_-(j)\right\} - \exp\left\{2\pi i\, 2^{-n-1}\, S_j\right\}\right] g_{\eta_j} = 0 \quad . \tag{7.2.16}$$

Like R_j, S_j is modulo 2^{n+1}.

We now completely specify the truncation, as follows:

$$g_{\eta_j}\left[x_-(j); r_{2j}, r_{2j+1}\right] = \exp\left\{iS_j \tfrac{1}{2} x_-(j)\right\} G_{S_j}\left[x_-(j)\right] t_{R_j r_{2j} r_{2j+1}} , \tag{7.2.17}$$

where by (7.2.16), G_s are (normalized) periodic functions with period $2\pi 2^{-n}$:

$$\begin{aligned} G_s(x_-) &= G_s\left(x_- + 2\pi 2^{-n}\right) \quad , \\ \left(G_s, G_s\right) &\equiv \int_0^{4\pi} dx_- \left|G_s(x_-)\right|^2 \quad . \end{aligned} \tag{7.2.18}$$

In (7.2.17) we have truncated the quase-spins in the simplest possible way, with a pure spin wave-function t that may be treated variationally along with $G_s(x_-)$.

Symmetries. We are building a trial wave function that obeys all the model symmetries listed in Section 2.1, and in particular the symmetries

$$\left.\begin{aligned} x_j &\to -x_j \\ p_j &\to -p_j \end{aligned}\right\} \quad \text{(field-reflections)} \quad , \tag{7.2.19}$$

$$\left.\begin{array}{l} x_j \to x_{-j} \\ p_j \to p_{-j} \end{array}\right\} \quad \text{(space-reflection)} \quad . \qquad (7.2.20)$$

We now derive the consequences of these symmetries for G_s and $t_{Rr_1r_2}$. Due to (7.2.8), the quasi-spins transform as follows:

$$\begin{array}{ll} r_j \to -r_j & \text{(field-reflection)} \\ r_j \to r_{-j} & \text{(j-reflection)} \quad . \end{array} \qquad (7.2.21)$$

Replacing the dummy indices η_j in (7.2.14) by $(1-\eta_j)$, we find for the block variables

$$\begin{array}{lll} R_j \to -R_j \,, & S_j \to -S_j & \text{(field-reflection)} \\ R_j \to R_{-j} \,, & S_j \to -S_{-j} & \text{(space-reflection)} \quad . \end{array} \qquad (7.2.22)$$

The symmetry conditions on the wave-function are

$$\psi\{x_j, r_j\} = \psi\{-x_j, -r_j\} = \psi\{x_{-j}, r_{-j}\} \quad . \qquad (7.2.23)$$

By imposing the same symmetry on the (n+1)-th wave function, ψ_{res}, and using (7.2.12), (7.2.17) and (7.2.21)-(7.2.23), we obtain the desired symmetry conditions:

$$G_s(x_-) = G_{-s}(-x_-) \quad , \qquad (7.2.24)$$

$$t_{Rr_1r_2} = t_{(-R)(-r_1)(-r_2)} = t_{Rr_2r_1} \quad . \qquad (7.2.25)$$

We satisfy (7.2.24) by choosing $G_s(x_-)$ to be symmetric in s and x_-; we will also choose G_s,t to be real.

There is one more constraint: from the norm condition

$$(\psi,\psi) = \left(\psi_{res},\psi_{res}\right) = 1 \quad , \tag{7.2.26}$$

and from (7.2.18), we obtain

$$\sum_{r_1 r_2} \left(t_{Rr_1r_2}\right)^2 = 1 \quad . \tag{7.2.27}$$

Note that t vanishes unless the addition rule

$$R = r_1 + r_2 + 2^n\eta \quad , \quad \eta = 0 \text{ or } 1 \tag{7.2.13)'}$$

is obeyed.

In Appendix C, the derivation of the renormalization group transformation for the matrices $\mathcal{O}_1,\mathcal{O}_2$ is outlined. These matrices specify the iterated effective Hamiltonians, $H^{(n)}$, via (7.2.7). We also give the outlines of the minimal quasi-spin renormalization-group, the one where five spin states are kept:

$$-2 \le R_j \le 2 \quad , \quad -2 \le S_j \le 2 \quad . \tag{7.2.28}$$

In that Appendix we also explain why keeping less spins than (7.2.28) leads once more, as happened in Section 7.1, to a trivial evolution of the Hamiltonian. We will not pursue the minimal scheme, as it turns out that the full r-spin towers are needed to recover the free-field physics in the $\lambda \to \infty$ limit (see Section 7.5 below). The minimal scheme will, however, prove useful for studying the $\lambda << 1$ region, where the full towers are not needed.

We now proceed to derive a quasi-spin scheme that keeps the full r-spin towers.*

7.3 The periodic Gaussian scheme: evolution of the partition sum

Let us return to the periodic Gaussian trial wave-function, (4.1). We will evaluate the norm partition sum Z, (4.2)', by truncating the propagator $\Delta(j)$ in a way that corresponds exactly with the free-field simple blocking scheme with a look-ahead, described in Part II. That is, the propagator is characterized by one Gaussian parameter per length scale; this is the parameter γ_- appearing in the truncating wave function, Part II Eqs. (4.2), (4.4). We first derive the iterative renormalization-group transformation for Z and for various expectation values, and then iterate the trial wave-function. The latter iteration shows that this scheme is just a special case of our quasi-spin formalism of the last subsection.

This scheme, a periodic Gaussian wave function blocked as a free-field theory, will henceforth be called the NPBG scheme, or schemes: Naively Blocked Periodic Gaussian. The plural is used because the number of look-ahead steps is arbitrary. All of the computations reported in Section 7 were done for the NBPG schemes, or variants thereof.

For the N_j effective Coulomb gas, the norm partition sum is [(4.2)']

$$Z \equiv \langle\psi|\psi\rangle = \sum_{\substack{\{N\} \\ -\infty<N_j<\infty}} \exp\left\{ - \pi^2 \sum_{jj'} N_j \, \Delta(j-j') \, N_{j'} \right\} . \qquad (7.3.1)$$

*This does not mean the r-spins will not be truncated, but rather that all the 2^n sectors allowed by (7.2.12) will be kept.

We block the lattice sites as in Section 7.2, and define slow and fast N variables in a block:

$$N_{\pm}(j) = N_{2j} \pm N_{2j+1} \quad . \tag{7.3.2}$$

Z is next rewritten in terms of the $N_{\pm}$ variables,

$$Z = \sum_{\{N\}} \exp\left\{ - \sum_{jj'} N_{+}(j)\, \Delta_{++}(j-j')\, N_{+}(j') \right. \tag{7.3.3}$$
$$\left. - \sum_{jj'} N_{-}(j)\, \Delta_{--}(j-j')\, N_{-}(j') - 2 \sum_{jj'} N_{+}(j)\, \Delta_{+-}(j-j')\, N_{-}(j') \right\} ,$$

where the three blocked propagators are

$$\Delta_{++}(j) = \frac{\pi^2}{4} \left[2\Delta(2j) + \Delta(2j+1) + \Delta(2j-1) \right] ,$$
$$\Delta_{+-}(j) = \frac{\pi^2}{4} \left[\Delta(2j-1) - \Delta(2j+1) \right] , \tag{7.3.4}$$
$$\Delta_{--}(j) = \frac{\pi^2}{4} \left[2\Delta(2j) - \Delta(2j+1) - \Delta(2j-1) \right] .$$

The simple (no-shift) truncation consists of setting Δ_{+-}, the part of the propagator that couples the fast and slow variables, to zero, and using a mean-field (zero-range) approximation to evaluate the $N_{-}(j)$ summations; that is, (δ is a variational parameter)

$$\Delta_{+-}(j) \equiv 0, \Delta_{--}(j) = \left(\pi^2 \delta\right) \delta_{j0} \quad . \tag{7.3.5}$$

The truncation next calls for defining $N_{+}(j)$ as the new effective variable in a block, and summing over the $N_{-}(j)$ variables. There is, however, a complication arising from the discreteness of {N}: N_{+} and N_{-}

do not vary independently. Namely, $\{N_+ - N_-\}$ must be even, due to (7.3.2). This constraint may be taken care of by introducing the factor

$$p\{N_\pm\} = \left(\prod_j \sum_{\eta_j=0}^{1} \right) \prod_j \left(\exp \left\{ \pi i \eta_j \left[N_+(j) - N_-(j) \right] \right\} \right) \quad , \tag{7.3.6}$$

inside the summation (7.3.3). This factor vanishes unless $N_+(j) - N_-(j)$ are even, and so the summations over $\{N_+, N_-\}$ may now be carried out independently. Making use of (7.3.5), we obtain

$$Z = \sum_{\{r\}, \{N_+\}} \exp\left\{ -\sum_{jj'} N_+(j) \Delta_{++}(j-j') N_+(j') + i\pi \sum_j r_j N_+(j) \right\} A^{(1)}(r_j) \quad ,$$

$$0 \le r_j \le 1 \tag{7.3.7}$$

$$A^{(1)}(r_j) = \sum_{N_-=-\infty}^{\infty} \exp\left\{ -\pi^2 \delta N_-^2 - i\pi r_j N_- \right\} \quad .$$

We renamed the dummy indices η_j as r_j, to signal the fact that they correspond to the quasi-spin variables for the $n = 1$ iteration; hence also the superscript of the function A. We now redefine $N_+(j)$ as $N(j)$, define a decimated lattice with the blocks as its new sites, and set Δ_{++} to be the new iterated propagator:

$$\pi^2 \Delta^{(1)}(j) \equiv \Delta_{++}(j) \quad . \tag{7.3.8}$$

The iterated form of Z will turn out to be, for all $n \ge 0$,

$$Z = \sum_{\substack{\{r\}, \{N_+\} \\ 0 \le r_j \le 2^{n-1}}} \exp\left\{ -\pi^2 \sum_{jj'} N(j) \Delta^{(n)}(j-j') N(j') + 2^{1-n} \pi i \sum_j r_j N(j) \right\} \prod_j A^{(n)}(r_j) . \tag{7.3.9}$$

In particular, for $n = 0$, $A^{(0)}(r)$ has only one component,

$$A^{(0)}(0) = 1 \quad . \tag{7.3.10}$$

We next set out to derive the recursion relations for the parameters $A^{(n)}(r)$. Let us start from (7.3.9) and block the lattice. Define $N_{\pm}(j)$ according to (7.3.2), and truncate the propagator $\Delta^{(n)}(j)$ via (7.3.3)-(7.3.5). We again insert $p\{N_{\pm}\}$, and carry out the N_- summations by defining:

$$I_n(\omega) = \sum_{N_-=-\infty}^{\infty} \exp\left\{ - \pi^2 \delta_n (N_-)^2 + i\pi 2^{-n} N_- \omega \right\} \quad . \tag{7.3.11}$$

Here δ_n is the propagator parameter for this length scale. We then find,

$$Z = \sum_{\substack{\{\eta\},\{r\},\{N_+\} \\ 0\le\eta_j\le 1 \\ 0\le r_j\le 2^n-1}} \exp\left\{ - \sum_{jj'} N_+(j)\, \Delta_{++}^{(n)}(j-j')\, N_+(j') + i\pi 2^{-n} \sum_j N_+(j)\left(r_{2j} + r_{2j+1} + 2^n\eta_j\right)\right\} \tag{7.3.12}$$

$$\times \prod_j A^{(n)}(r_{2j})\, A^{(n)}(r_{2j+1})\, I_n\left(r_{2j} - r_{2j+1} - 2^n \eta_j\right) .$$

In order to cast this in the fixed form (7.3.9), we must also block and truncate the r indices: let

$$\begin{aligned} R_j &= r_{2j} + r_{2j+1} + 2^n\eta_j \quad , \\ S_j &= r_{2j} - r_{2j+1} - 2^n\eta_j = -2r_{2j} - R_j \quad . \end{aligned} \tag{7.3.13}$$

At this point, we recognize these as the quasi-spin addition rules, (7.2.13) and (7.2.15). Replacing the sum over η_j, r_{2j} and r_{2j+1} by sums over

$$0 \le R_j \le 2^{n+1} - 1 \quad , \qquad 0 \le S_j \le 2^{n+1} - 1 \quad ,$$

we arrive again at the form (7.3.9) for the (n+1)-th iteration. The recursion relation for $A^{(n)}$ is

$$A^{(n+1)}(R) = \sum_{r_1} A^{(n)}(r_1)\, A^{(r)}(R - r_1)\, I_n(2r_1 - R) \quad . \tag{7.3.14}$$

As in Section 7.2, r_1 ranges from 0 to $2^n - 1$, R over 0 to $2^{n+1} - 1$ and R, r_1 are defined modulo 2^{n+1} and 2^n, respectively. This completes the iterative blocking of the partition sum; the initial condition for the recursion relation (7.3.14) is (7.3.10).

7.4 NPBG as a quasi-spin scheme

We could now proceed to iterate statistical-mechanics averages computed in the partition sum. It is evident, however, that the NBPG scheme is related to our quasi-spin formalism; we now show that it is, in fact, a particular case of the formalism, with a particular choice of truncating wave function; we will then analyze NBPG using the formalism.

The periodic-Gaussian wave function is [by (4.1)],

$$\psi\{x\} = \sum_{\{N\}} \exp\left\{ -\frac{1}{2} \sum_{jj'} (x_j - 2\pi N_j)\, \Delta(j - j')\, (x_{j'} - 2\pi N_{j'}) \right\}. \tag{7.4.1}$$

We block the lattice sites, and define block variables $x_\pm$, $N_\pm$ through (7.1.2), (7.3.2). The propagator is blocked and truncated via (7.3.3)-(7.3.5). We also insert the factor $p\{N_\pm\}$ of (7.3.6) into the $\{N_\pm\}$ summation, and carry out the N_- sums. This gives

$$\psi\{x\} = \sum_{\substack{\{N_+\},\{r_j\} \\ 0\le r_j\le 1}} \exp\left\{ -\frac{1}{2} \sum_{jj'} \left[N_+(j) - \frac{1}{\pi}\tilde{x}_j \right] \Delta_{++}(j-j') \right. \tag{7.4.2}$$

$$\left. \times \left[N_+(j') - \frac{1}{\pi}\tilde{x}_{j'} \right] + i\pi \sum_j r_j N_+(j) \right\} \prod_j J_{r_j}\left[x_-(j)\right] ,$$

where

$$J_r(x_-) = \sum_{N_-=\infty}^{\infty} \exp\left\{ -\frac{1}{4}\,\delta_0\left(x_- - 2\pi N_-\right)^2 - i\pi r N_- \right\} . \tag{7.4.3}$$

Formula (7.4.2) specifies the truncation of the x_- (fast) modes.

By making use of the Poisson summation formulae (5.1.1) - (5.1.2), we may rewrite J_r as

$$J_r(x_-) = \exp\left\{ -i\frac{r}{2}x_- \right\} \sqrt{\frac{1}{\pi\delta_0}} \sum_{m=-\infty}^{\infty} \exp\left\{ imx_- \right\} \exp\left\{ -\frac{1}{\delta_0}\left(m-\frac{1}{2}r\right)^2 \right\} \tag{7.4.4}$$

We note that $J_r(x_-)$ are periodic (antiperiodic) functions for $r = 0,1$ respectively; we thus identify them as the trial x_- wave-functions of (7.2.1). The $\tilde{x}$ dependent factor in the sum (7.4.2) is the residual wave-function, and depends on the quasi-spin variables as well as continuous variables. From (7.3.8)

$$\psi_{res}\{\tilde{x},r\} = \psi^{(1)}\{\tilde{x},r\} ,$$

$$\psi^{(1)}\{x,r\} = \sum_{\{N\}} \exp\left\{ -\frac{1}{2} \sum_{jj'} \left(x_j - \pi N_j\right) \Delta^{(1)}(j-j') \left(x_{j'} - \pi N_{j'}\right) \right.$$

$$\left. + i\pi \sum_j r_j N_j \right\} \tag{7.4.5}$$

The residual wave function is therefore once more a periodic Gaussian, but with a Bloch wave-number r_j for the sum over degenerate vacua; the period of $\psi^{(1)}$ is π, rather than 2π. We also note that the wave-functions $J_r(x_-)$, used to truncate the x_- modes in (7.4.2), are themselves periodic Gaussians.

Using the above, and the results of Section 7.3, it is straightforward to prove the following facts:

(1) The n-th iterated NBPG wave-function is

$$\psi^{(n)}\{x,r\} = \sum_{\{N\}} \exp\left\{ -\frac{1}{2}\sum_{jj'} \left(x_j - 2\pi 2^{-n}N_j\right) \Delta^{(n)}\left(j-j'\right)\left(x_{j'} - 2\pi 2^{-n}N_{j'}\right) \right. \tag{7.4.6}$$

$$\left. + 2\pi i 2^{-n} \sum_j r_j N_j \right\}, \quad 0 \le r_j \le 2^n - 1, \quad 0 \le x_j \le 2\pi \quad ,$$

and obeys the periodicity constraints, (7.2.8).

(2) $\psi^{(n)}$ obeys the recursion relation (7.2.14) derived in the quasi-spin formalism, where the spin-truncation wave function is

$${}^{t}R r_1\left(R-r_1\right) = \left[\frac{I_n\left(2r_1 - R\right) A^{(n)}\left(r_1\right) A^{(n)}\left(R - r_1\right)}{A^{(n+1)}(R)} \right]^{1/2},$$

and the fast-mode wave-function is a periodic Gaussian,

$$G_s\left(x_-\right) = \sum_{m=-\infty}^{\infty} \exp\left\{ -i2^n m x_- \right\} \exp\left\{ -\frac{4^n}{2\delta_n} \left(m - s2^{-1-n}\right)^2 \right\} . \tag{7.4.8}$$

G_s satisfies the periodicity property, Eq. (7.2.18). Note that t satisfies the normalization condition, (7.2.27), by virtue of Eq. (7.3.14).

(3) The parameters $D^{(n)}(r)$ and $E^{(n)}(r)$ defined through (7.2.7) and (C.3) are

$$D^{(n)}(r) = \frac{C^{(n)}(r)}{A^{(n)}(r)} \quad ,$$

$$E^{(n)}(r) = \frac{R^{(n)}(r)}{\left[A^{(n)}(r)\, A^{(n)}(r-1)\right]^{1/2}} \quad , \tag{7.4.9}$$

where $A^{(n)}$, $C^{(n)}$, $R^{(n)}$ obey the recursion relations,

$$A^{(n+1)}(r) = \sum_{r_1=0}^{2^n-1} A^{(n)}(r_1)\, A^{(n)}(r-r_1)\, I_n(2r_1-r) \quad ,$$

$$R^{(n+1)}(r) = \exp\left\{-\frac{1}{16\delta_n}\right\} \sum_{r_1=0}^{2^n-1} R^{(n)}(r_1)\, A^{(n)}(r-r_1)\, I_n\left(2r_1 - r + \frac{1}{2}\right) \quad ,$$

$$C^{(n+1)}(r) = \sum_{r_1=0}^{2^n-1} C^{(n)}(r_1)\, A^{(n)}(r-r_1)\, I_n(2r_1-r) + \frac{1}{2} \sum_{r_1=0}^{2^n-1} A^{(n)}(r_1)$$

$$\times A^{(n)}(r-r_1)\, \bar{I}_n(2r_1-r) - 2^{-n-1} \exp\left\{-\frac{1}{4\delta_n}\right\}$$

$$\times \sum_{r_1=0}^{2^n-1} R^{(n)}(-r_1)\, R^{(n)}(r-r_1)\, I_n(2r_1-r-1) \quad . \tag{7.4.10}$$

Here $0 \le r \le 2^{n+1}$, and

$$I_n(S) = \left(\pi\delta_n\right)^{-1/2} \sum_{m=-\infty}^{\infty} \exp\left\{-\frac{4^n}{\delta_n}\left(m - 2^{-n-1}S\right)^2\right\} \quad ,$$

$$\bar{I}_n(S) = \left(\pi\delta_n\right)^{-1/2} \sum_{m=-\infty}^{\infty} \left(m - 2^{-n-1}r\right)^2 \exp\left\{-\frac{4^n}{\delta_n}\left(m - 2^{-n-1}S\right)^2\right\} \quad . \tag{7.4.11}$$

This expression for $I_n(S)$ was obtained from the definition, (7.3.11), via Poisson's summation equation. The number of parameters iterated grows proportionally to the size of the quasi-spin towers, i.e., as 2^n. The initial conditions are

$$\begin{aligned} A^{(0)}(0) &= 1 \quad , \\ C^{(0)}(0) &= 0 \quad , \\ R^{(0)}(0) &= \sqrt{\lambda} \quad ; \end{aligned} \tag{7.4.10}'$$

this is the only part where λ enters the equations.

Look-ahead schemes and the trial energy. Since the parameters $D^{(n)}(r)$, $E^{(n)}(r)$ completely specify the effective Hamiltonian, we are now in a position to compute a trial energy $\langle H^{(n+1)}\rangle$. The renormalization-group transformation in the NBPG scheme is characterized by a single parameter, δ_n, that specifies the propagator truncation, (7.3.5). We will minimize $\langle H^{(n+1)}\rangle$ with some suitable mean-field look-ahead wave function in the slow modes $x^{(n)} \equiv x^{(n+1)}$; this will give us the parameter δ_n and the look-ahead wave function. The latter will be discarded, as explained in Part II.

The look-ahead wave function is chosen as the product state,

$$\psi_{\text{look}}^{(n+1)}\{x;r\} = \prod_j F_{r_j}^{(n+1)}\left[x_j^{(n+1)}\right] \quad , \tag{7.4.12}$$

where $x_j^{(n+1)}$ are the variables in the (n+1)-th iteration, and $F^{(n+1)}$ is (naturally) chosen to be a periodic Gaussian, with period $2\pi 2^{-n}$. This period is chosen so that $\psi_{look}^{(n+1)}$ obeys the periodicity constraint (7.2.8). In Section 5, we saw the disadvantages of using U(1) noninvariant wavefunctions such as (7.4.12) in the x basis; but ψ_{look} is merely a guess for the slow modes and is not part of the final ψ_{trial}, so this violation of U(1) should not matter too much. In Section 7.5, we will see that this is indeed the case.

Let $F_r^{(n+1)}$ be the periodic Gaussian given in (C.6); it depends on the variational parameter δ'_{n+1}. With the look-ahead (7.4.12), the trial energy at the (n+1)-st iteration comes out to be

$$\rho_{look}^{(n+1)} = \frac{1}{L} \left\langle H^{(n+1)} \right\rangle_{look}$$

$$= \frac{\sum_r I'_{n+1}(r)\, C^{(n+1)}(r)}{\sum_r I'_{n+1}(r)\, A^{(n+1)}(r)} + \frac{1}{2} \frac{\sum_r \bar{I}'_{n+1}(r)\, A^{(n+1)}(r)}{\sum_r I'_{n+1}(r)\, A^{(n+1)}(r)} \qquad (7.4.13)$$

$$- 2^{-1-n} \exp\left\{ - \frac{1}{2\delta'_{n+1}} \right\} \left(\frac{\sum_r I'_{n+1}\left(r+\frac{1}{2}\right) R^{(n+1)}(r)}{\sum_r I'_{n+1}(r)\, A^{(n+1)}(r)} \right)^2, \quad 0 \le r \le 2^{n+1}-1 \ ,$$

where $I'_{n+1}(r)$, $\bar{I}'_{n+1}(r)$ are the same as $I_n(r)$, $\bar{I}_n(r)$, but with δ_n replaced by δ'_{n+1}. $\rho_{look}^{(n+1)}$ is a function of both δ_n and δ'_{n+1} and should be minimized with respect to both of them.

Correlation Functions. By using the quasi-spin formalism, it is possible to iterate not only the Hamiltonian, but any operator. In particular, we find for the two dual correlation functions,

$$\left\langle \cos\left(x_j - x_{j'}\right)\right\rangle \sim \exp\left\{-\frac{1}{4}\sum_{n=0}^{\log_2|j'-j|}\delta_n^{-1}\right\}$$

$$\left\langle \exp\left\{i\ \text{const.}\sum_{k=j+1}^{j'} p_k\right\}\right\rangle \sim \exp\left\{-\ \text{const.}\sum_{n=0}^{\log_2|j'-j|}\delta_n\right\} \quad . \tag{7.4.14}$$

Symmetries. It is easy to prove by induction that

$$\begin{aligned} A^{(n)}(-r) &= A^{(n)}(r) \quad , \\ C^{(n)}(-r) &= C^{(n)}(r) \quad , \\ R^{(n)}(r) &= R^{(n)}(-r-1) \quad , \end{aligned} \tag{7.4.15}$$

where r is treated modulo 2^n.

7.5 The results

The recursion relations (7.4.10), with initial conditions (7.4.10)', give the evolution of the 2^{n+1} Hamiltonian parameters $D^{(n)}(r)$ and $E^{(n)}(r)$, and of the auxiliary parameters $A^{(n)}(r)$ governing the iteration of the partition sum Z. Unlike in ordinary renormalization-group transformations, or even the minimal scheme described in Appendix C, the number of iterated parameters grows with n; this is because the NBPG scheme keeps the full r-towers. We saw in Section 7.4 that it is necessary to keep

them for the case of the periodic Gaussian wave-function. Since in the $\lambda \to \infty$ limit the exact wave function is a Gaussian, we conclude that the full quasi-spin towers are needed, if one is to recover the free-field regime.

Keeping all the parameters numerically proved easy, up to n values sufficiently high (n = 6) so the scaling properties of the large-distance correlation functions can be seen.

We have analyzed the physics of the NBPG renormalization-group equations in three ways: analytically, in the $\lambda << 1$ and $\lambda >> 1$ regions, and numerically for all coupling values. What follows is a review of the results in each of these approaches.

(1) *Small-λ region*. For $\lambda << 1$, only the lowest-lying spins in the r-spin towers are activated, and NBPG reduces, approximately, to the minimal quasi-spin scheme. It is then sufficient to iterate only five parameters: $R^{(n)}(1)/A^{(n)}(0)$, $R^{(n)}(0)/A^{(n)}(0)$, $C^{(n)}(0)/A^{(n)}(0)$, $C^{(n)}(1)/A^{(n)}(0)$, $A^{(n)}(1)/A^{(n)}(0)$. This is due to the symmetries (7.4.15), and due to the fact that only ratios of the parameters A, C, R appear in physical quantities.*

The results are as follows: The final ground-state trial energy is

$$\rho_{g.s.}(\lambda) = \lim_{n \to \infty} \rho^{(n)}_{look}(\lambda) = -.28\lambda^2 + \bar{0}(\lambda^4) \quad , \qquad (7.5.1)$$

as compared with the exact perturbative result, $-(1/2)\lambda^2 + 0(\lambda^4)$. The discrepancy is due to the use of the $\{x_j\}$ basis, rather than the $\{y_j\}$

---

*Since $A^{(n)}(r)$ are related to the norm (Section 7.3) and hence unphysical; e.g., see the expression for the energy, (7.4.13).

basis defined in Section 5 (Eq. 5.3.3). That this is indeed true is proven in the following subsection. Figure 21 shows $\rho_{g.s.}$. [The recursion relations for the five parameters, from which the results reported here were derived, follow easily from (7.4.10) - (7.4.10)', and are listed in (C.7).]

By minimizing the trial energy (7.4.13) we got for the Gaussian parameter of the n-th iteration, for large n,

$$\exp\left\{-\frac{1}{4\delta_n}\right\} \simeq \lambda^{\left(2^{-n}\right)} \frac{1}{4} \quad (\lambda << 1,\ n >> 1) \quad , \tag{7.5.2}$$

and thus from (7.4.14), the correlation function is:

$$\left\langle \cos\left(x_j - x_{j'}\right)\right\rangle \propto \lambda^2 |j-j'|^{-2} \quad , \quad |j-j'| >> 1 \quad . \tag{7.5.3}$$

This is, of course, the wrong behavior, since the falloff with distance should be exponential. This problem as well may be corrected by working in the $\{y_j\}$ basis, as shown in Section 7.6.

(2) *Large-λ region*. In this regime, the tunnelings between degenerate classical vacua are suppressed as* $\exp\{-\text{const.}\sqrt{\lambda}\}$, and the correct physics is that of the free massless field, corrected by $O(\lambda^{-m/2})$ perturbative corrections to the power-falloff and to the energy; see Section 2.3. In the NBPG approximation, too, one obtains the free-field physics — but only that which the naive blocking of the propagator allows. As we recall from Part II, that means a spurious

---

*See Section 6 for a discussion of the strength of tunneling effects.

long-range order rather than power falloff:[†]

$$\left\langle \cos\left(x_j - x_{j'}\right)\right\rangle \sim \exp\left\{-\frac{\text{const.}}{|j-j'|^2}\right\}, \qquad |j-j'| \gg 1 \quad . \tag{7.5.4}$$

This behavior violates Coleman's theorem,[§] that forbids local operators from having vacuum expectation values in (1+1)-dimensional models. The true correlation function in this region falls off as a power, but this discrepancy can be corrected via adiabatic truncation, as showed in Part II. In Section 7.6 we discuss a way to extend the adiabatic method to intermediate couplings.

(3) *Numerical results.* Our numerical calculations yield a phase transition between the asymptotic behaviors (7.5.3) and (7.5.4), i.e., between power-law disorder in the $\lambda < \lambda_c$ regime and long-range order in the $\lambda > \lambda_c$ regime, with $\lambda_c \simeq .35$. While this is not the correct transition of the XY model, it is an order-disorder transition, and it appears to be of infinite order — in the sense explained below.

The transition is found to have the following properties:

(A) $\delta_n(\lambda)$ have a weak singularity at $\lambda = \lambda_c$, which becomes weaker when n_ℓ is increased from 1 to 2. [n_ℓ is the number of look-ahead steps; see Part II.] This singularity is a spurious one, caused by the U(1) violation in $\psi^{(n+1)}_{\text{look}}$. We encountered such a transition in Section 5.2. Here it manifests itself merely as a nonanalyticity, since the violation occurs only in the look-ahead part of ψ, which is not present in the

---

[†]We recall that there, $\langle x(k)x(-k)\rangle_{\text{trial}} \sim k^{-1/2}$ in momentum basis; that translates to (7.5.4) in the position basis. See Ref. 16 of Part II for a discussion of this long-range order vis-á-vis Colemans theorem.

[§]Or, more accurately, the Mermin-Wegner theorem.

full wave-function. Figure 22 shows $-1/(4\delta_n)$ versus λ, for $0 \le n \le 6$, in the case $n_\ell = 1$. Figure 23 shows the same parameters, for $0 \le n \le 4$, in the $n_\ell = 2$ case. Figure 24 shows $-1/(4\delta_0)$ near $\lambda = \lambda_c$ for both look-ahead schemes. Here we note that the change is only several percent at its largest, but that the $n_\ell = 2$ curve is smoother at $\lambda \simeq \lambda_c$. This is as it should be, since when n_ℓ is increased, the U(1) violation occurs at larger length scales and affects δ_n less. The look-ahead parameters exhibit the full spurious transition, but these parameters are unphysical (See Fig. 25). This spurious singularity should disappear altogether when the $\{y_j\}$ basis is used, because of its manifest U(1) invariance.

(B) Apart from the above-mentioned weak singularity, the functions $\delta_n(\lambda)$ are smooth for finite n; but as n increases, they become steeper near $\lambda = \lambda_c$ (Fig. 26). The numerical results indicate that $1/\delta_n$ approaches a step-function as $n \to \infty$,

$$\frac{1}{\delta_n(\lambda)} \longrightarrow \begin{cases} 0 & \lambda > \lambda_c \quad , \\ \\ 4\ \ell n\ 4 & \lambda < \lambda_c \quad . \end{cases} \tag{7.5.5}$$

Thus, any physical quantity involving finite length-scales is smooth, but the asymptotic large-distance behavior (large-n) of correlation functions is discontinuous. This is an important feature of the true Kosterlitz-Thouless transition; and so although we cannot determine the λ-dependence at $\lambda \simeq \lambda_c$ analytically, we have found (in a numerical sense) an infinite-order transition. With the aid of the improvements

suggested in the next subsection, we hope to turn this into a more realistic phase transition in the near future.

7.6 Improvements using our methods.

The NBPG scheme is the first quasi-spin scheme for which we obtained the results, but much better schemes are easy to implement using the quasi-spin formalism. In this section we describe two such improvements, which when combined will yield the correct physics in both extreme regions of the coupling axis — and hence will also give a more realistic phase transition.

The first improvement consists of working in the $\{y_j\}$ basis ($y_j = x_{j+1} - x_j$) rather than the $\{x_j\}$ basis. We then easily recover the plane-wave perturbative excitation, (7.2.2), as a special case of the periodic Gaussian, to order (λ). This is because

$$1 + \sum_j \lambda\cos\left(x_j - x_{j+1}\right) = \prod_j \left[1 + \lambda\cos\left(x_{j+1} - x_j\right)\right] + O\left(\lambda^2\right)$$
$$\cong \prod_j F\left(x_j - x_{j+1}\right) \equiv \psi_1\{x\} \tag{7.6.1}$$

where F(x) is a very flat periodic Gaussian. It is trivial to show that for the wave-function ψ_1, naive blocking is exact — and so the correct perturbative wave-function falls within our trial Hilbert subspace, to lowest order in λ. Thus, to that order, we will get the correct results for energy and correlation,

$$\rho_{g.s.} = -\frac{1}{2}\lambda^2 + O\left(\lambda^3\right) \quad ,$$
$$\left\langle \cos\left(x_j - x_{j'}\right)\right\rangle \sim \left[\lambda + O\left(\lambda^3\right)\right]^{|j-j'|}; \quad |j-j'| >> 1 \, , \, \lambda << 1 \quad . \tag{7.6.2}$$

Therefore, the massive ($\lambda < \lambda_c$) regime indeed possesses a mass gap in the {y} basis NBPG, and one can study how it vanishes as $\lambda \to \lambda_c$.

The second improvement would be to use shifted periodic Gaussians, i.e., to use an adiabatic truncation similar to the one employed in Part II. To preserve periodicity, it would be necessary to shift x_- by a sine-function of the surrounding slow modes,

$$x_-(j) \to x_-(j) - \xi \sin\left[2^n\left(\tilde{x}_{j+1} - \tilde{x}_{j-1}\right)\right] \quad , \tag{7.6.3}$$

rather than the linear shift used in the free-field case [(4.2) - (4.3) in Part II]. It is possible to incorporate this periodic shift in our quasi-spin approach.

APPENDIX A

A PERTURBATIVE CALCULATION FOR HIGH λ

We temporarily drop the primes in (2.3.2). To second order in the small expansion parameter, $1/\sqrt{\lambda}$,

$$H = \frac{1}{2}\left[\sum_j p_j^2 + \sum_j \left(x_{j+1} - x_j\right)^2\right] - \frac{1}{4!}\lambda^{-1/2}\sum_j \left(x_{j+1} - x_j\right)^4 + \frac{1}{6!}\lambda^{-1}\sum_j \left(x_{j+1} - x_j\right)^6 + \left(\lambda^{-3/2}\right) \quad . \tag{A.1}$$

In the momentum basis,

$$x_j = \frac{1}{\sqrt{L}}\sum_k e^{-ijk}\, x(k) \quad ,$$

$$p_j = \frac{1}{\sqrt{L}}\sum_k e^{-ijk}\, p(k) \quad , \tag{A.2}$$

where L is the volume, k ranges over $2\pi\, n_k/L$, $0 \le n_k < L$, and $x(k)$; $p(k)$ satisfy the canonical commutation relations

$$\left[p(k), x(k')\right] = i\delta_{k+k'} \quad . \tag{A.3}$$

[Due to the existence of a momentum lattice cutoff, a Kronecker delta involving momenta is always modulo 2π.]

We rewrite in terms of annihilation and creation operators

$$H = \sum_k \left[2(1 - \cos k)\right]^{1/2}\left[a^\dagger(k)\, a(k) + \frac{1}{2}\right] + H_I \quad , \tag{A.4}$$

where H_I is the interaction part

$$H_I = -\frac{1}{4!}\ \lambda^{-1/2} \sum_j \left(x_{j+1} - x_j\right)^4 + \frac{1}{6!}\ \lambda^{-1} \sum_j \left(x_{j+1} - x_j\right)^6 \quad . \qquad (A.4)'$$

$a(k)$, $a^\dagger(k)$ are defined in the usual way, namely

$$\begin{aligned} x(k) &= \left[2\omega(k)\right]^{-1/2} \left[a(k) + a^\dagger(-k)\right] \quad , \\ p(k) &= i\left[\frac{\omega(k)}{2}\right]^{1/2} \left[a^\dagger(k) - a(-k)\right] \quad , \end{aligned} \qquad (A.5)$$

where

$$\omega(k) = \left[2(1 - \cos k)\right]^{1/2} \quad . \qquad (A.6)$$

The effects of H_I are treated perturbatively by means of Feynman diagrams. Since this is a routine calculation, we skip the gory details and highlight the main steps in the derivation.

H_I in momentum basis. For the quartic term in H_I we have

$$\begin{aligned} \sum_j \left(x_{j+1} - x_j\right)^4 = \frac{1}{L} \sum_{\{k_a\}} \delta\left(\sum_{a=1}^4 k_a\right) \prod_a \Bigg\{ a(k_a)\left[e^{-ik_a} - 1\right] \\ \times \left[2\omega(k_a)\right]^{-1/2} \Bigg\} + \text{crossed terms} \quad , \end{aligned} \qquad (A.7)$$

where by 'crossed terms' we mean those obtained through the replacement

$$a(k) \to a^\dagger(-k)$$

in one or more of the four momenta. A similar expansion holds for the second term in H_I.

Normal ordering. The interaction terms H_I are not normal-ordered, and in the process of normal ordering them self-energy terms arise. Those can be eliminated by a Bogoliubov-Shirkov transformation: we define new operators,

$$\begin{aligned} a(k) &= vb(k) + ub^{\dagger}(-k) \quad , \\ a(k) &= v^{*}b^{\dagger}(k) + u^{*}b(-k) \quad , \\ |v|^2 - |u|^2 &= 1 \quad ; \end{aligned} \tag{A.8}$$

u and v are chosen to eliminate b(k)b(-k) terms in H.

Let y_j be a new field, with canonical momentum π_j, defined in terms of b and $b^{\dagger}$; in the momentum basis,

$$\begin{aligned} y(k) &= \left[\frac{1}{2\omega(k)}\right]^{1/2}\left[b(k) + b^{\dagger}(-k)\right] \quad , \\ \pi(k) &= i\left[\frac{\omega(k)}{2}\right]^{1/2}\left[b^{\dagger}(k) - b(-k)\right] \quad . \end{aligned} \tag{A.9}$$

Our results are:

$$\begin{aligned} u &= -\frac{1}{4\pi\lambda^{1/2}} + \frac{3}{4\pi^2\lambda} + O\left(\lambda^{-3/2}\right) \quad , \\ v &= 1 + \frac{1}{32\pi^2\lambda} + O\left(\lambda^{-3/2}\right) \quad , \\ H' &= L\cdot\left(\frac{2}{\pi} - \frac{1}{2\pi^2\lambda^{1/2}} + \frac{1}{3\pi^3\lambda}\right) + \left(1 + \frac{1}{2\pi\lambda^{1/2}} - \frac{21}{32\pi^2\lambda}\right) \\ &\quad \times \sum_k \omega(k)\, b^{\dagger}(k)\, b(k) - \lambda^{-1/2}\left(1 - \frac{3}{2\pi\lambda^{1/2}}\right)\frac{1}{4!} : \sum_j \left(y'_{j+1} - y'_j\right)^4 : \\ &\quad + \lambda^{-1}\,\frac{1}{6!} : \sum_j \left(y'_{j+1} - y'_j\right)^6 : + O\left(\lambda^{-3/2}\right) \quad , \end{aligned} \tag{A.10}$$

where the colons mean normal-ordering with respect to the b-s and we have reinserted the primes. The rest of the calculation is straightforward, old-fashioned perturbation theory; the results for ground-state energy density and long-range correlation function are

$$\begin{aligned} \rho_{g.s.} &= \frac{1}{L} \langle H \rangle_{\text{ground state}} \\ &= \sqrt{\lambda}\left[\frac{2}{\pi} - \frac{1}{2\pi^2}\lambda^{-1/2} + \lambda^{-1}\left(\frac{1}{3\pi^3} + I\right) + O\left(\lambda^{-3/2}\right)\right] , \\ C(n) &= \left\langle \cos\left(x_j - x_{j+1}\right)\right\rangle_{\text{ground state}} \\ &\xrightarrow[n >> 1]{} \left[\left(4 \exp\left\{\gamma_E\right\} n\right) \exp\left\{-\left[\frac{\lambda^{-1/2}}{2\pi} + \frac{\lambda^{-1}}{8\pi^2}\right]\right\}\right] + O\left(\lambda^{-3/2}\right) , \end{aligned} \tag{A.11}$$

where I is the Feynman integral resulting from the one-loop diagram:

$$\begin{aligned} I &= \frac{3}{1152\pi^3} \prod_{a=1}^{4} \int_{-\pi}^{\pi} dk_a \left[\prod_{a=1}^{4} \left| \sin\left(\frac{k_a}{2}\right)\right|\right] \\ &\times \delta\left(\sum_{a=1}^{4} k_a\right)\left[\sum_{a=1}^{4} \left| \sin\left(\frac{k_a}{2}\right)\right|\right]^{-1} \sim 0.03 . \end{aligned} \tag{A.12}$$

γ_E in (A.11) is Euler's constant, and the infinite-volume limit is understood.

APPENDIX B

{ℓ}-BASIS TRANSFER MATRIX FORMULAE

The matrices $\overleftrightarrow{A}$ and $\overleftrightarrow{B}$ appearing in (5.4.14) are:

$$\begin{aligned} \overleftrightarrow{A} &= \overleftrightarrow{A}_1 \cdot P \cdot \overleftrightarrow{A}_2 \quad , \\ \overleftrightarrow{B} &= \overleftrightarrow{P} \cdot \overleftrightarrow{A}_2 \quad , \end{aligned} \tag{B.1}$$

where P is the transfer matrix (5.4.6), and

$$\begin{aligned} A_1(L,L') &= \delta_{LL'} \exp\left\{-\frac{\delta_1}{2}\ \ell_2 - \frac{\delta_2}{2}\ \ell_1\right\} , \\ A_2(L,L') &= \theta\left(\ell_1 + 1\right) \delta_{LL'} \exp\left\{-2\beta\ell_1 - \frac{\delta_1}{2}\ \ell_2\right\} , \\ A_3(L,L') &= \delta_{LL'} \exp\left\{-\frac{\delta_2}{2}\ \ell_1\right\} . \end{aligned} \tag{B.2}$$

Here $\theta(n)$ is 0 if $n > \ell_c$ and 1 otherwise. L,L' are the variables enumerating the two-site blocks:

$$\begin{aligned} L &= \left(\ell_1, \ell_2\right) \quad , \\ L' &= \left(\ell_1', \ell_2'\right) \quad . \end{aligned} \tag{B.3}$$

Derivation of large-distance correlation. We now compute the exponential falloff of the correlation function C(n) for $n \gg 1$. The correlation is a special case of the expression on the left-hand side of (5.4.12), with

$$q_j = \begin{cases} 1 & 0 \le j < n \quad , \\ 0 & \text{otherwise} \quad ; \end{cases} \tag{B.4}$$

Thus

$$\left\langle \psi \middle| \cos(x_0 - x_n) \middle| \psi \right\rangle = \left\langle \psi \middle| \exp\left\{ i \sum_j q_j y_j \right\} \middle| \psi \right\rangle \quad .$$

From (5.4.1) and (B.4)

$$\sum_{jj'} q_j \, \Delta_1^{-1}(j - j') \, q_{j'} = 4\beta n + 2\delta_1(n-1) + 2\delta_2(n-2) \quad ;$$

(5.4.12) then yields

$$C(n) \equiv \left\langle \psi \middle| \cos(x_0 - x_n) \middle| \psi \right\rangle \tag{B.5}$$

$$= \exp\left\{ \frac{\delta_1}{2} + \delta_2 \right\} \exp\left\{ - \left(\beta + \frac{\delta_1}{2} + \frac{\delta_2}{2} \right) n \right\} (p_1)^{-n/2-1} \; \vec{V}_1^5 \cdot \overleftrightarrow{\Pi}_n \cdot \vec{V}_1 \, ,$$

where

$$\overleftrightarrow{\Pi}_n = \overleftrightarrow{F}_1 \cdot \left(\overleftrightarrow{E}^{\frac{n}{2}-3} \right) \cdot \overleftrightarrow{F}_2 \quad . \tag{B.6}$$

Here $\overleftrightarrow{F}_{1,2}$ are n-independent matrices, and

$$E(L,L') = \exp\left\{ - \left(\beta + \frac{\delta_1}{2} + \frac{\delta_2}{2} \right) \left(\ell_1 + \ell_2 + \ell_1' + \ell_2' \right) \right\} \tag{B.7}$$

$$\times \; \theta(\ell_1 + 1) \, \theta(\ell_2 + 1) \, \theta(\ell_1' + 1) \, \theta(\ell_2' + 1) \, P(L,L') \quad .$$

The above formulae readily yield (5.4.18); the matrices $\overleftrightarrow{F}_{1,2}$ are irrelevant for the asymptotic behavior.

APPENDIX C

QUASI-SPIN FORMULAE

We continue the derivation of the renormalization-group transformation in the quasi-spin formalism, begun in Section 7.2. By truncating the internal ('fast') block variables $x_-(j), S_j$ according to the decomposition (7.2.14), and using (7.2.17)-(7.2.18), we may truncate any operators that act on the spins and/or the x-variables. Let us truncate the general block operator,

$$M_{r_1'r_2';r_1r_2}(x_-,p_-) = f(x_-,p_-)\,\mu^{I}_{r_1'r_1}\,\mu^{II}_{r_2'r_2} \tag{C.1}$$

where I and II act on the first (1) and second (2) sites of the block, respectively. Integrating over x_- and summing over S and S', we get the truncated spin matrix acting on the total block spin:

$$(M_{tru})_{R'R} =$$

$$= \sum \int dx_- G_{2r_1'-R'}(x_-)\,\exp\left\{i\left(\frac{R'}{2}-r_1'\right)x_-\right\} M_{r_1'(R'-r_1');r_1(R-r_1)}(x_-,p_-)$$

$$\times \exp\left\{i\left(r_1-\frac{R}{2}\right)x_-\right\} G_{2r_1-R}(x_-)\; t_{R'r_1'(R'-r_1')}\; t_{Rr_1(R-r_1)}$$

$$= \sum_{r_1r_1'} C_f(2r'-R;2r_1-R)\,\mu^{I}_{r_1'r_1}\,\mu^{II}_{(R'-r_1')(R-r_1)}\; t_{R'r_1'(R'-r_1')}\; t_{Rr_1(R-r_1)} \tag{C.2}$$

where

$$C_f(S';S) = \int_0^{4\pi} dx_-\, G_{S'}(x_-)\exp\left\{-iS'\frac{1}{2}x_-\right\} f(x_-,p_-)\exp\left\{iS\frac{1}{2}x_-\right\} G_S(x_-)\ .$$

In arriving at (C.2) we have also made use of (7.2.15). It is straightforward, although tedious, to iterate the matrices $\overleftrightarrow{\mathcal{O}}_1$, $\overleftrightarrow{\mathcal{O}}_2$ characterizing the Hamiltonian $H^{(n)}$. From the field-reflection and space-reflection symmetries, we have proven that for all n,

$$\begin{aligned} \left(\mathcal{O}_1\right)_{r'r} &= \delta_{r',r}\, D(r) \\ \left(\mathcal{O}_1\right)_{r'r} &= \delta^{m}_{r'_1,r-1}\, E(r) \end{aligned} \tag{C.3}$$

There are thus 2^{n+1} parameters describing the Hamiltonian $H^{(n)}$. δ^m is a Kronecker delta modulo 2^n.

Summations. All sums over r_1, r'_1 range from 0 to $2^n - 1$, and are treated modulo 2^n.

From (7.2.17), (C.2) and (C.3) we find

$$\begin{aligned} D^{(n+1)}(R) = \sum_{r_1=1}^{2^n} \left[t_{Rr_1}(R-r_1)\right]^2 \left\{\left[\frac{(2r_1-R)^2}{4} + \int dx\_\, G'^2_{2r_1-R}\right] 2^{-n} + D^{(n)}(r_1)\right\} \\ - \sum_{r_1,r'_1=1}^{2^n} t_{R(r_1-1)(R-r_1+1)}\, t_{Rr_1(R-r_1)}\, E(r_1)\, E(R-r_1+1)\, C(2r_1-R)\ , \end{aligned} \tag{C.4}$$

$$E^{(n+1)}(R) = \sum_{r_1=1}^{2^n} t_{Rr_1(R-r_1)}\, t_{(R-1)r_1(R-1-r_1)}\, E(R+1-r_1)\, C_2(2R-r_1+1)\ ,$$

where

$$C_1(S) = \frac{1}{2}\int_0^{4\pi} dx_- \, G_S(x_-)\left[G_{S+2}(x_-)\, G_{S-2}(x_-)\right] \quad ,$$

$$C_2(S) = \int_0^{4\pi} dx_- \, G_S(x_-)\, G_{S+1}(x_-) \quad . \tag{C.5}$$

Minimal quasi-spin towers. The smallest spin towers consistent with field-reflection symmetry are of dimension three,

$$-1 \le r_j \le 1$$

Since under the symmetry, $r_j \to -r_j$. The exception is at n = 1, where $r_j = \pm 1$ are identical (r_j are defined modulo 2^n). But from (C.4)-(C.5) it is easy to prove that in that scheme, $\overleftrightarrow{\mathcal{O}}_2$ vanishes for $n \ge 3$ and the long-range renormalization group is thus trivial. If, however, we keep $-2 \le r_j \le 2$, and truncate $t_{Rr_1r_2}$ so that $-2 \le S_j \le 2$, the evolution is nontrivial. Due to the symmetries (7.2.25) of t, it has only five independent nonvanishing components in this minimal quasi-spin scheme; these are for the spin values listed in the table below.

R	S	r_1	r_2
0	0	0	0
0	2	1	-1
1	-1	0	1
2	0	1	1
2	-2	0	2

The t components, along with parameters characterizing the five periodic functions $G_S(x_-)$, are varied to minimize the trial energy in this scheme. All those parameters may also be expanded in powers of λ in the small-λ region.

Mean-Field Look Ahead. The crude guess for the slow-mode wave function, called for by the look-ahead approach, is chosen in the NBPG scheme to be the product state (7.4.12), where $F^{(n+1)}$ is the periodic Gaussian,

$$F_r^{(n+1)}(\tilde{x}) = \sum_{m=-\infty}^{\infty} \exp\left\{-i2^{n+1} m \tilde{x}\right\} \exp\left\{-\frac{4^{n+1}}{\delta'_{n+1}}\left(m - r2^{-n-1}\right)^2\right\} \quad , \quad (C.6)$$

where δ'_{n+1} is another parameter to be determined variationally.

Minimal scheme for $\lambda << 1$. For small couplings, we may neglect all but the lowest-lying quasi-spin components of A,R,C: thus the renormalization-group equations, (7.4.10), simplify. We retain only $-2 \leq R \leq 2$, and further neglect $A(\pm 2)$, $C(\pm 2)$, $R(2)$. Then by (7.4.15) we are left with only A(0), A(1), C(0), C(1), R(0), R(1) as independent parameters; and only their five ratios appear in physical quantities. The recursion-relations for small λ become:

$$A_{n+1}(1) \simeq 2\alpha_n A_n(1) \quad ,$$

$$C_{n+1}(0) \simeq C_n(0) - 2^{-n}\alpha_n^2 R_n(0)^2 + \alpha_n^4 \left[2\theta_{n1} A_n(1) C_n(1) + 4^{-n}\theta_{n1} A_n(1)^2 + \delta_{n0} \right] \quad ,$$

$$C_{n+1}(1) \simeq \alpha_n \left[\theta_{n1} C_n(1) + 4^{-n-1} A_n(1) - 2^{-n-1} R_n(0)^2 \right] \quad , \qquad \text{(C.7)}$$

$$R_{n+1}(0) \simeq \sqrt{\alpha_n}\ R_n(0) \quad ,$$

$$R_{n+1}(1) \simeq \sqrt{\alpha_n}\ R_n(0) A_n(1) \quad ,$$

where

$$\alpha_n = \exp\left\{ -\frac{1}{4\delta_n} \right\}$$

and

$$\theta_{nm} = \begin{cases} 0 & n < m \\ 1 & n \geq m \end{cases}$$

Unlike in a normal renormalization-group, n occurs explicitly in these recursions.

REFERENCES

1. J. M. Kosterlitz and D. J. Thouless, J. Phys. C6, 1181 (1973).

2. J. M. Kosterlitz, J. Phys. C7, 1046 (1974).

3. S. Elitzur, R. B. Pearson and Shigemitsu, Phys. Rev. D19, 3698 (1979).

4. J. V. Jose, L. P. Kadanoff, S. Kirkpatrick and D. R. Nelson, Phys. Rev. B16, 1217 (1977).

5. E. Fradkin and L. Susskind, Phys. Rev. D17, 2637 (1978); there a correspondence is pointed out between the vortices and kink configurations in one spatial dimension; our $\{M_j\}$ variables count such kinks.

6. In the two-dimensional vortex gas, there is a different volume element for the summation over the location of the 'small' pairs, and one should replace $\sum_r$ by $2\pi \sum_r r$, in both sums appearing in (6.2.10). This can easily be seen to lead to a screening of the logarithm coefficient in the propagator, at large distances.

FIGURE CAPTIONS

Fig. 1. A vortex in the Euclidean XY model.

Fig. 2. The function f(p).

Fig. 3. The energy density for pure Gaussian wave-function.

Fig. 4. 1/p vs. coupling λ for pure Gaussian wave-function.

Fig. 5. z vs. λ.

Fig. 6. $\rho_{g.s.}$ vs. λ.

Fig. 7. z_1, z_2 vs. λ.

Fig. 8. z vs. λ ($\{\ell\}$ basis).

Fig. 9. $\rho_{g.s.}$ vs. λ ($\{\ell\}$ basis).

Fig. 10. Correlation parameter α vs. λ.

Fig. 11. Parameter $e^{-\beta}$ vs. λ for $\ell_c = 1, 2, 3$ (going up).

Fig. 12. Parameter $\exp\{\delta_1/2\}$ vs. λ for $\ell_c = 2$ (dotted curve is $\ell_c = 3$).

Fig. 13. Parameter $\exp\{\delta_2/2\}$ vs. λ for $\ell_c = 2$ (dotted curve is $\ell_c = 3$).

Fig. 14. Ground-state energy density curves. Going from top to bottom: energy for the {m} basis mean-field, exhibiting the spurious transition (second order); mean-field, $\{\ell\}$ basis; transfer matrix results for $\ell_c = 1, 2, 3$ (last two are indistinguishable).

Fig. 15. Transfer-matrix results for α vs. λ, with $\ell_c = 2,3$.

Fig. 16. α,η vs. λ for $\ell_c = 2$.

Fig. 17. Additive screening constant vs λ'.

Fig. 18. Screening distance j_1 vs. λ'.

Fig. 19. From top to bottom: bare and screened propagators for $\lambda' = .19$.

Fig. 20. Effective coupling λ' vs. λ for the pure-Gaussian case. The critical point resulting from self-consistent screening is above the spurious critical point of Section 4.

Fig. 21. Again the $\{\ell\}$-basis energy results of Fig. 14, but with (NBPG) $\rho_{g.s.}$ superimposed (plotted curve).

Fig. 22. $-1/(4\delta_n)$ vs. $\ell n\ \lambda$ for $n_\ell = 1$ and $0 \le n \le 6$.

Fig. 23. $-1/(4\delta_n)$ vs. $\ell n\ \lambda$ for $n_\ell = 2$ and $0 \le n \le 4$.

Fig. 24. $-1/(4\delta_0)$ near $\ell n\ \lambda = \lambda_c$, for $n_\ell = 1, 2$.

Fig. 25. Exp $\{-1/(4\delta'_{n+1})\}$ vs. $\ell n\ \lambda$ for $0 \le n \le 4$, $n_\ell = 1$.

Fig. 26. Seven plots, of $-1/(4\delta_n(\lambda))$ vs. $\ell n\ \lambda$ for $0 \le n \le 6$, $n_\ell = 1$.

Fig. 27. From top to bottom: a,b and ground-state energy-density exhibiting a spurious first-order transition.

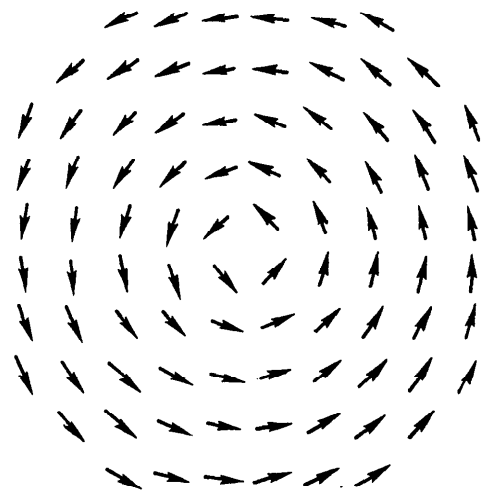

Fig. 1

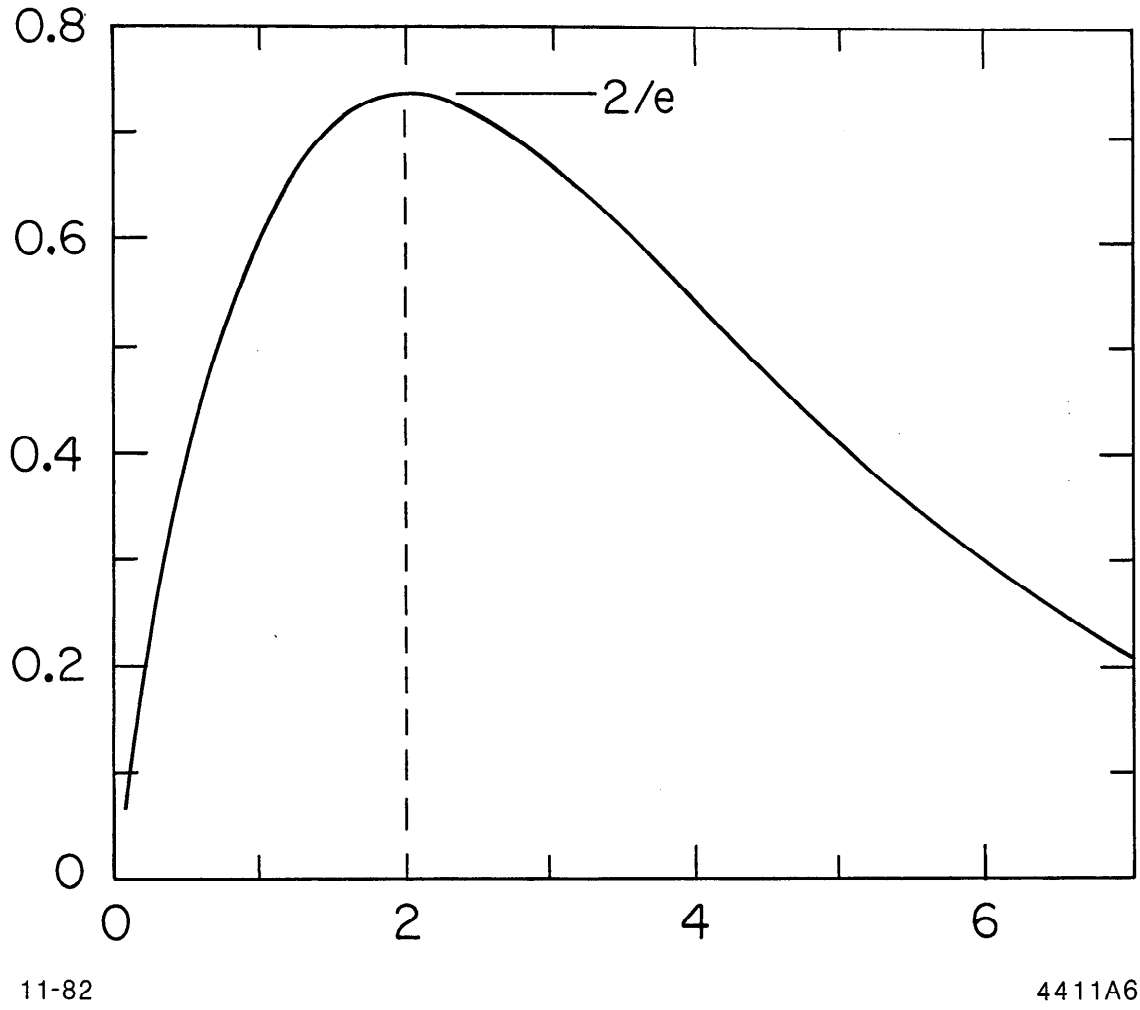

Fig. 2

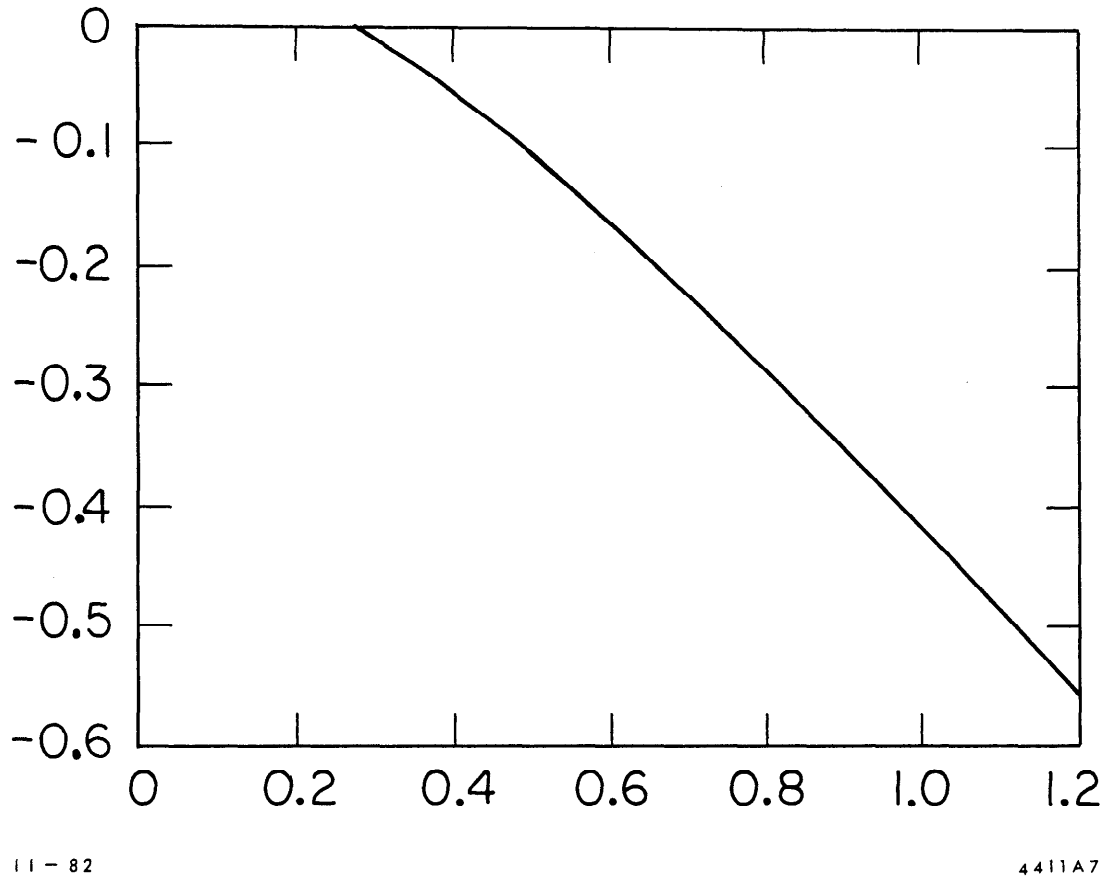

Fig. 3

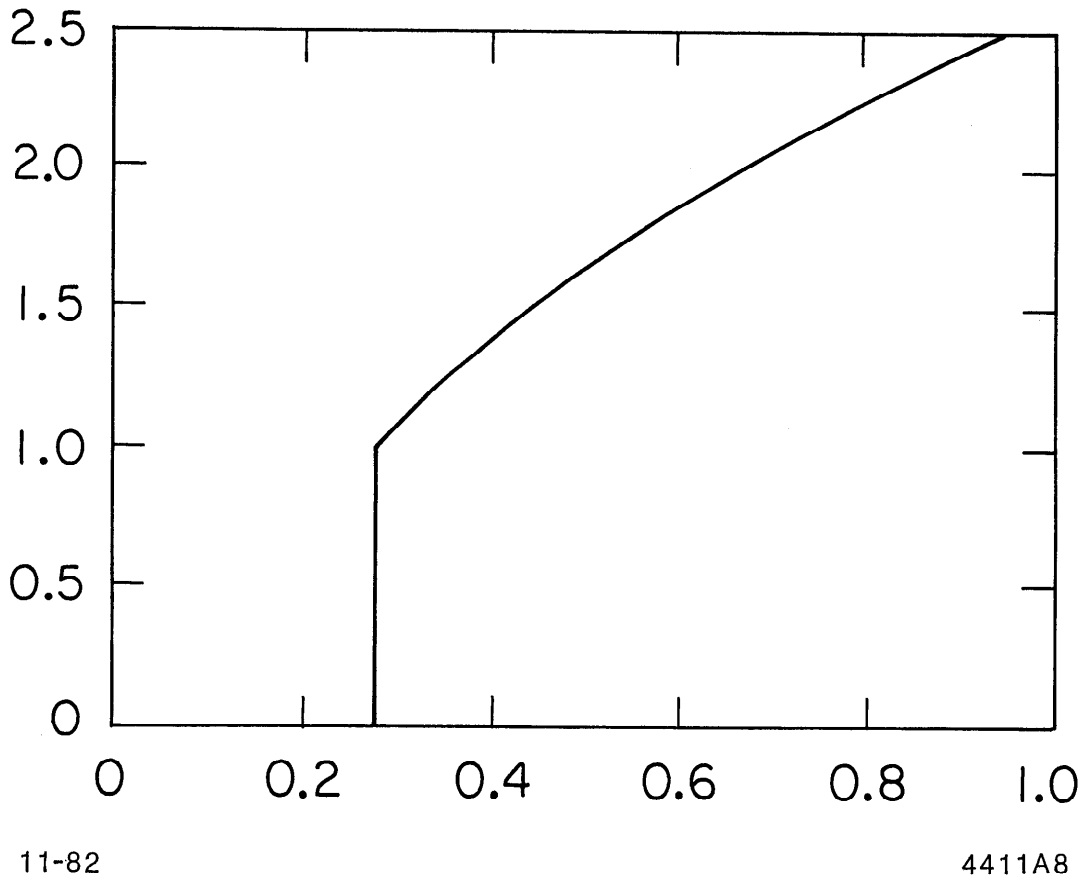

Fig. 4

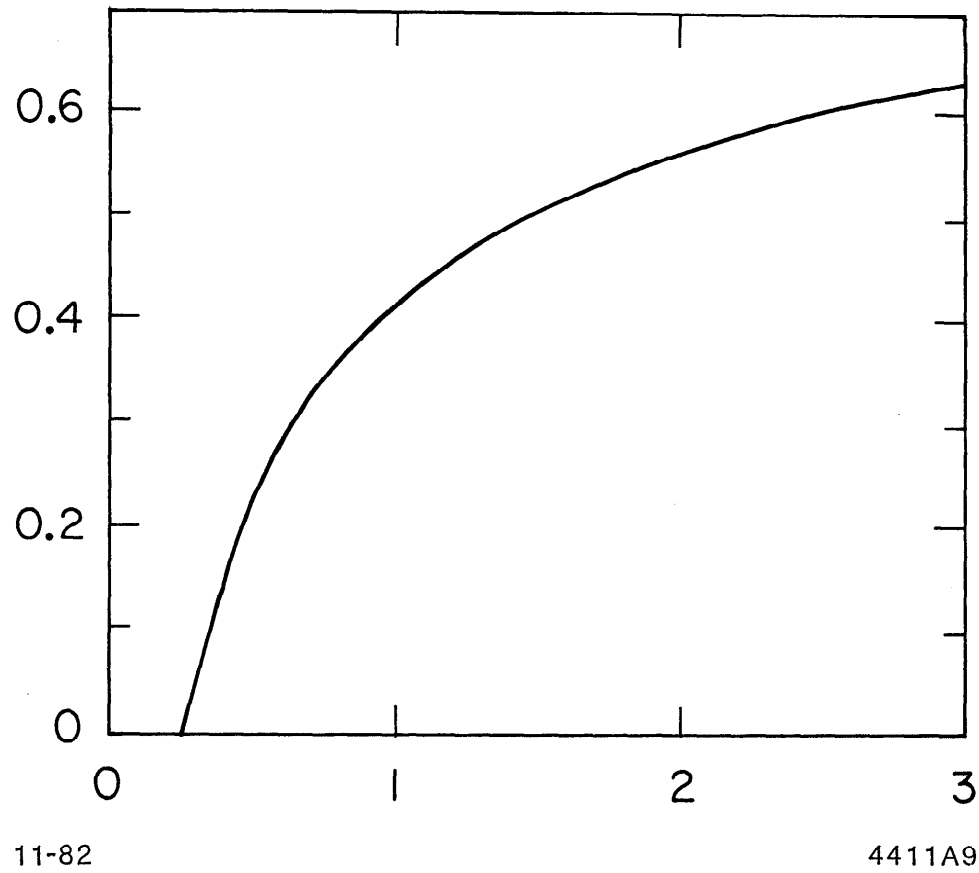

Fig. 5

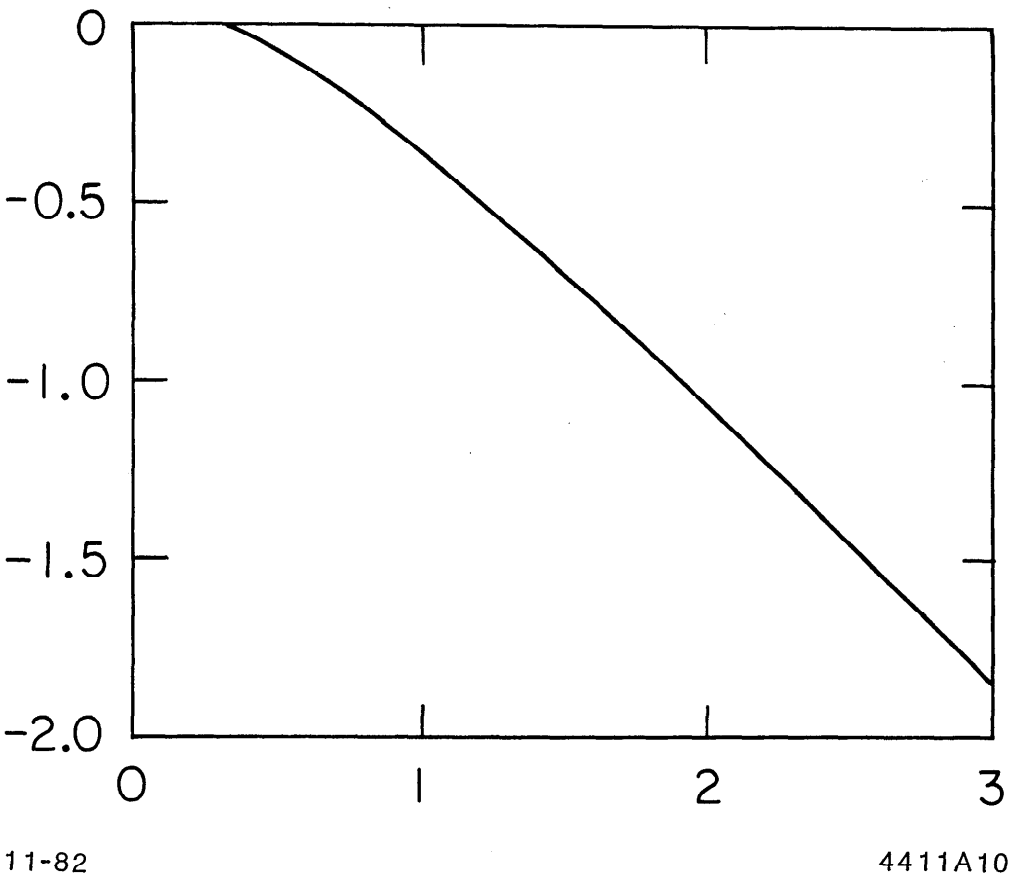

Fig. 6

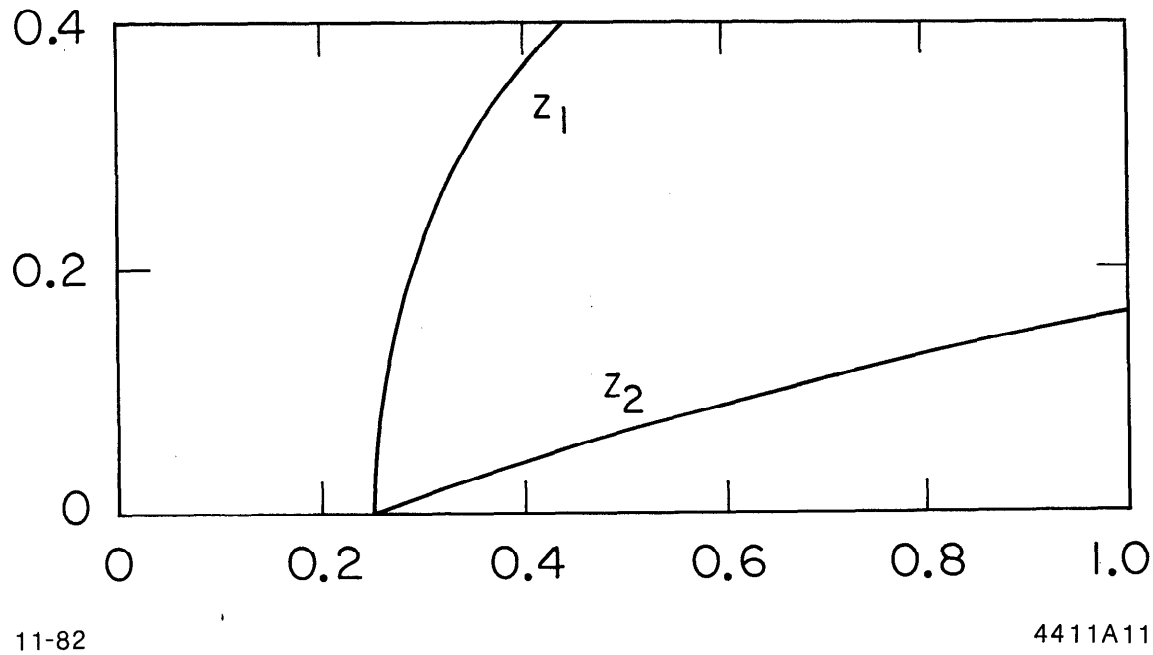

Fig. 7

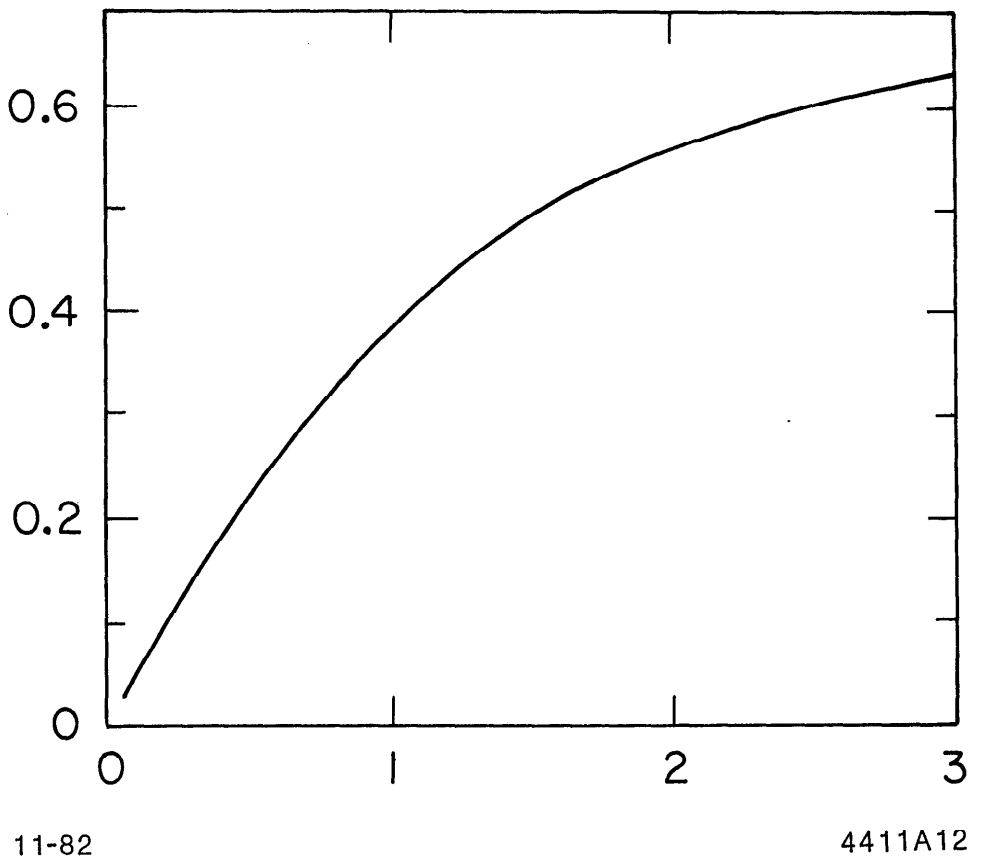

Fig. 8

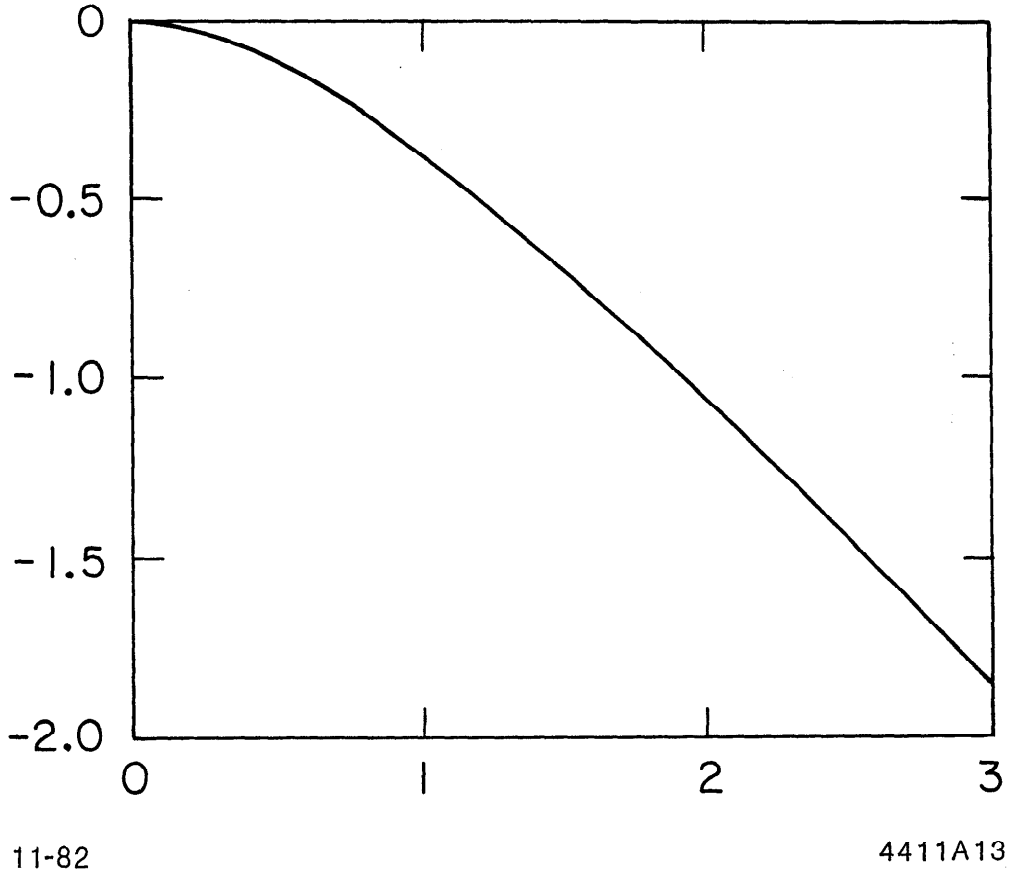

Fig. 9

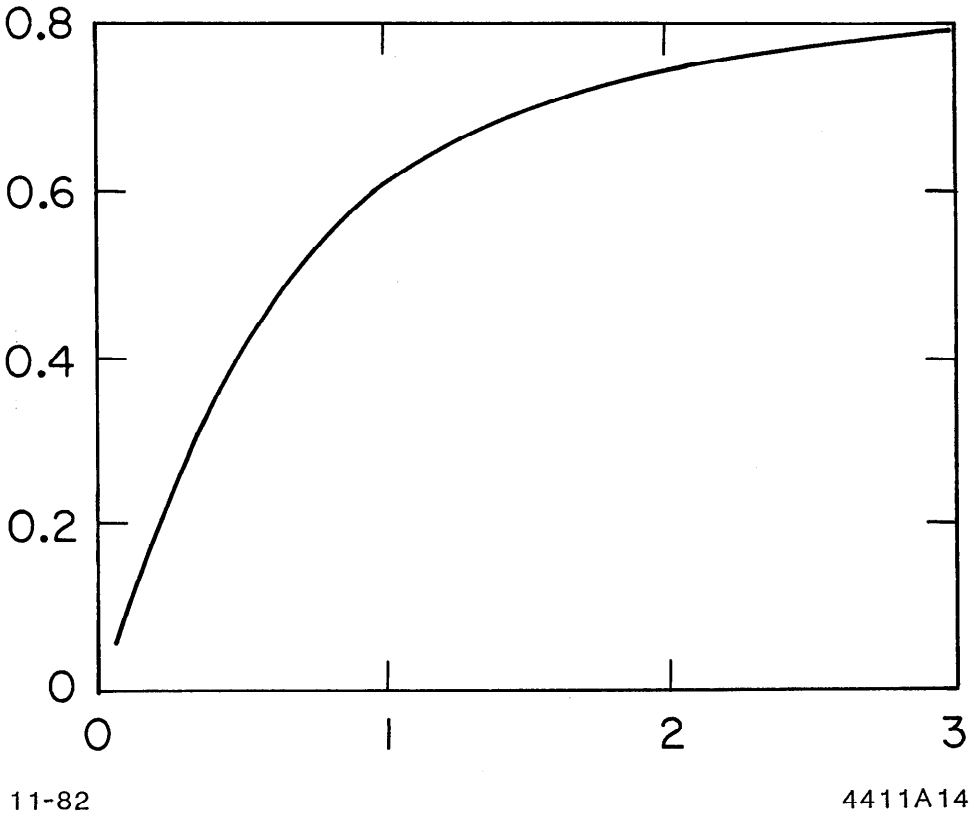

Fig. 10

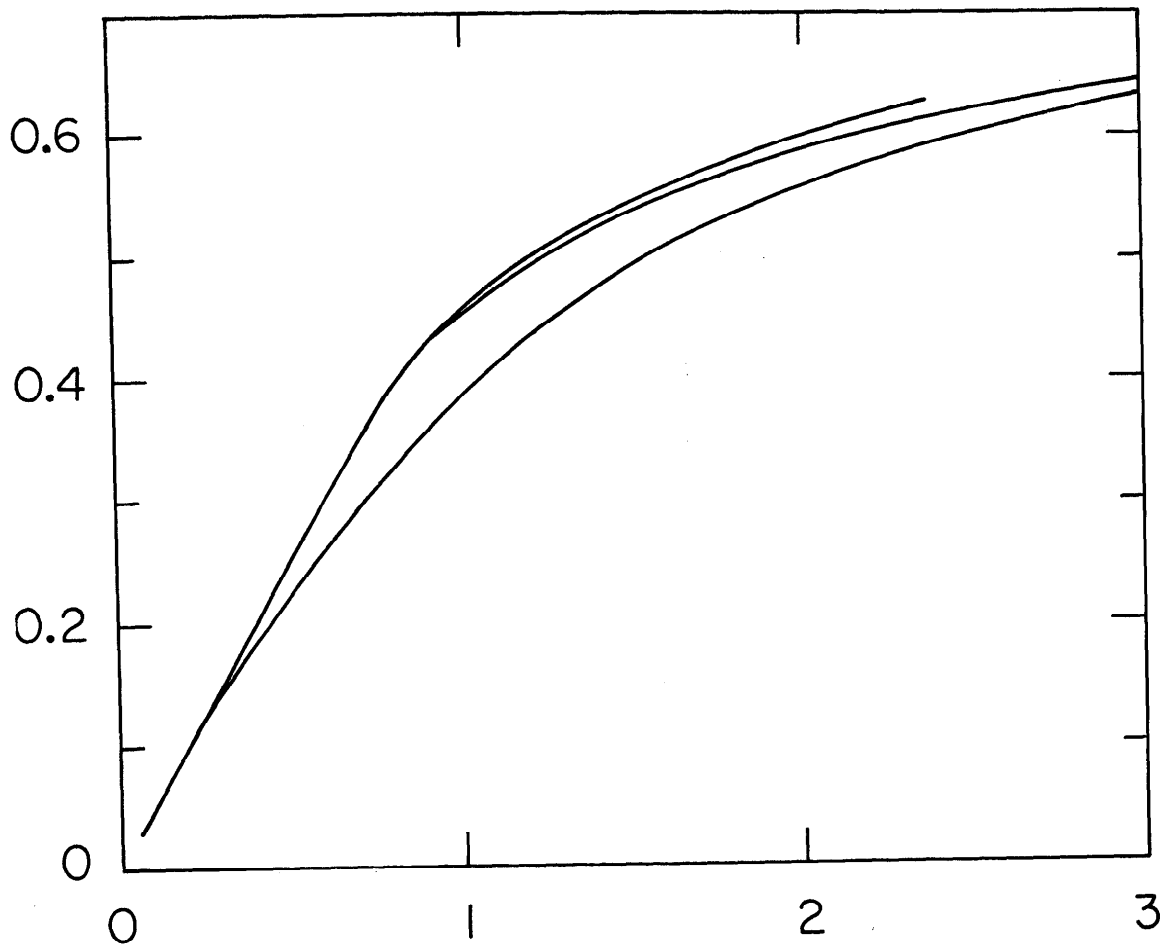

Fig. 11

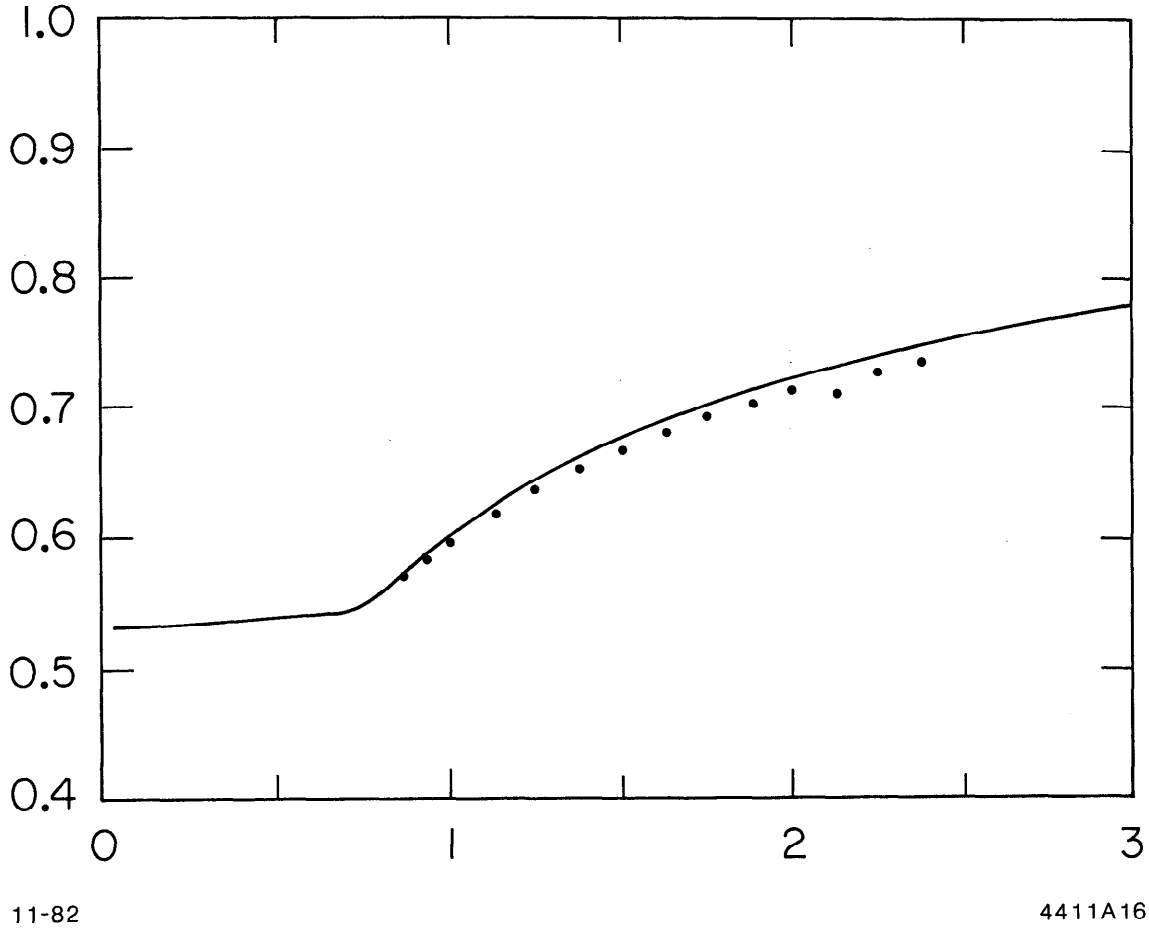

Fig. 12

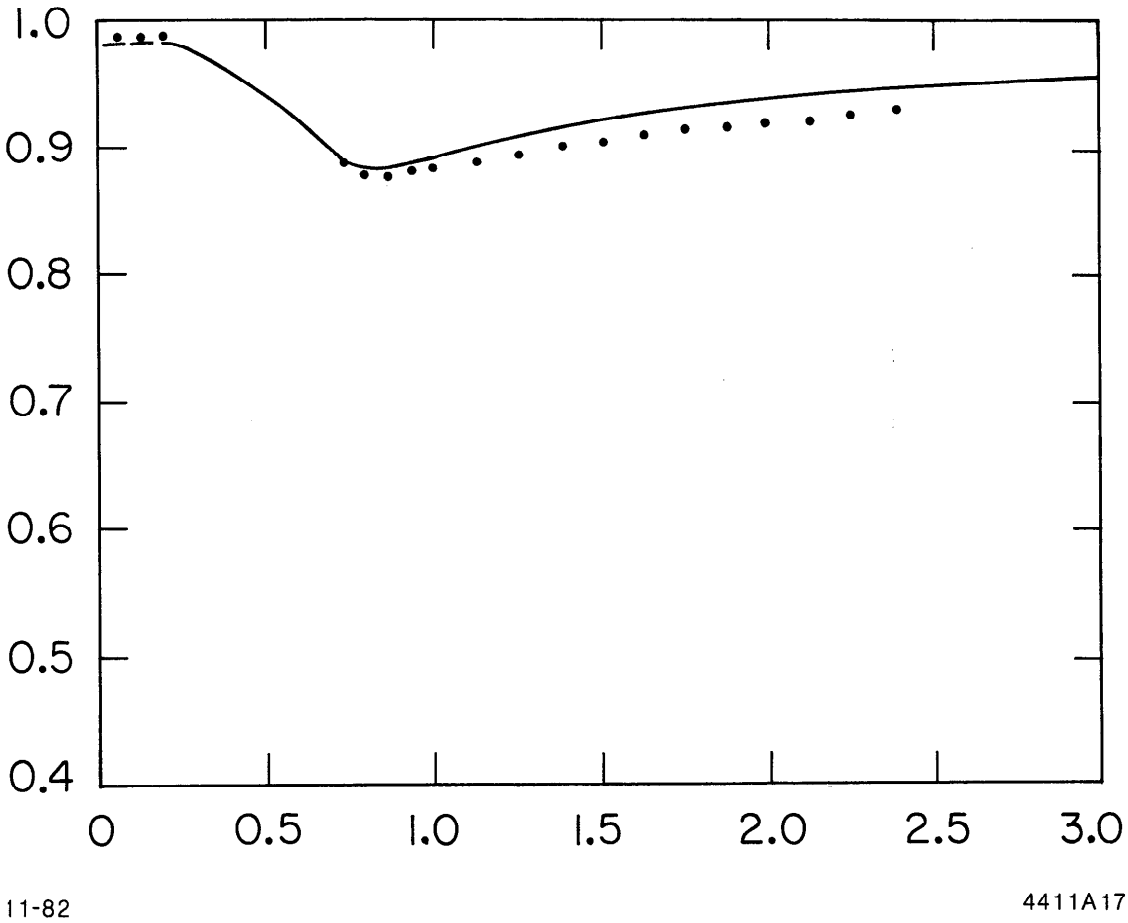

Fig. 13

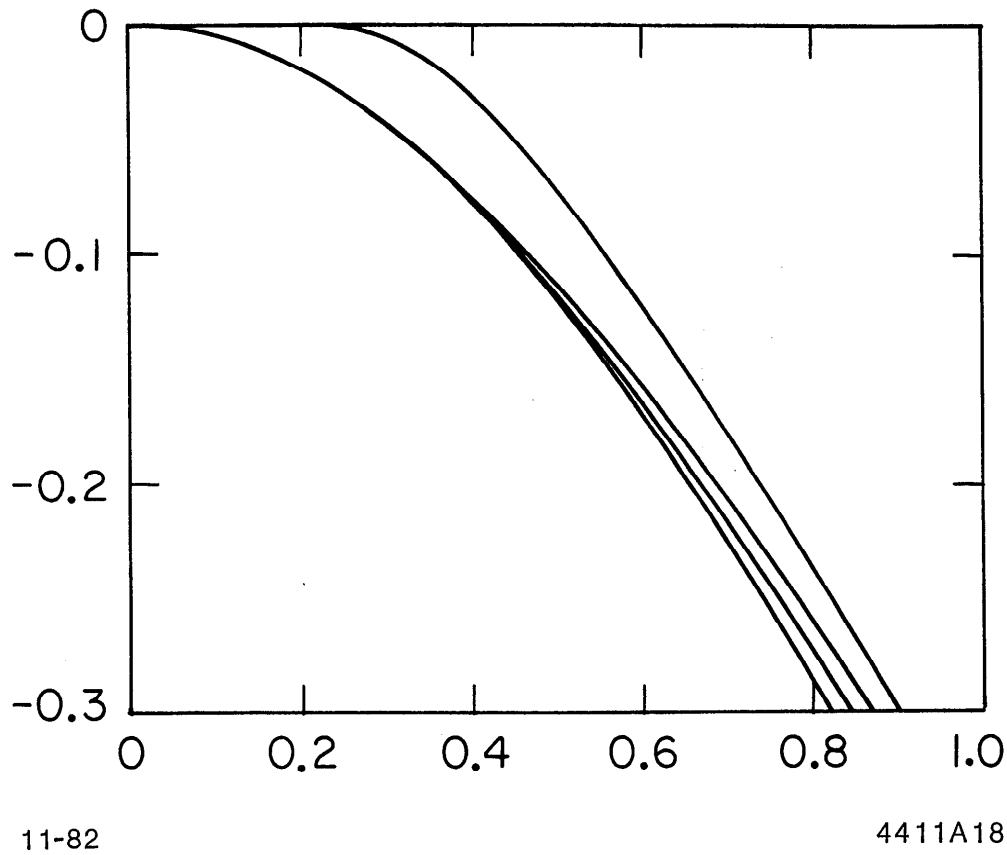

Fig. 14

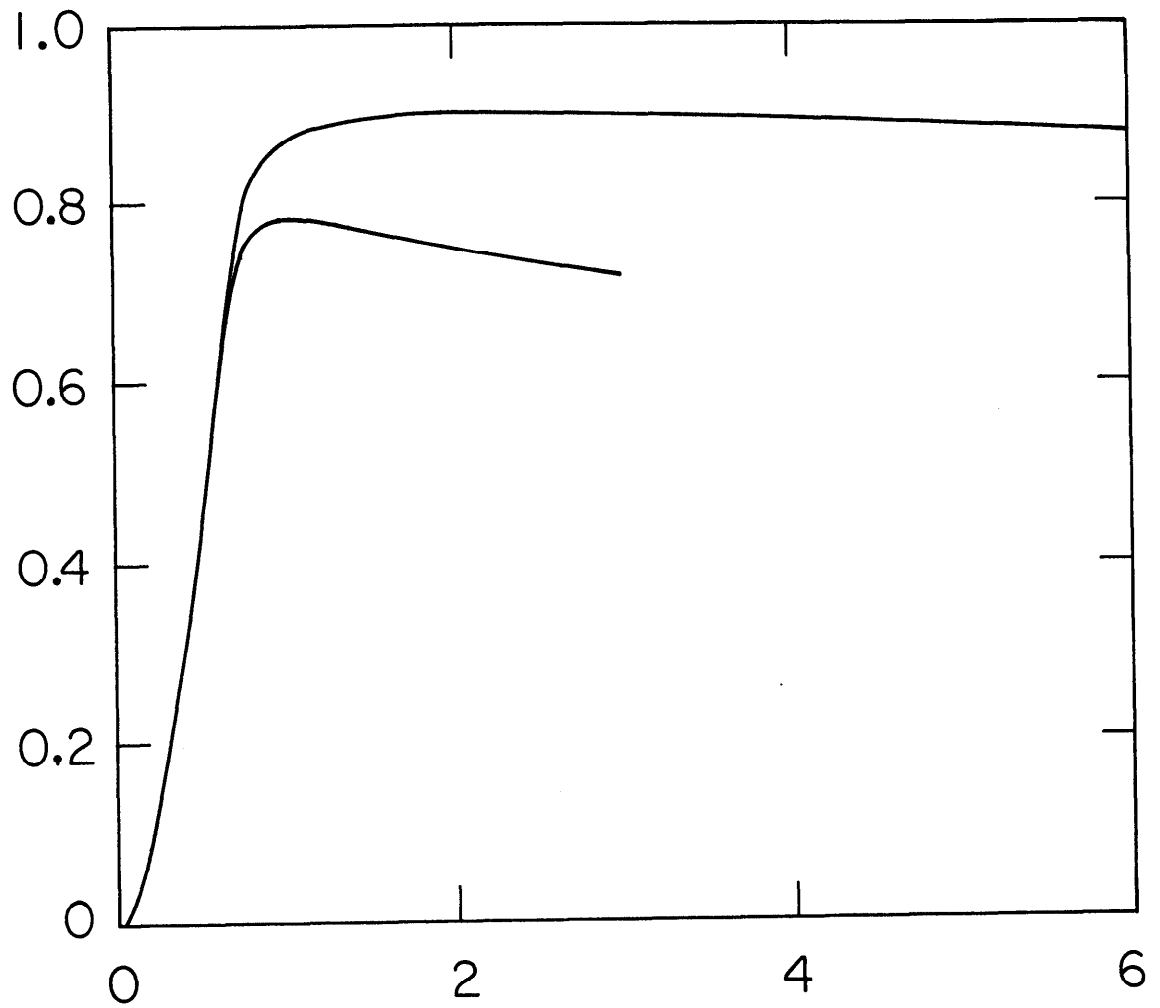

Fig. 15

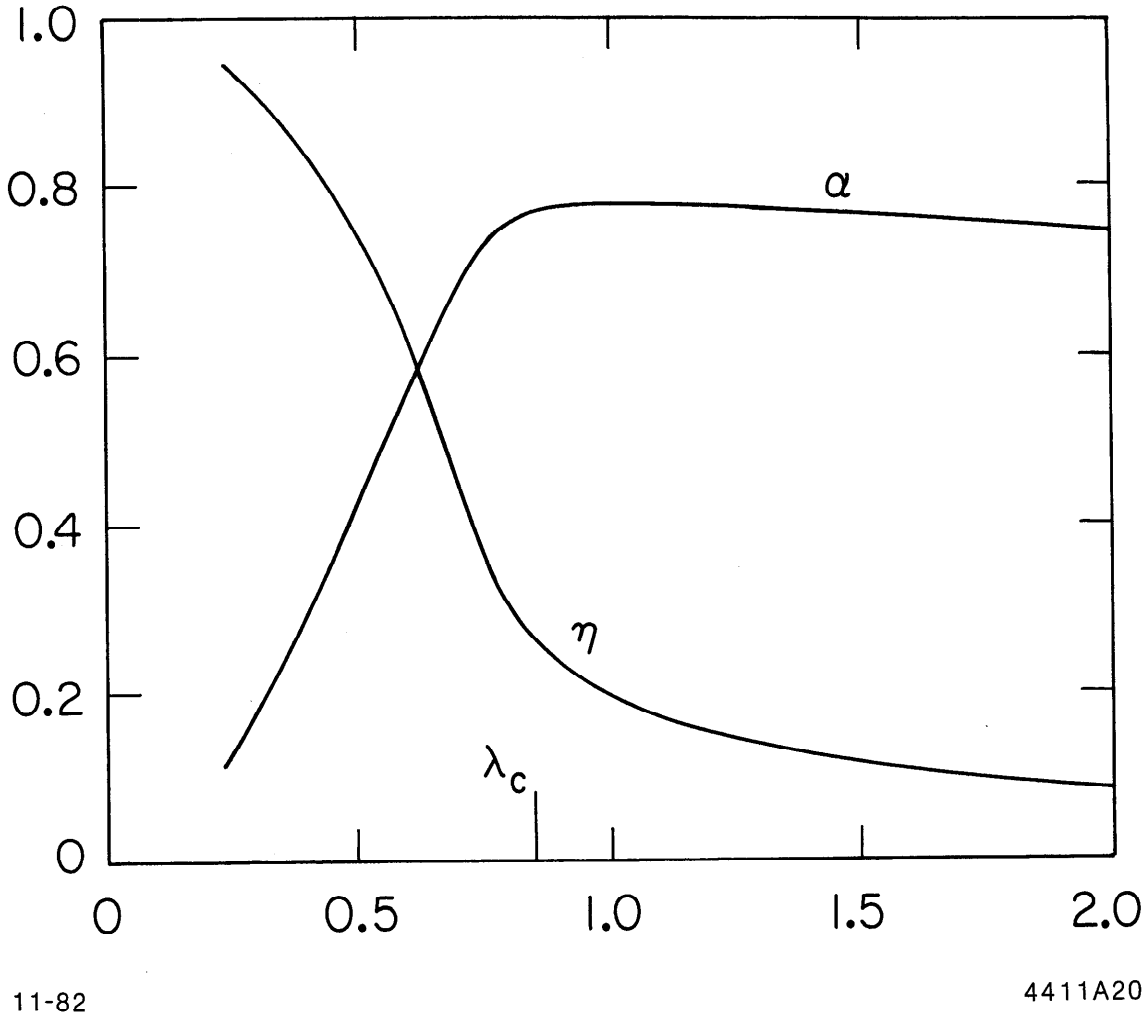

Fig. 16

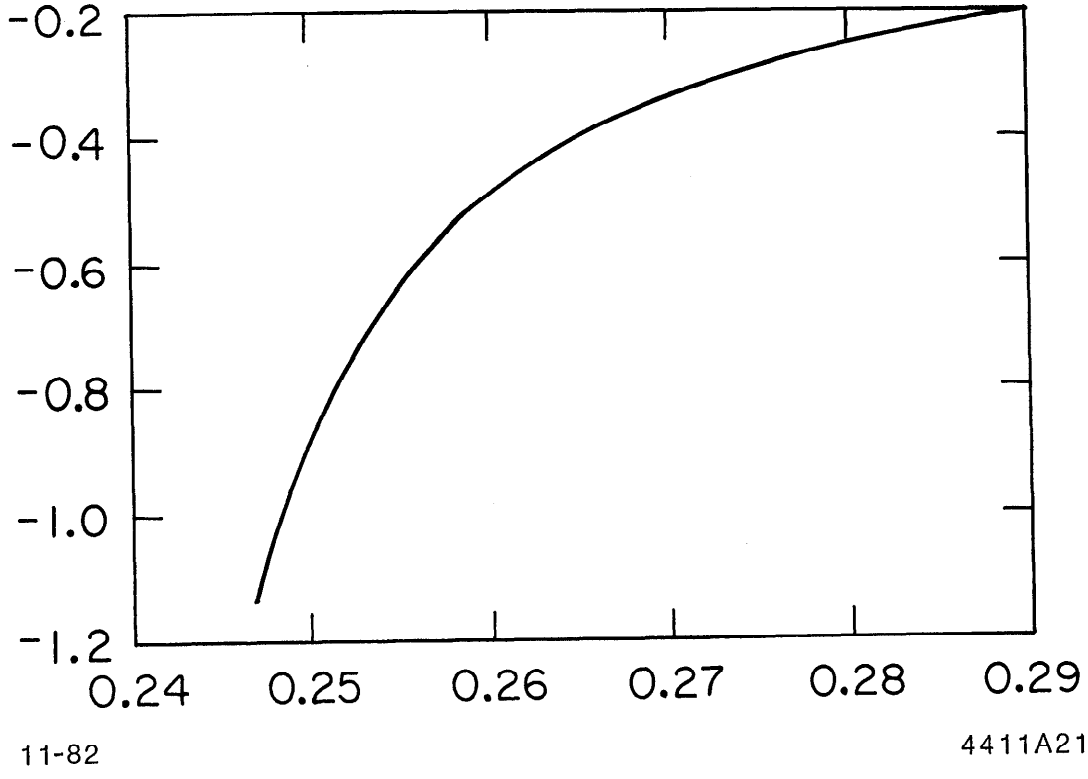

Fig. 17

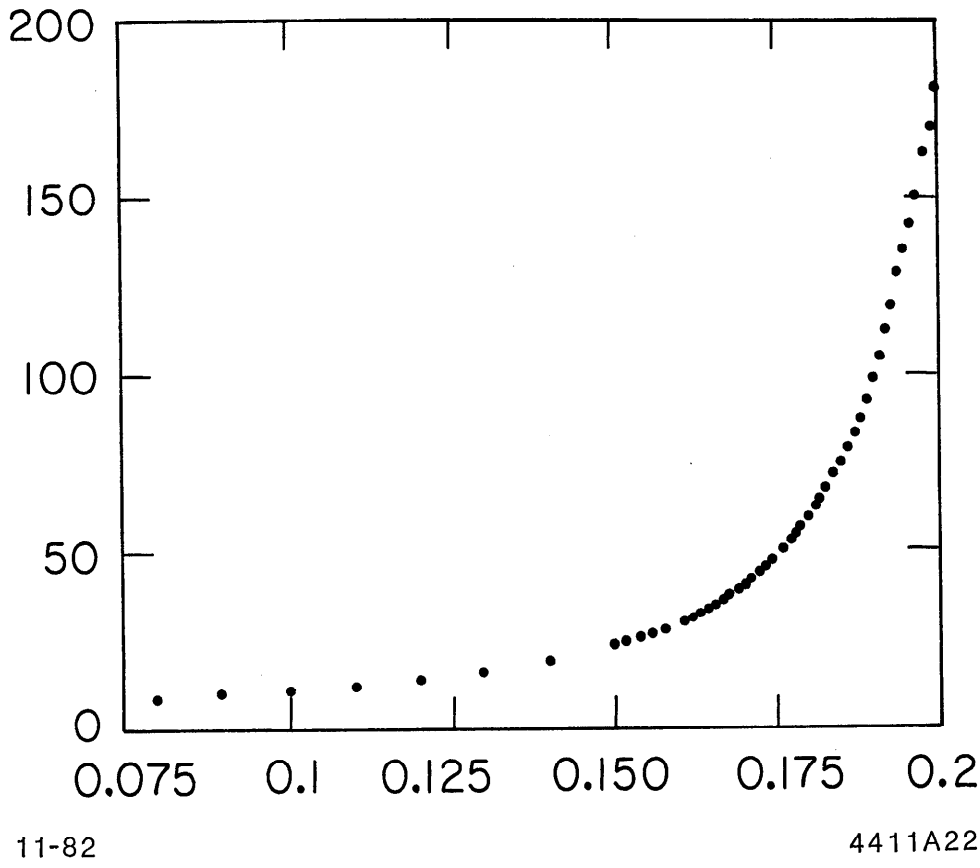

Fig. 18

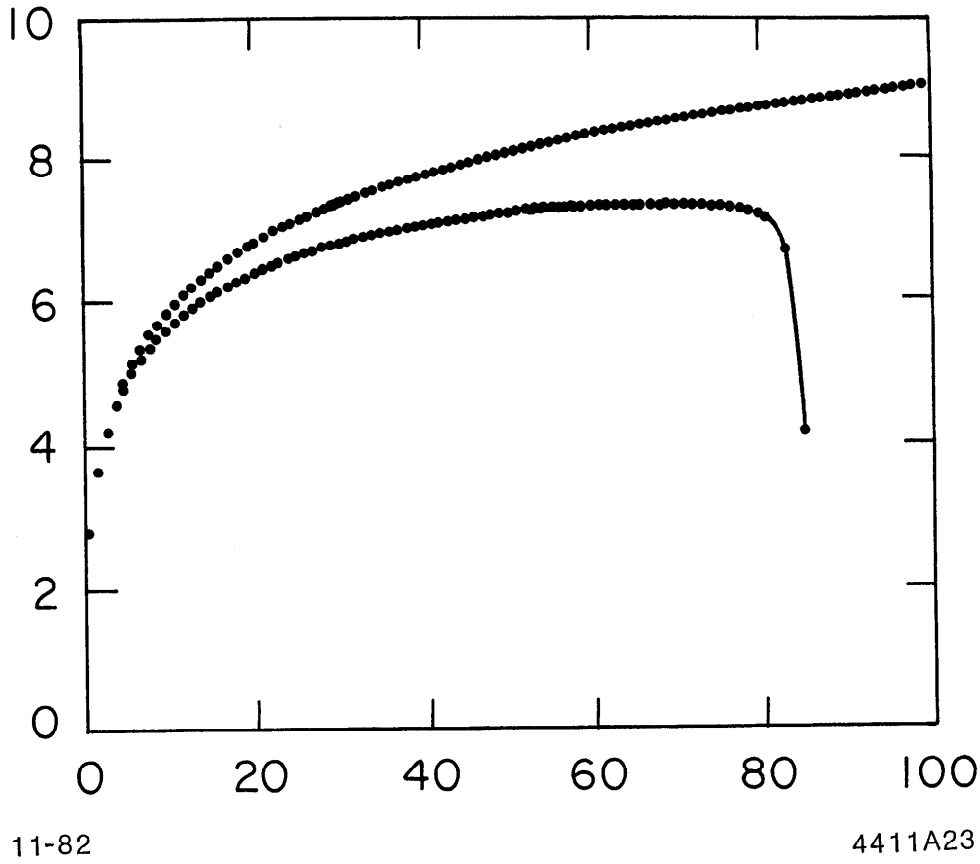

Fig. 19

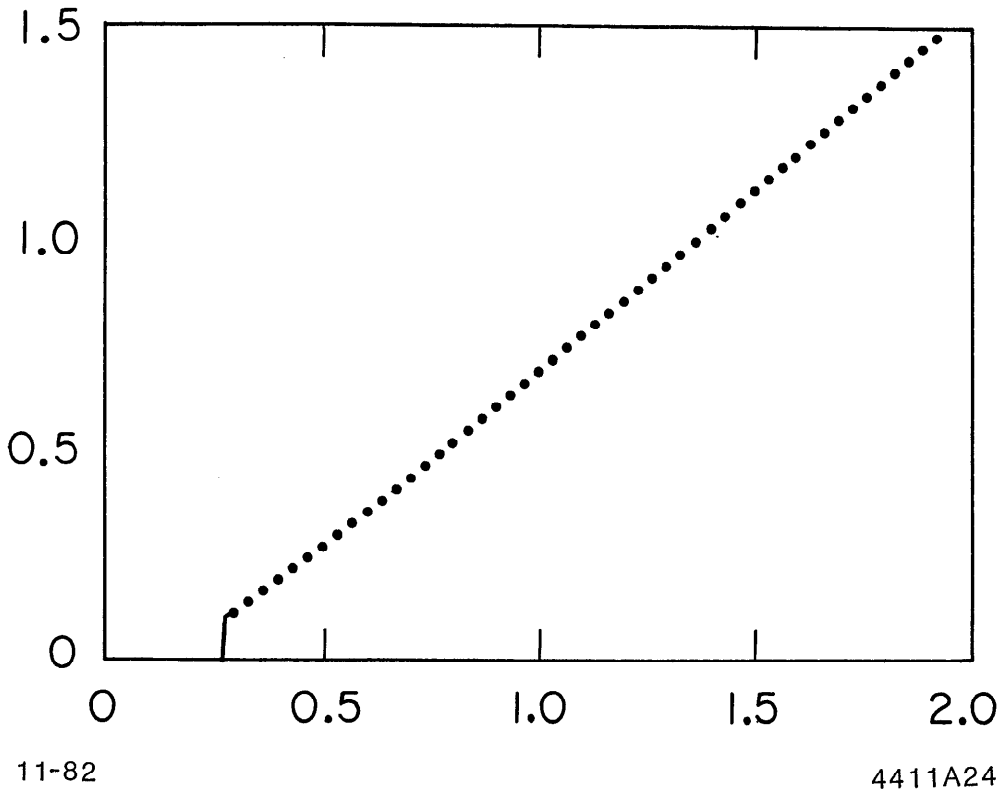

Fig. 20

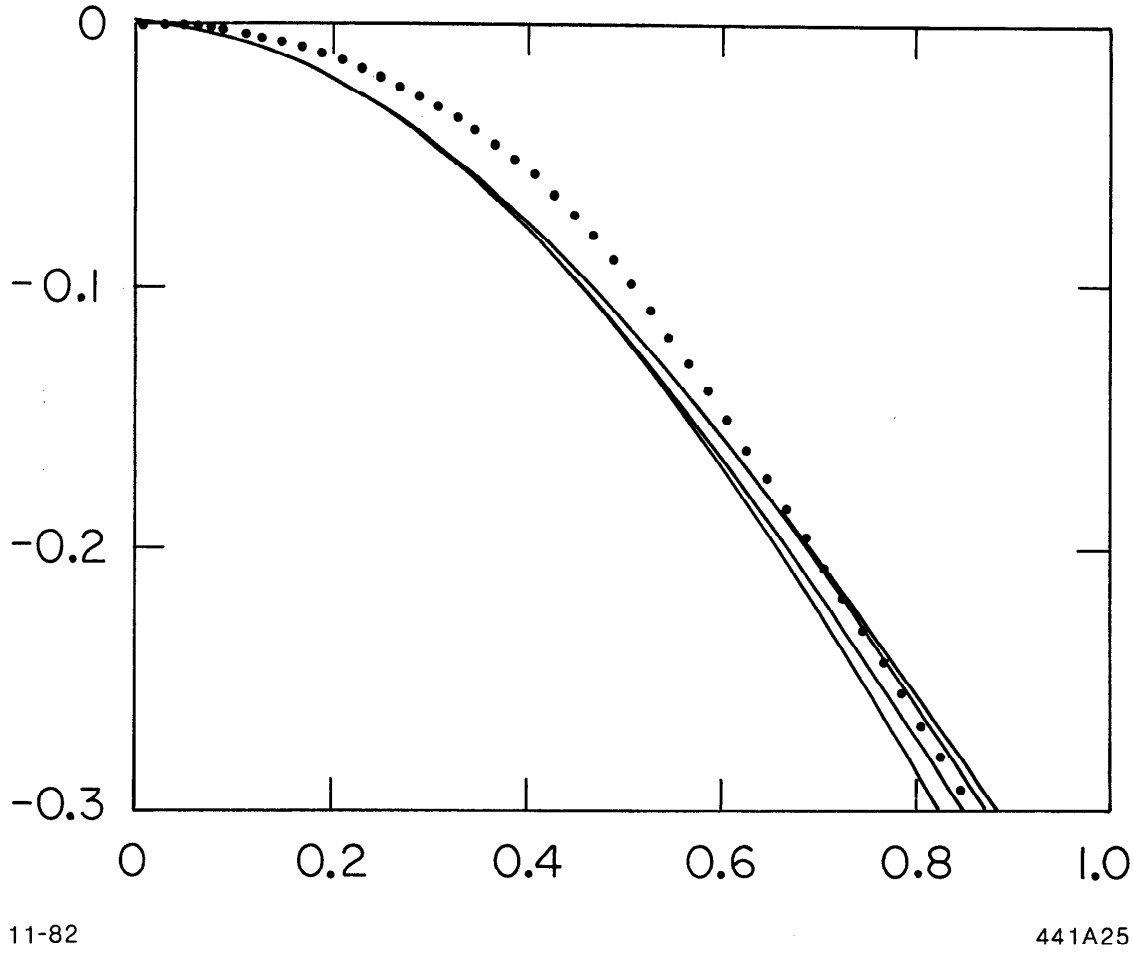

Fig. 21

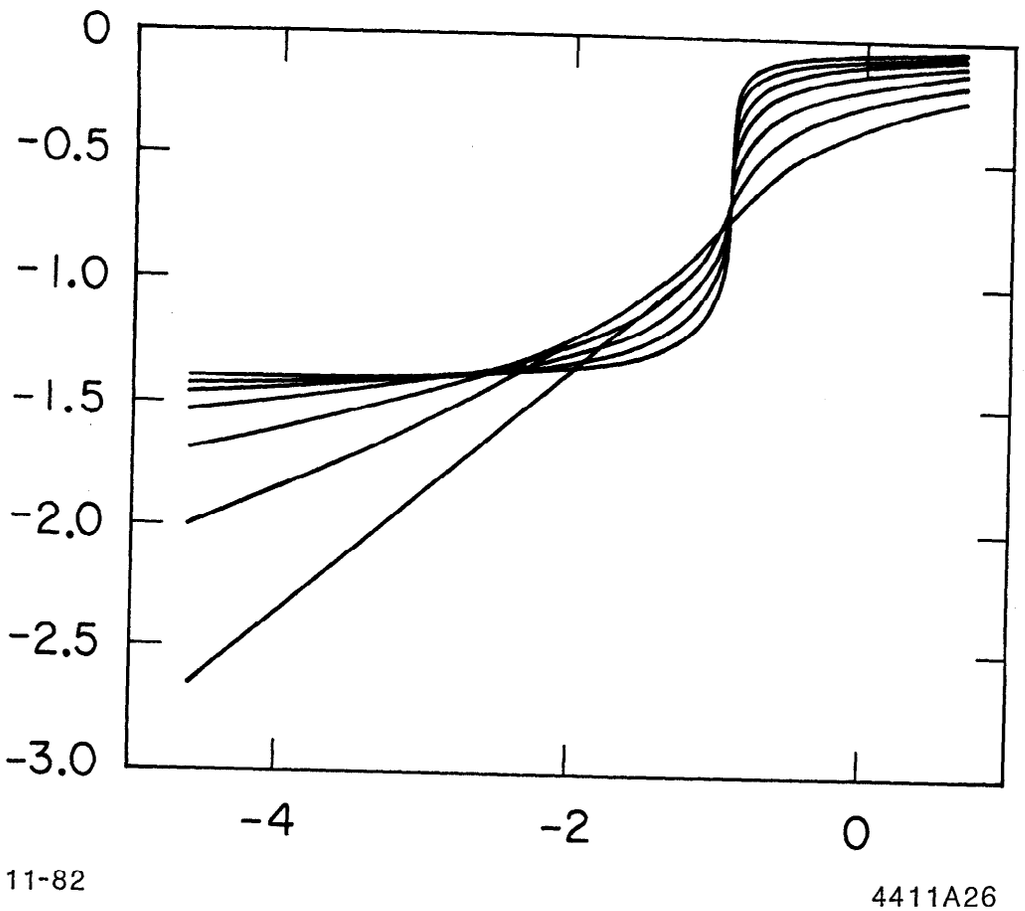

Fig. 22

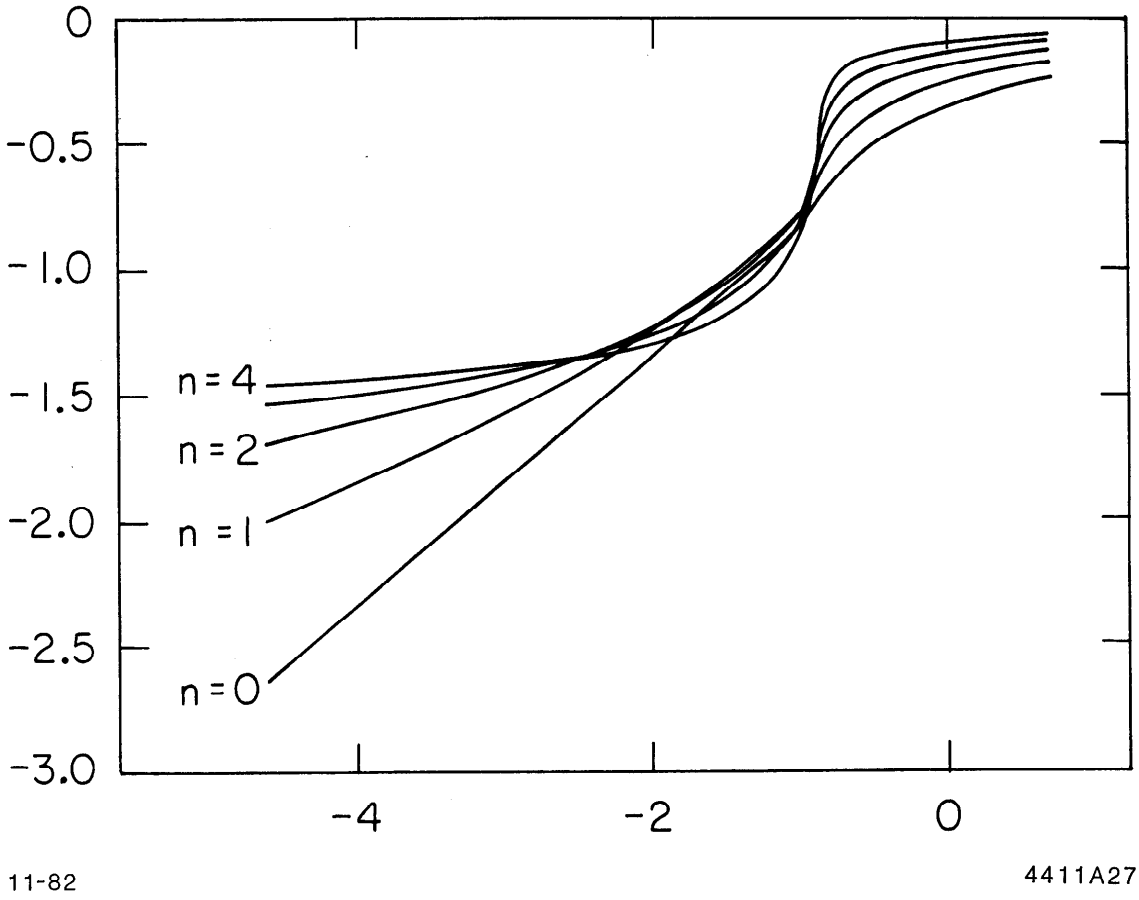

Fig. 23

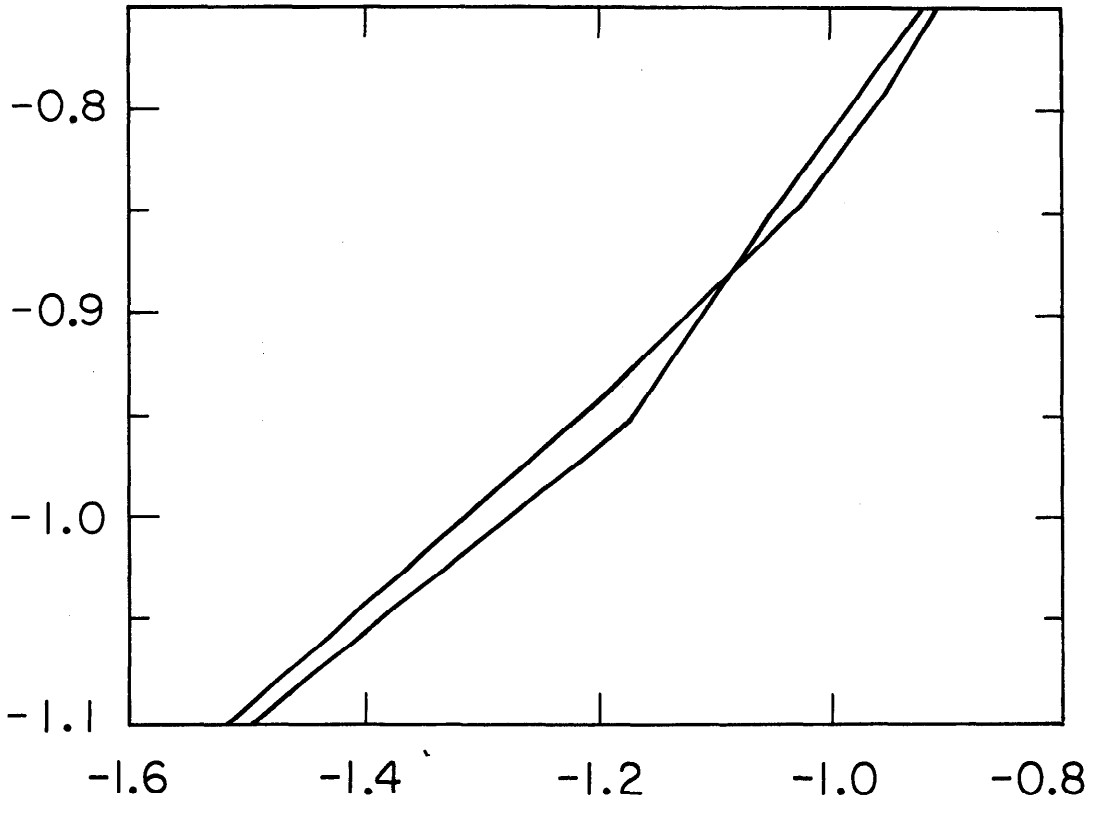

Fig. 24

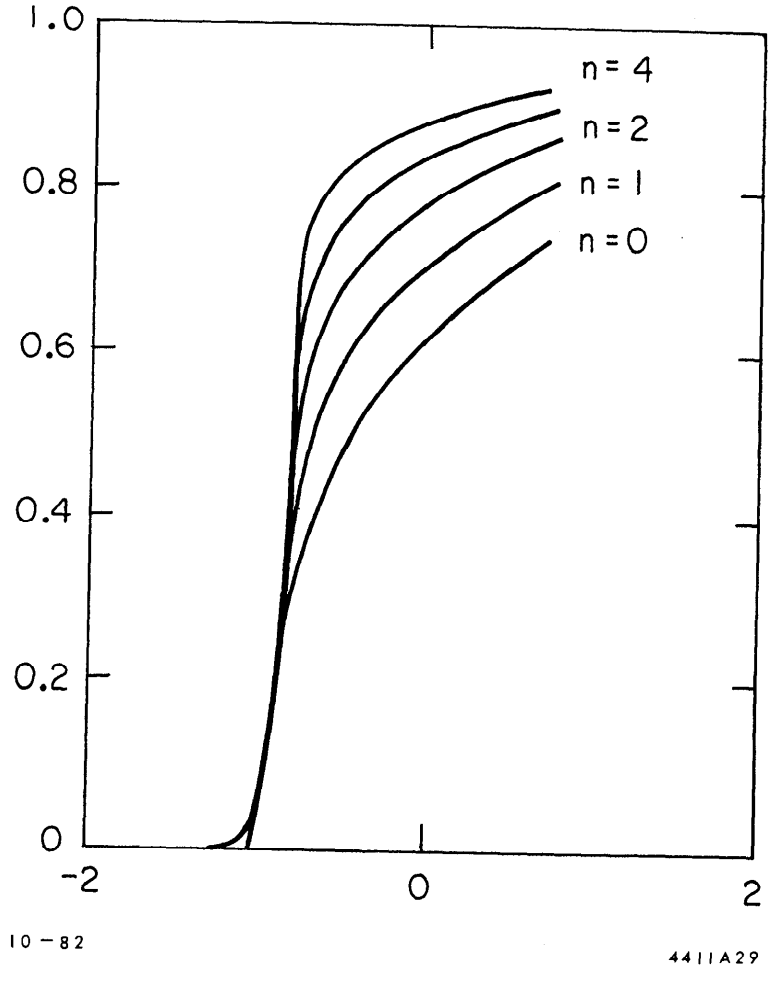

Fig. 25

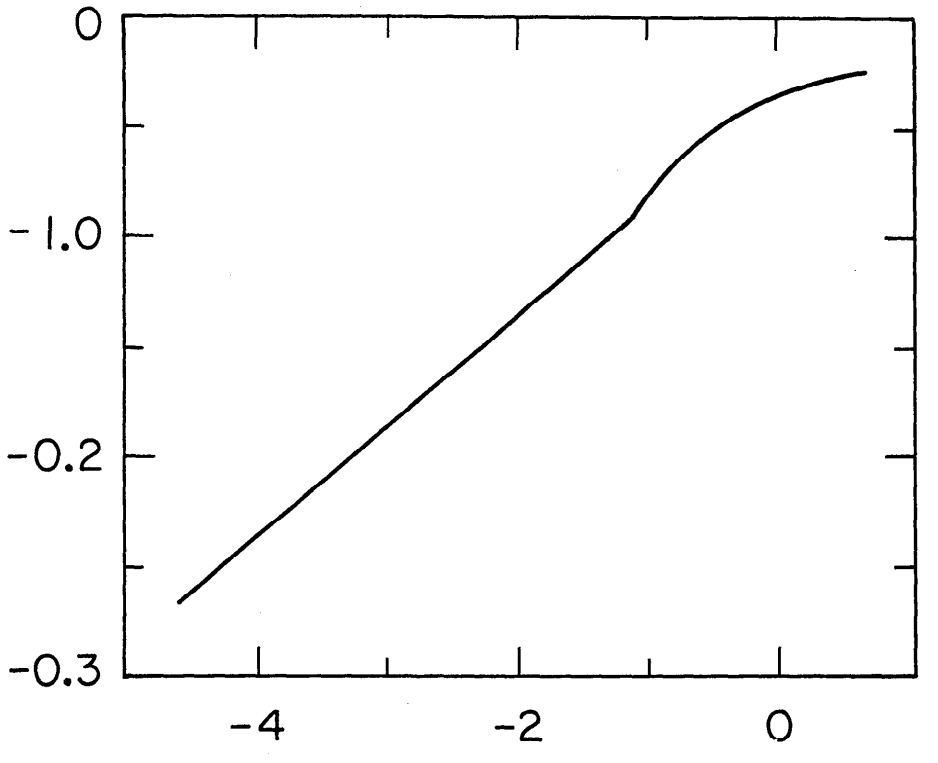

Fig. 26 (a)

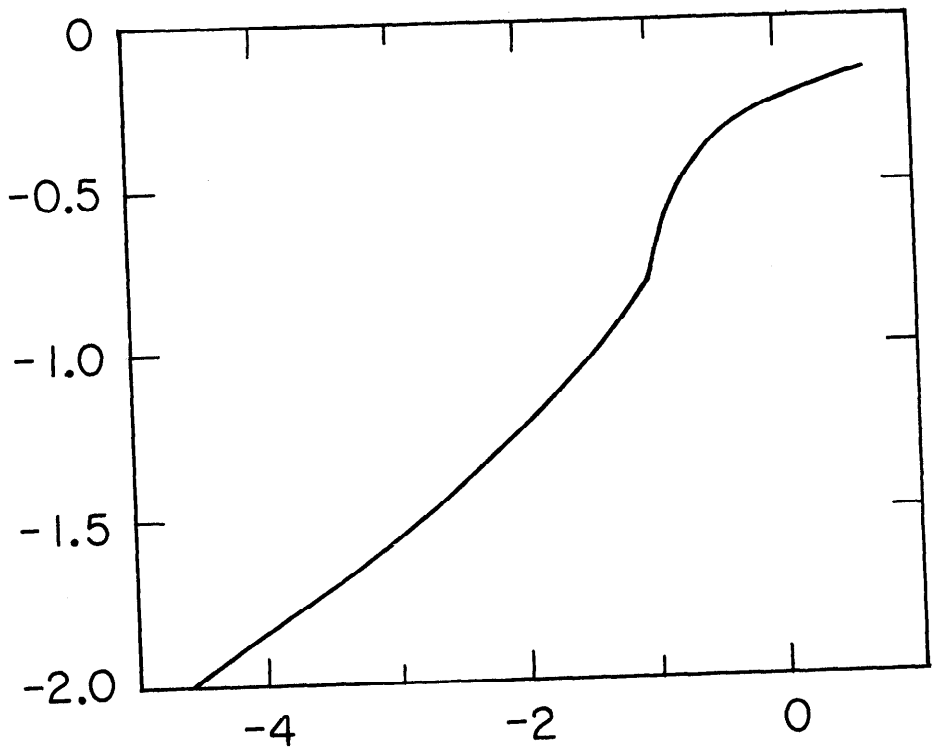

Fig. 26 (b)

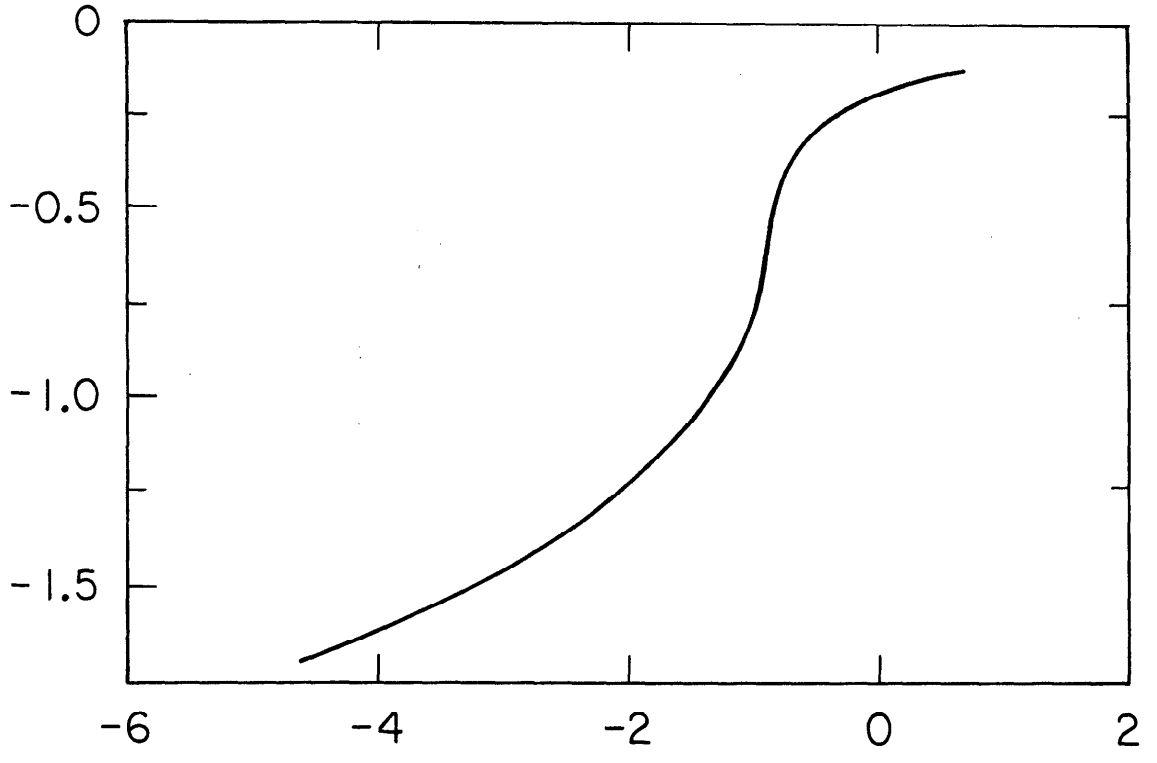

11-82

4411A32

Fig. 26 (c)

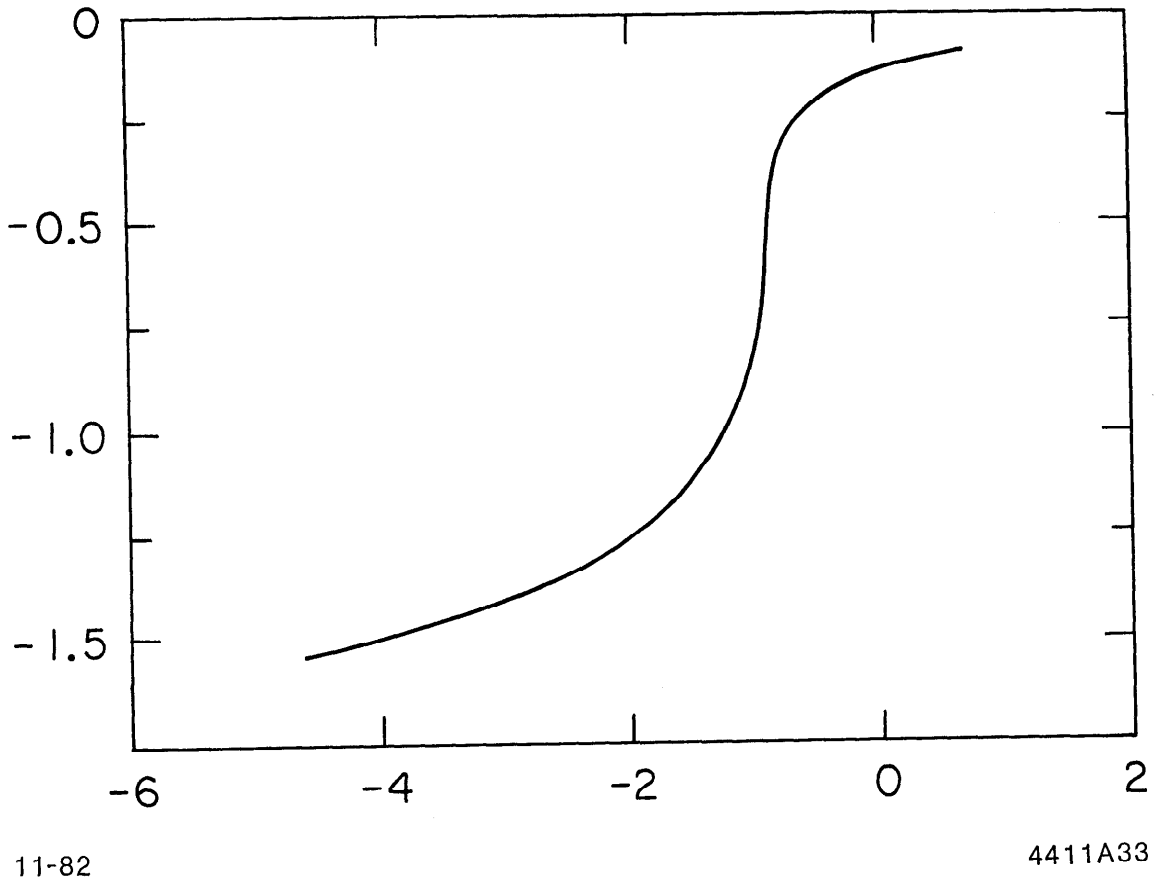

Fig. 26 (d)

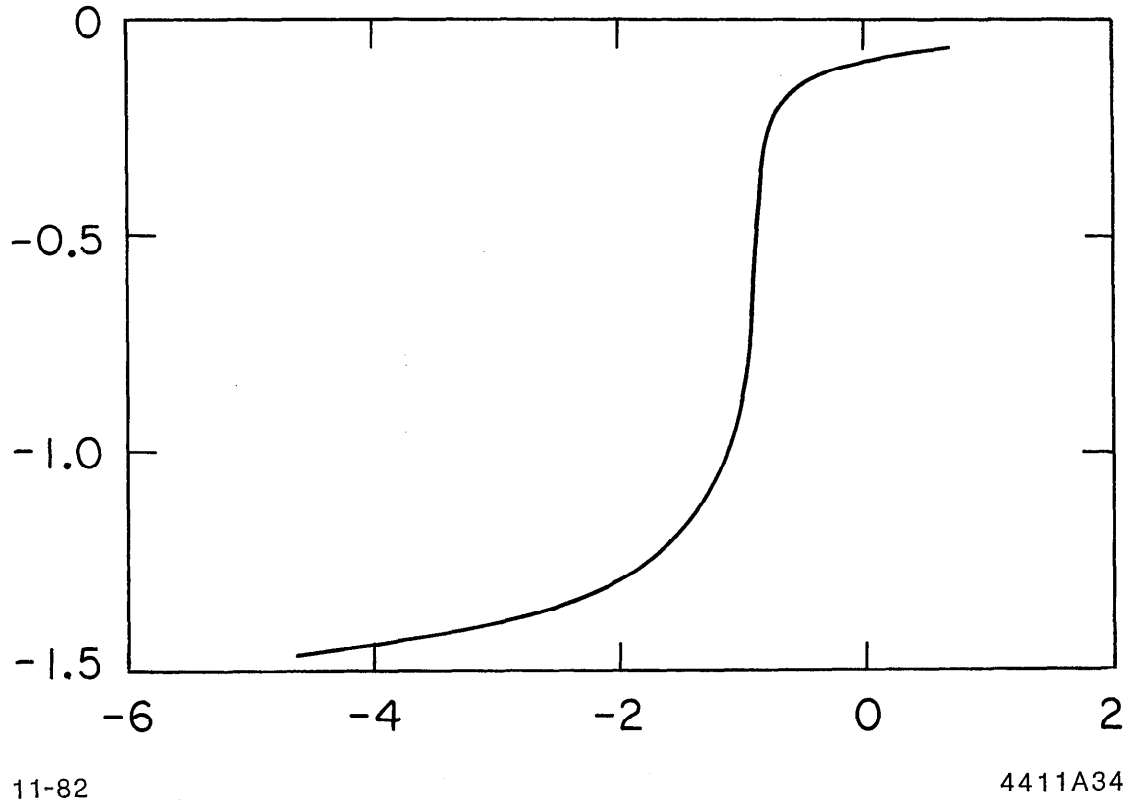

Fig. 26 (e)

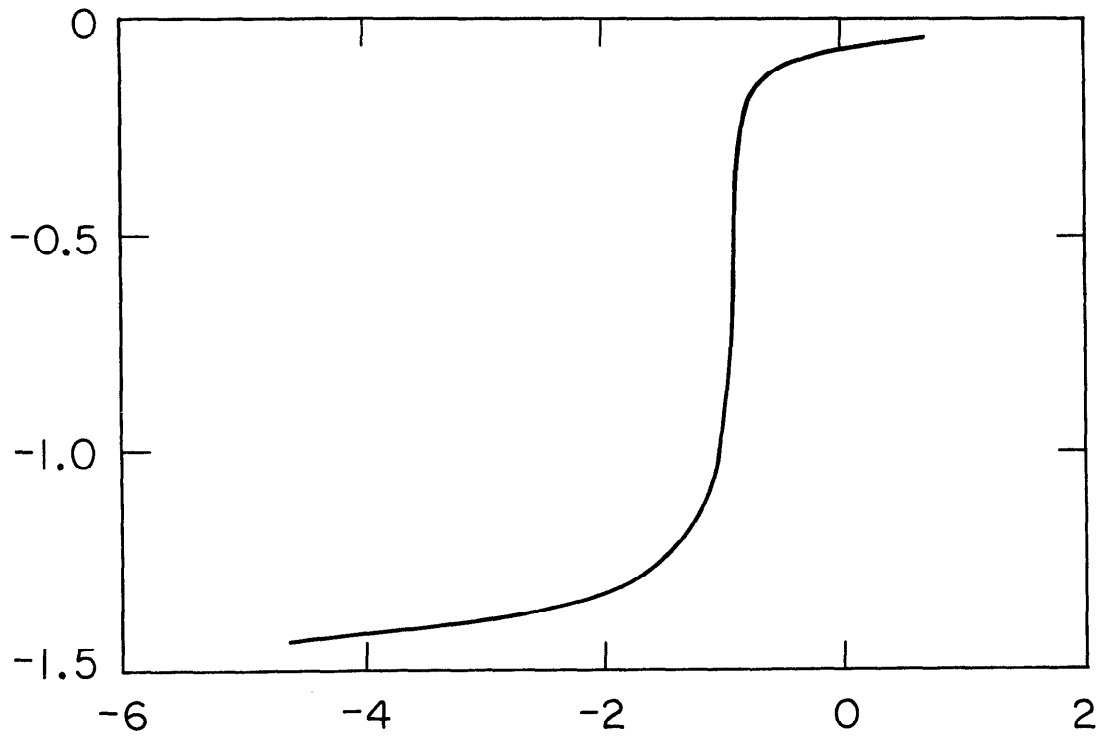

11-82

4411A35

Fig. 26 (f)

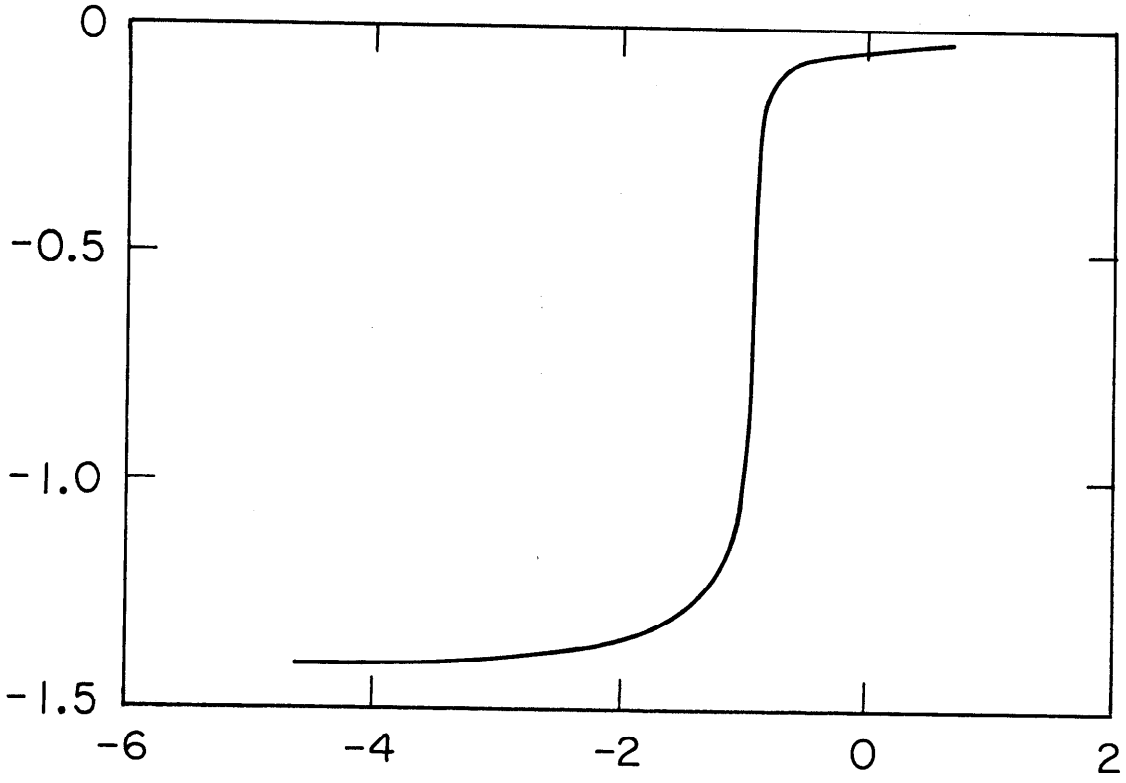

Fig. 26 (g)

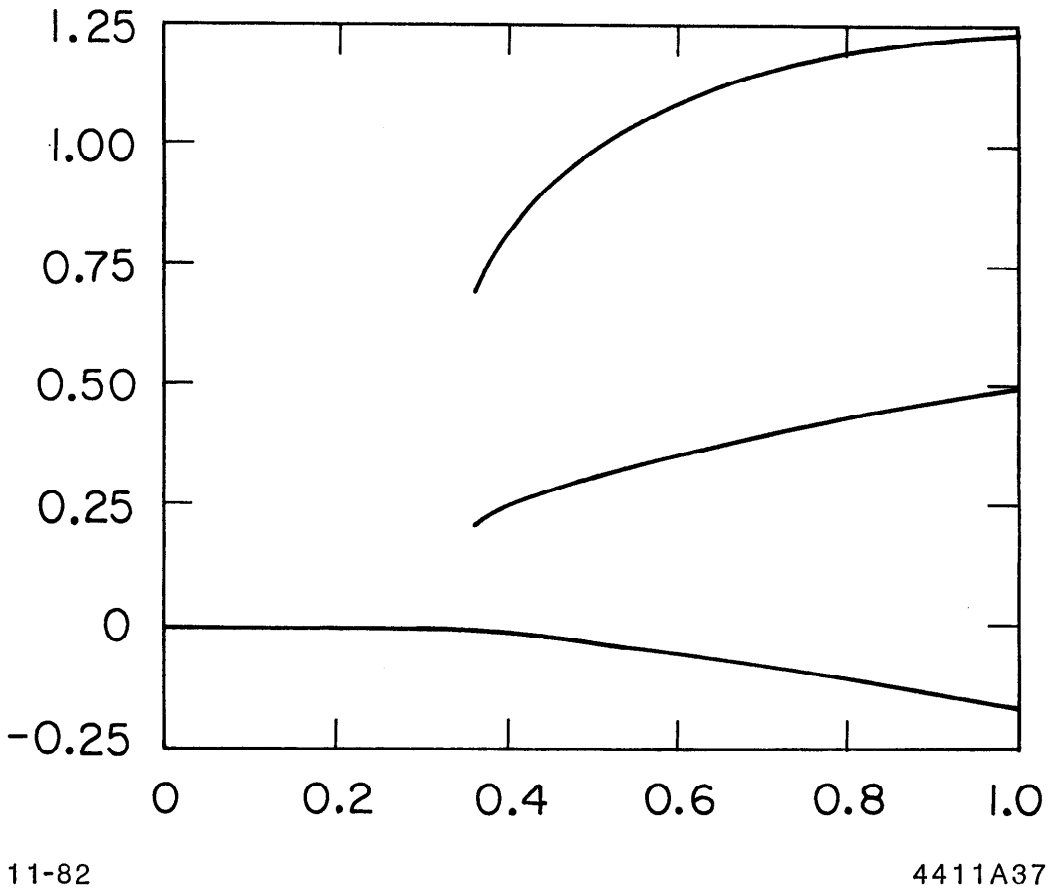

Fig. 27

PART IV

TRANSFER MATRIX METHODS FOR THE ISING CHAIN IN A TRANSVERSE MAGNETIC FIELD

1. Introduction

In Parts I and III of the thesis, we have seen the usefulness of periodic Gaussian trial wave-functions for studying lattice models posessing a compact U(1) symmetry. Such models may be formulated as spin models with infinite spin towers. [See Part III, Sec. 2.2.] In that language, the trial wave-function became a (long-range) Gaussian in the discrete spin variables. [See Part III, Sec. 5.7.] The long-range Gaussian propagator characterizing the wave-function is varied to minimize the ground-state energy density, so the method is in fact a generalized Hartree-Fock variational calculation.

In this part of the thesis, we use such a trial ground-state for the soluble one-dimensional Ising chain in a transverse magnetic field. The resulting statistical-mechanics sums are evaluated via the transfer-matrix method, used in Part III Sec. 5 for the XY model.

The presentation is organized as follows. In Sec. 2, the model is defined, the Hartree-Fock trial state introduced and the quantum-mechanical problem converted to statistical-mechanics language. In Secs. 3, 3.1, the transfer-matrix formalism is presented for a nearest-neighbor propagator (a calculation by Pearson[1]), and perturbative results are derived in the two extreme limits of the coupling constant. In Sec. 3.2, the transfer matrix method is extended to propagators of arbitrary (finite) range. In 3.3, numerical results for ranges up to four lattice spacings are presented and discussed.

2. A Trial Ground State for the Model

2.1 The model

The model is an Ising chain in one space dimension in a transverse magnetic field. Its Hamiltonian is

$$H = \sum_j \left[\sigma_z(j) - \Delta\sigma_x(j)\ \sigma_x(j+1)\right] \quad , \tag{2.1.1}$$

where $\sigma_x(j)$, $\sigma_y(j)$, $\sigma_z(j)$ are the Pauli spin matrices acting on site j. Δ is the coupling constant, ranging from 0 to ∞. The first term is the interaction with an external magnetic field in the z direction, while the second term is the spin-spin interaction. In the $\Delta \to 0$ limit, the spins are aligned in the negative z direction. In the $\Delta \to \infty$ limit the system is a pure zero-temperature Ising model, with all the spins aligned in the same (plus or minus x) direction. Our convention for spin states is

$$\left.\begin{aligned}
\sigma_z|\uparrow\rangle &= |\uparrow\rangle \quad , \\
\sigma_z|\downarrow\rangle &= -|\downarrow\rangle \quad , \\
\sigma_x|+\rangle &= |+\rangle \quad , \\
\sigma_x|-\rangle &= -|-\rangle \quad , \\
|+\rangle &= \frac{1}{\sqrt{2}}\ (|\uparrow\rangle + |\downarrow\rangle) \quad , \\
|-\rangle &= \frac{1}{\sqrt{2}}\ (-|\uparrow\rangle + |\downarrow\rangle) \quad .
\end{aligned}\right\} \tag{2.1.2}$$

The Hamiltonian (2.1.1) is symmetric under the σ_x-reflection transformation, effected by the operator

$$P_z = \prod_j \sigma_z(j) \ , \quad \left[H, P_z \right] = 0 \ . \tag{2.1.3}$$

For $\Delta < 1$, there is a single ground state, whereas for $\Delta > 1$, the symmetry is spontaneously broken and there are two ground states related by P_z.

2.2 A discrete Hartree-Fock trial ground state

In a field theory, the variational Hartree-Fock approximation consists of

(1) Expressing the fields in terms of creation and annihilation operators, with an arbitrary single-particle spectrum $\omega(\vec{k})$ and arbitrary single-particle Schrödinger wave functions (this defines a Fock space);

(2) taking the trial vacuum to be the naive Fock space vacuum; and

(3) varying over the single particle wave function to minimize the vacuum energy density.

If the single-particle wave-functions are to be in the momentum basis, the wave-functions are just plane waves, exp{ikj}. Then only $\omega(k)$, or in other words the propagator, is left undetermined, to be found variationally.

In the position basis, the above procedure is equivalent to taking the vacuum wave functional to be

$$\psi_{HF}\{\phi\} = \exp\left\{ - \sum_{jj'} \phi_j \ \Delta_{jj'} \ \phi_{j'} \right\} \ , \tag{2.2.1}$$

where $\Delta_{jj'}$ is the position basis propagator from site j to site j', and ϕ_j is the field.

For a field theory where the field develops a vacuum expectation value, (2.2.1) is modified to

$$\psi'_{HF}\{\phi\} = \exp\left\{-\sum_{jj'}(\phi_j - c)\,\Delta(j-j')\,(\phi_{j'} - c)\right\}, \qquad (2.2.2)$$

where c is an additional variational parameter.

In order to apply these ideas to a spin model, we will take the trial ground state for the Ising model to be

$$|\psi_t(\theta)\rangle = \exp\left\{i\frac{\theta}{2}\sum_j \sigma_y(j)\right\} \sum_{\{m\}} \exp\left\{-\frac{1}{2}\sum_{jj'} m_j \Delta(j-j') m_{j'} + \frac{1}{2}\sum_j m_j \zeta_j\right\} |\{m\}\rangle$$

$$\equiv \exp\left\{i\frac{\theta}{2}\sum_j \sigma_y(j)\right\} \prod_{m_j=\pm 1} |\psi_t(0)\rangle \quad , \qquad (2.2.3)$$

where the σ_x-spin basis of states is

$$|\{m\}\rangle = \prod_j |m_j\rangle_j \quad , \qquad m_j = \pm 1 \quad , \qquad (2.2.4)$$

and from parity symmetry $\Delta(j) = \Delta(-j)$.

The main conceptual difference between (2.2.2) and (2.2.3) is the extra rotation operator in front; both θ and ζ are mean-field parameters, i.e., characterizing the mean-field wave-function at a single site. In that sense, they both correspond to c in the field theory.

In the case of pure mean-field,[2] $\Delta(j)$ vanishes. The parameters θ,ζ then over-specify the state and we may set one of them to zero. The results are a transition at $\Delta_c = .5$, and a critical power-law vanishing of

the magnetization at the transition:

$$\langle \sigma_x(j) \rangle \sim \left(\Delta - \frac{1}{2}\right)^{1/2}, \quad \Delta \gtrsim \frac{1}{2} \quad , \tag{2.2.5}$$

whereas the correct critical power is 1/8.

For nonvanishing Δ of range greater than zero, both θ and ζ are needed.

2.3 Statistical mechanics formulation of the model

From (2.2.3), the norm of the state $|\psi_t\rangle$ is the partition sum

$$\begin{aligned} Z &\equiv \langle \psi_t(0) | \psi_t(0) \rangle \\ &= \sum_{\{m\}} \exp\left\{ \zeta \sum_j m_j - \sum_{j,n} m_j m_{j+n} \Delta(n) \right\} \\ &\equiv \sum_{\{m\}} Z_{\{m\}} \quad , \end{aligned} \tag{2.3.1}$$

where n ranges over all nonvanishing integers. (This is because $\Delta(0)$ multiplies $m_j^2 \equiv 1$ and therefore drops out.)

Expectation values of operators in $|\psi_t\rangle$ are expressible as averages weighted by the partition sum. We will need the expectations of the following five operators.

Single-site operators

The single-site matrix elements of σ_z are [(2.1.2)]

$$\langle m' | \sigma_z | m \rangle = - \delta_{m+m',0} \quad , \tag{2.3.2}$$

so from (2.2.3),

$$A \equiv \langle \psi_t(0) | \sigma_z(j) | \psi_t(0) \rangle$$
$$= - \sum_{\{m\}} \exp \left\{ \zeta \sum_{r \neq j} m_r - \sum_{\substack{r \neq j \\ r+n \neq j}} m_r m_{r+n} \Delta(n) \right\} \qquad (2.3.3)$$
$$= \sum_{\{m\}} Z_{\{m\}} \exp \left\{ -\zeta m_j + 2 \sum_n m_j m_{j+n} \Delta(n) \right\} .$$

Likewise for σ_x, which is diagonal in the $|m\rangle$ basis,

$$B \equiv \langle \psi_t(0) | \sigma_x(j) | \psi_t(0) \rangle = \sum_{\{m\}} Z_{\{m\}} m_j . \qquad (2.3.4)$$

By folding back the rotation matrices in (2.2.3) on the operators, we find for the expectations of the single site operators in the θ-rotated trial states

$$\langle \psi_t(\theta) | \sigma_z(j) | \psi_t(\theta) \rangle = A\cos\theta + B\sin\theta ,$$
$$\langle \psi_t(\theta) | \sigma_x(j) | \psi_t(\theta) \rangle = - A\sin\theta + B\cos\theta . \qquad (2.3.5)$$

Two-site operators

The two-site operator appearing in the Hamiltonian is $\langle \sigma_x(j)\sigma_x(j+1) \rangle$ and through θ rotation this will mix with $\langle \sigma_x(j)\sigma_z(j+1) \rangle$, $\langle \sigma_z(j)\sigma_x(j+1) \rangle$ and $\langle \sigma_z(j)\sigma_z(j+1) \rangle$. The first two are the same because of parity and translation symmetries, so we have three two-site expectations values to compute.

From (2.2.3) and (2.3.2),

$$E \equiv \langle \psi_t(0) | \sigma_z(j)\sigma_z(j+1) | \psi_t(0) \rangle$$

$$= \sum_{\{m\}} Z_{\{m\}} \exp\left\{ -\zeta(m_j - m_{j+1}) + 2\sum_n m_j m_{j+n} \Delta(n) + 2\sum_n m_{j+1} m_{j+1+n} \Delta(n) \right\},$$

$$D \equiv \langle \psi_t(0) | \sigma_z(j)\sigma_x(j+1) | \psi_t(0) \rangle \tag{2.3.6}$$

$$= -\sum_{\{m\}} Z_{\{m\}} m_{j+1} \exp\left\{ -\zeta m_j + 2\sum_n m_j m_{j+n} \Delta(n) \right\} ,$$

$$C \equiv \langle \psi_t(0) | \sigma_x(j)\sigma_x(j+1) | \psi_t(0) \rangle = \sum_{\{m\}} Z_{\{m\}} m_j m_{j+1} .$$

By (2.1.1), (2.3.3) - (2.3.6), the trial energy density is

$$\rho_{g.s.} = \frac{1}{\text{volume}} \langle \psi_t(\theta) | H | \psi_t(\theta) \rangle \tag{2.3.7}$$

$$= A\cos\theta + B\sin\theta - \Delta\left[C\cos^2\theta - D\sin(2\theta) + E\sin^2\theta \right] .$$

3. Transfer matrix method for range 1 and higher

The case where $\Delta(j)$ is of range one was done by Pearson. In this case, the partition sum is reduced to [(2.3.1)]

$$Z = \sum_{\{m\}} Z_{\{m\}} = \sum_{\{m\}} \exp\left\{ \zeta \sum_n m_j - 2\Delta_1 \sum_j m_j m_{j+1} \right\} , \tag{3.1}$$

where $\Delta_1 = \Delta(1)$. The transfer matrix method consists in this case of decomposing $Z_{\{m\}}$ as follows:

$$Z_{\{m\}} = \prod_j P(m_j, m_{j+1}) , \tag{3.2}$$

and defining P as a 2×2 matrix. if we demand that P be symmetric, we find

$$\overleftrightarrow{P} = \begin{pmatrix} \exp\left\{-\zeta - 2\Delta_1\right\} & \exp\left\{2\Delta_1\right\} \\ \exp\left\{2\Delta_1\right\} & \exp\left\{\zeta - 2\Delta_1\right\} \end{pmatrix} . \tag{3.3}$$

$\overleftrightarrow{P}$ is called the transfer matrix. We adopt the convention whereby the first row (column) corresponds to m = -1(m' = -1).

The partition sum is dominated by the leading eigenvalue of P,

$$p_1 = \sqrt{\exp\left\{-4\Delta_1\right\} \mathrm{sh}^2\zeta + \exp\left\{4\Delta_1\right\}} \quad , \quad , \tag{3.4}$$

with the corresponding normalized eigenvector

$$\vec{V}_1 = \begin{pmatrix} \frac{1}{t} \\ \frac{\sqrt{t^2 - 1}}{t} \end{pmatrix} . \tag{3.4}'$$

[See (A.1) in the Appendix for t.]

At this point, we note that when the symmetry operation P_z [see (2.1.3)] is applied to $|\psi_t(\theta)\rangle$, it flips the signs of θ and ζ and leaves $\Delta(n)$ invariant. Therefore, we may adopt the convention $\zeta \geq 0$ without loss of generality, since it suffices to study only one of the degenerate ground states. As we shall find later, this convention corresponds to positive magnetization: with the convention $\zeta \geq 0$,

$$\langle \sigma_x \rangle \geq 0 \quad . \tag{3.5}$$

The operator expectation values we need, (2.3.3)-(2.3.6), can be expressed as

$$\vec{v}_1 \cdot \overleftrightarrow{M} \cdot \vec{v}_1 \quad , \tag{3.6}$$

where $\vec{v}_1$ is the dominant eigenvector of P, and $\overleftrightarrow{M}$ are various matrices. The resulting expressions for A through E are given in (A.2).

3.1 Perturbative analysis

To find the best trial wave function $|\psi_t(0)\rangle$, the three parameters θ, ζ, Δ must be varied to minimize the energy density $\rho_{g.s.}$ [(2.3.7)]. For finite couplings Δ this must be carried out numerically, but for the two extremes, $\Delta << 1$ and $\Delta >> 1$, the variational analysis may be carried out perturbatively. Since the derivation of these results involves mainly tedious Taylor expansions, we shall omit most of the calculation and merely quote the results.

$\Delta << 1$ region. Since in the $\Delta < \Delta_c$ regime there is only one ground state, it is possible to prove that

$$\theta = \zeta = 0 \quad , \quad \Delta = \Delta_c \quad . \tag{3.1.1}$$

These parameters vanish because they violate the P_z symmetry [(2.1.3)]. Therefore, in the $\Delta << 1$ region we need only solve for Δ_1. The results are

$$\begin{aligned} \Delta_1 &= -\frac{\Delta}{4} + O(\Delta^3) \quad , \\ \rho_{g.s.} &= -1 - \frac{1}{4}\Delta^2 + O(\Delta^4) \quad , \\ \langle \sigma_x \rangle &\equiv 0 \quad . \end{aligned} \tag{3.1.2}$$

Thus the wave function in {m} basis is very flat, which corresponds to a probability distribution in the z-spin basis that is peaked around $\sigma_z \equiv -1$ [see (2.1.2)].

$\Delta >> 1$ region. Here we have found by minimizing $\rho_{g.s.}$ as a function of Δ_1, θ and ζ,

$$\begin{aligned} \Delta_1 &= -\frac{1}{4}\ \ell n\ 2 + O\left(\Delta^{-2}\right) \quad , \\ \zeta &= \ell n(2\Delta) + O\left(\Delta^{-2}\right) \quad , \\ \theta &= O\left(\Delta^{-3}\right) \quad , \\ \rho_{g.s.} &= -\Delta - \frac{1}{4\Delta} - \frac{1}{64\Delta^3} + O\left(\Delta^{-5}\right) \quad , \\ \langle \sigma_x \rangle &= 1 - \frac{1}{8\Delta^2} \quad . \end{aligned} \tag{3.1.3}$$

ζ is large, so the probability distribution is peaked around $\sigma_x = +1$; that is why the magnetization is near one. The first three terms in $\rho_{g.s.}$ agree with the exact perturbative result, as noted by Pearson.

3.2 Longer-range propagators

What we have done in this part of the thesis is to carry out the variational computation for propagators of ranges 2, 3 and 4 lattice spacings. This was done using the transfer matrix method, in the following way. For range r we divide the sites into blocks of r sites each. The spin configuration of the lattice is then classified as $\{M_J\}$ where M_J is an integer describing the spin configuration in the Jth block:

$$M_J = \sum_{i=0}^{r-1} 2^i\ m_{Jr+i+1} \equiv M\left(m_{Jr+1}, \cdots m_{(J+1)r}\right) \quad , \tag{3.2.1}$$

$$0 \le M_J \le 2^r - 1$$

Since by definition $\Delta(j) = 0$ for all $j > r$, every block interacts only with its nearest neighbors in the partition sum (2.3.1). Thus we can again decompose

$$Z_{\{m\}} = \prod P\left(M_J, M_{J+1}\right) \quad , \tag{3.2.2}$$

where now the product is over blocks, and the transfer matrix $\overleftrightarrow{P}$ is of rank 2^r.

As in the $r = 1$ case, operator expectation values are computed by diagonalizing $\overleftrightarrow{P}$ and finding its leading eigenvalue p_1 and eigenvector $\vec{v}_1$. The details of these derivations are given in the Appendix.

3.3 Results

In Figs. 1,2 we see θ and ζ, respectively, plotted versus Δ for range $r = 2$ (for higher ranges the curves look almost exactly identical). In fig. 3, the solid curves show Δ_1 for ranges 1, 2 and 3, and Δ_2, Δ_3 for range $r = 3$. To get these curves, Δ_1, Δ_2 and Δ_3 were varied independently; the dotted curves show the corresponding propagator components for $r = 4$, using an ansatz for the components:

$$\Delta(n) = \begin{cases} \Delta_1 \ , & n = 1 \quad ; \\ \dfrac{4\Delta_2}{n^2} \ , & n > 1 \quad . \end{cases} \tag{3.3.1}$$

These curves are for the vicinity of the true (and trial) critical point. The approximate agreement between the two sets of curves is probably a reflection of the fact that the exact theory becomes massless at $\Delta = \Delta_c = 1$.

Finally, Fig. 4 shows the magnetization curves for ranges r = 1, 2, 3 and 4. The critical points in these four calculations are Δ_c = .813 (the result of ref. 1); = .889 (for range 2); = .916 (range 3); and = .925 [for range four lattice spacings, with the hypothesis (3.3.1)]. For comparison, the mean-field result is $\Delta_c = 1/2$. Our conclusion is that the Δ_c value begins to converge, and in order to get closer to the exact result this method should be combined with a long-range (e.g., renormalization-group) approach.

APPENDIX A

The range = 1 (Pearson) calculation

The leading eigenvector is:

$$v_1 = \begin{pmatrix} \frac{1}{t} \\ \\ \frac{\sqrt{t^2 - 1}}{t} \end{pmatrix} , \tag{A.1}$$

where

$$t = \left[1 + \exp\left(-8\Delta\right) \left\{ \mathrm{sh}\zeta + \left[\mathrm{sh}^2\zeta + \exp\left(8\Delta_1\right) \right]^{1/2} \right\}^2 \right] .$$

The expectation values A through E defined in (2.3.3) - (2.3.6), are

$$\begin{aligned}
A \equiv \left\langle \sigma_z(j) \right\rangle &= -\frac{2}{t^2 p_1^2} \left(e^{-\zeta/2} + e^{\zeta/2}\sqrt{t^2 - 1} \right)^2 , \\
B \equiv \left\langle \sigma_x(j) \right\rangle &= \frac{t^2 - 2}{t^2} , \\
C \equiv \left\langle \sigma_x(j)\sigma_x(j+1) \right\rangle &= 1 - 4 \left[\frac{\exp\left(2\Delta_1\right)\sqrt{t^2 - 1}}{t^2 p_1} \right] . \\
D \equiv \left\langle \sigma_z(j)\sigma_x(j+1) \right\rangle &= -\frac{2}{t^2 p_1^2} \left[e^{\zeta}\left(t^2 - 1\right) - e^{-\zeta} \right] , \\
E \equiv \left\langle \sigma_z(j)\sigma_z(j+1) \right\rangle &= -\frac{2\mathrm{ch}\left(2\Delta_1\right)}{p_1} \quad A \quad .
\end{aligned} \tag{A.2}$$

Range r > 1 calculations: the transfer matrix

We will rewrite the partition weight $Z_{\{m\}}$ in (2.3.1) as a product over block-block factors, according to (3.2.2). This is not a unique

decomposition, but unlike the r = 1 case, $\overleftrightarrow{P}$ cannot be chosen to be symmetric; $\overleftrightarrow{P}$ does, however possess a related symmetry:

$$P(M,M') = P\left(M'^{S},M^{S}\right) , \tag{A.3}$$

where M^{S} is defined through (3.2.1) but with the block parity-reflected:

$$\begin{aligned} M &= M\left(m_1,m_2, \ldots, m_r\right) , \\ M^{S} &= M\left(m_r, m_{r-1}, \ldots, m_1\right) . \end{aligned} \tag{A.3}'$$

We have enumerated the block as J = 0 for convenience. The symmetry (A.3) is a manifestation of the parity ($m_j \to m_{-j}$) symmetry of the model.

Let M, M' be the block-spins for two adjacent blocks:

$$\begin{aligned} M &= M\left(m_1, m_2, \ldots, m_r\right) , \\ M' &= M\left(m'_1, m'_2, \ldots, m'_r\right) . \end{aligned} \tag{A.4}$$

Then we choose the transfer matrix as follows,

$$P(M,M') = \exp\left\{\frac{\zeta}{2}\sum_{1\le j\le r}\left(m_j + m'_j\right) - \frac{1}{2}\sum_{\substack{1\le j_1\le r \\ 1\le j_2\le r \\ j_1\neq j_2}}\Delta\left(j_1 - j_2\right)\left(m_{j_1}m_{j_2} + m'_{j_1}m'_{j_2}\right)\right.$$

$$\left. - 2\sum_{\substack{1\le j_1\le r \\ 1\le j_2\le r}}\Delta\left(j_1 - j_2 - r\right)m_{j_1}m'_{j_2}\right\} .$$

Operator insertions

The formalism for computing operator expectation values via the transfer matrix is identical to that of Part III, Sec. 5. For an operator $\mathcal{O}$, one starts from the statistical-mechanics average formula for $\langle \mathcal{O} \rangle$. It is rewritten in block-block matrix form as

$$\langle \mathcal{O} \rangle = \frac{\mathrm{tr}\Big(\overbrace{\overleftrightarrow{P}\cdot\overleftrightarrow{P}\cdot\ \ldots\ \cdot\overleftrightarrow{P}}^{V/2}\cdot\overleftrightarrow{M}_0\cdot\overbrace{\overleftrightarrow{P}\cdot\ \ldots\ \cdot\overleftrightarrow{P}}^{(V/2-n)}\Big)}{\mathrm{tr}\Big(\overbrace{\overleftrightarrow{P}\cdot\overleftrightarrow{P}\cdot\ \ldots\ \cdot\overleftrightarrow{P}}^{V\ \text{factors}}\Big)} \quad , \tag{A.6}$$

where M_0 is a square matrix of rank 2^r and V is the volume of the lattice. n is related to the number of blocks affected by $\mathcal{O}$.

In the infinite-volume limit, $\overleftrightarrow{P}$ may be replaced by

$$\overleftrightarrow{P} \rightarrow p_1 \vec{v}_1 \vec{v}_1^{\,s} \quad , \tag{A.7}$$

where p_1 is the dominant eigenvalue of $\overleftrightarrow{P}$, $\vec{v}_1$ is its corresponding eigenvector, and $\vec{v}_1^{\,s}$ is the transpose of $\vec{v}_1$ a la (A.3)'. We choose $\vec{v}_1$ to be normalized as follows,

$$\vec{v}_1^{\,s}\cdot\vec{v}_1 = 1 \quad . \tag{A.8}$$

(A.6) - (A.8) yield for the expectation value:

$$\lim_{V\to\infty}\langle \mathcal{O} \rangle = \frac{\vec{v}_1^{\,s}\cdot\overleftrightarrow{M}_0\cdot\vec{v}_1}{(p_1)^2} \quad . \tag{A.9}$$

For the five expectation values (2.3.3) - (2.3.6), we get using this formalism:

$$A = \frac{\vec{v}_1^{\,s} \cdot \overleftrightarrow{A}_1^{z} \overleftrightarrow{A}_2^{z} \cdot \vec{v}_1}{p_1^2} \quad ,$$

$$B = \vec{v}_1^{\,s} \cdot \overleftrightarrow{A}^{x} \cdot \vec{v}_1 \quad ,$$

$$C = \vec{v}_1^{\,s} \cdot \overleftrightarrow{A}^{xx} \cdot \vec{v}_1 \quad , \tag{A.10}$$

$$D = \frac{\vec{v}_1^{\,s} \cdot \overleftrightarrow{A}_1^{zx} \overleftrightarrow{A}_2^{z} \cdot \vec{v}_1}{p_1^2} \quad ,$$

$$E = \frac{\vec{v}_1^{\,s} \cdot \overleftrightarrow{A}_1^{zz} \overleftrightarrow{A}_2^{zz} \cdot \vec{v}_1}{p_1^2} \quad ,$$

where the seven matrices introduced here are

$$A_1^z(M,M') = P(M,M') \exp\left\{-\frac{1}{2}\zeta m_1' + m_1 \sum_{1<j\le r} \Delta(j-1) m_j' + 2 \sum_{1\le j\le r} \Delta(j-1-r) m_1' m_j\right\} \quad ,$$

$$A_2^z(M,M') = P(M,M') \exp\left\{-\frac{1}{2}\zeta m_1 + m_1' \sum_{1<j\le r} \Delta(j-1) m_j + 2 \sum_{1\le j\le r} \Delta(j-1+r) m_1 m_j'\right\} \quad ,$$

$$A^x(M,M') = \delta_{MM',m_1} \quad , \qquad A^{xx}(M,M') = \delta_{MM',m_1 m_2} \quad , \qquad A_1^{zx}(M,M') = A_1^z(M,M') m_2' \quad ,$$

$$A_1^{zz}(M,M') = P(M,M') \exp\left\{-\frac{1}{2}\zeta\left(m_1' + m_2'\right) + m_1' \sum_{2<j\le r} \Delta(j-1) m_j' + m_2' \sum_{2<j\le r} \Delta(j-2) m_j'\right.$$

$$\left. + 2m_1' \sum_{1\le j\le r} \Delta(j-1-r) m_j + 2m_2' \sum_{1\le j\le r} \Delta(j-2-r) m_j\right\} \quad ,$$

$$A_2^{zz}(M,M') = P(M,M') \exp\left\{-\frac{1}{2}\zeta(m_1+m_2) + m_1 \sum_{2<j\le r} \Delta(j-1)m_j + m_2 \sum_{2<j\le r} \Delta(j-2)m_j \right.$$

$$\left. + 2m_1 \sum_{1\le j\le r} \Delta(j-1+r)m_j' + 2m_2 \sum_{1\le j\le r} \Delta(j-2+r)m_j' \right\} . \qquad (A.11)$$

REFERENCES

1. R. B. Pearson, Phys. Rev. A18, 2655 (1978).

2. H. R. Quinn and M. Weinstein, Phys. Rev. D25, 1661 (1982).

FIGURE CAPTIONS

Fig. 1. θ versus the coupling Δ for $r = 2$. The transition is at .889.

Fig. 2. ζ versus the coupling Δ for $r = 2$.

Fig. 3. Propagator components versus Δ (see text, Sec. 3.3).

Fig. 4. Magnetization versus Δ for ranges 1, 2, 3 and 4.
The range increases towards the right.

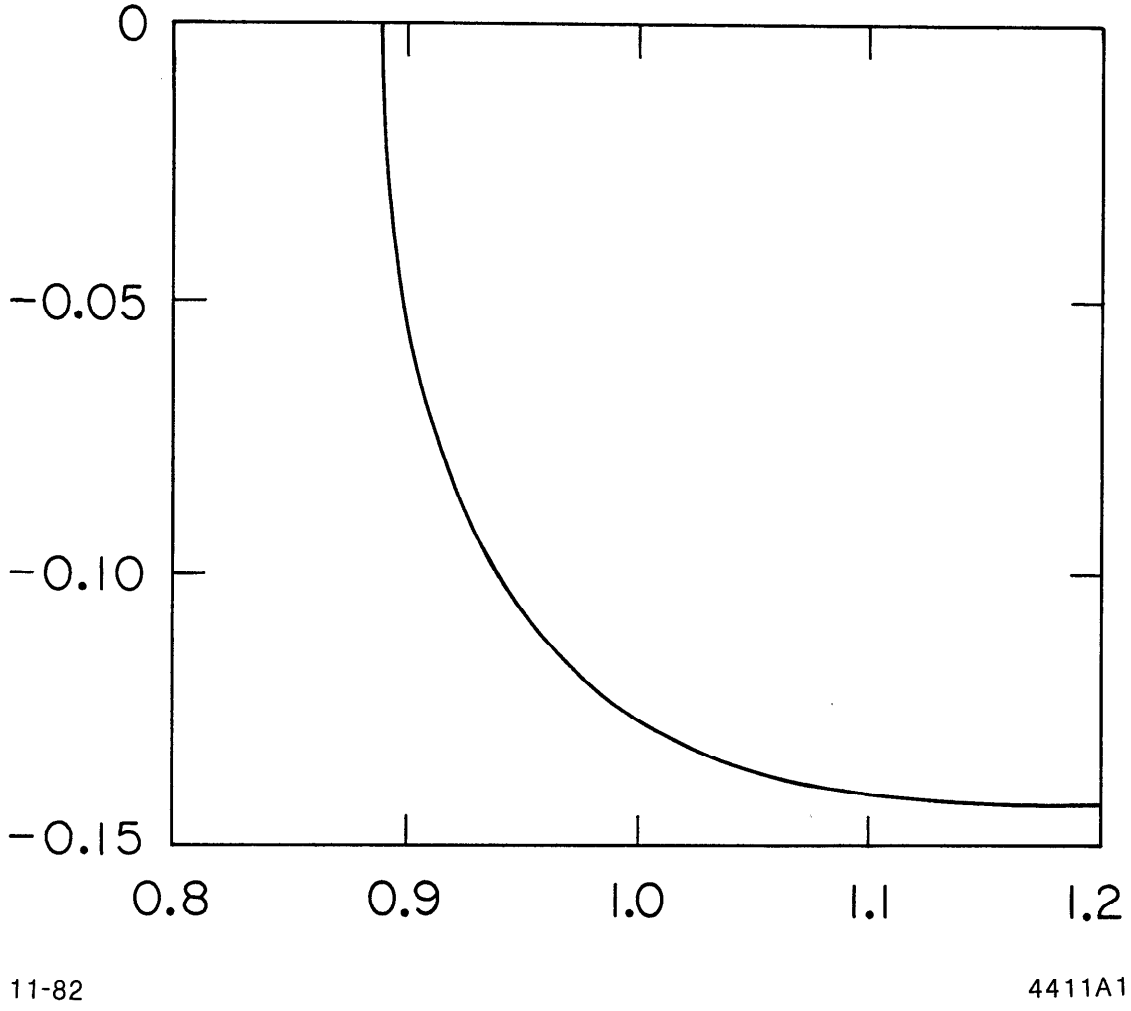

Fig. 1

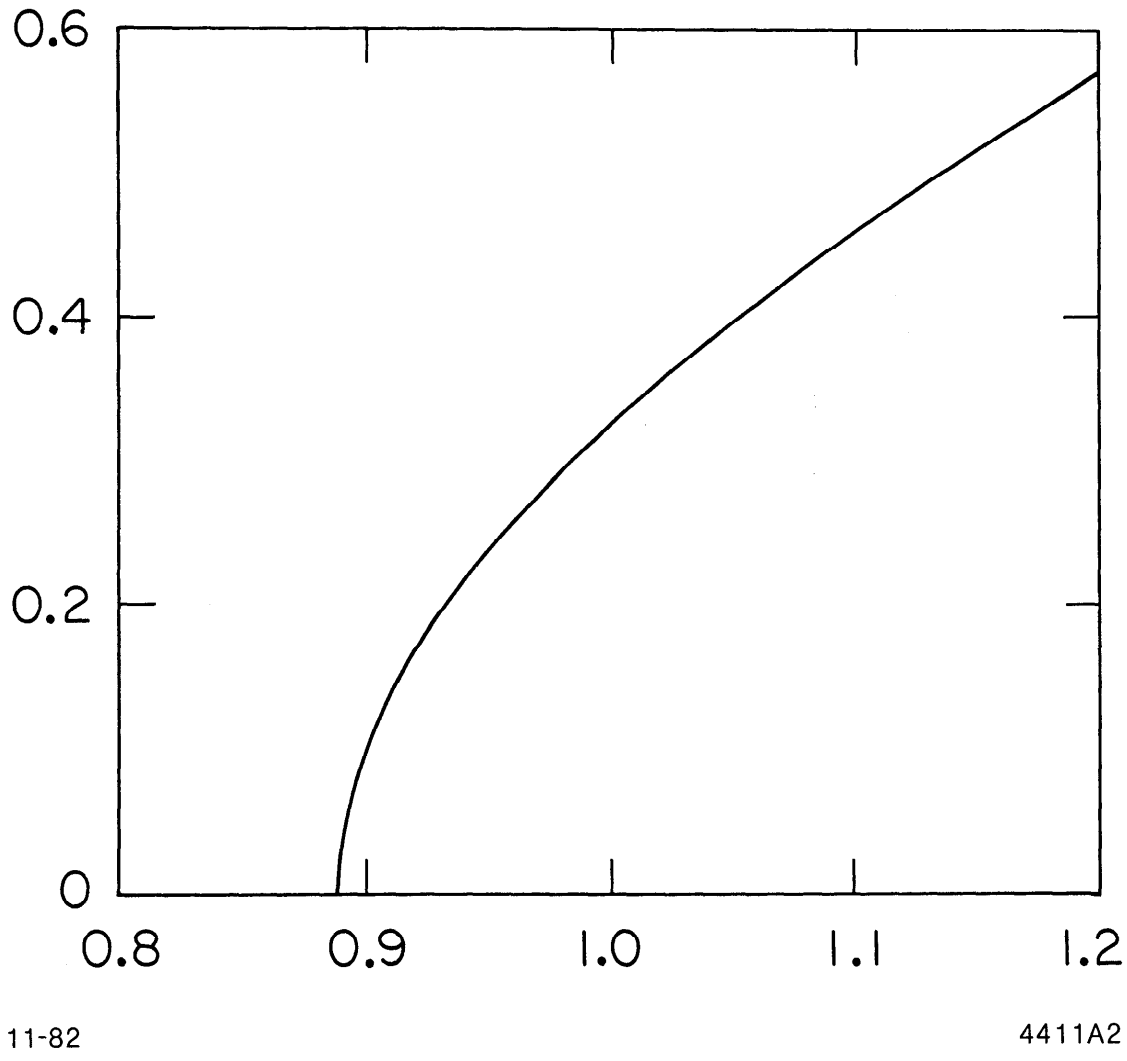

Fig. 2

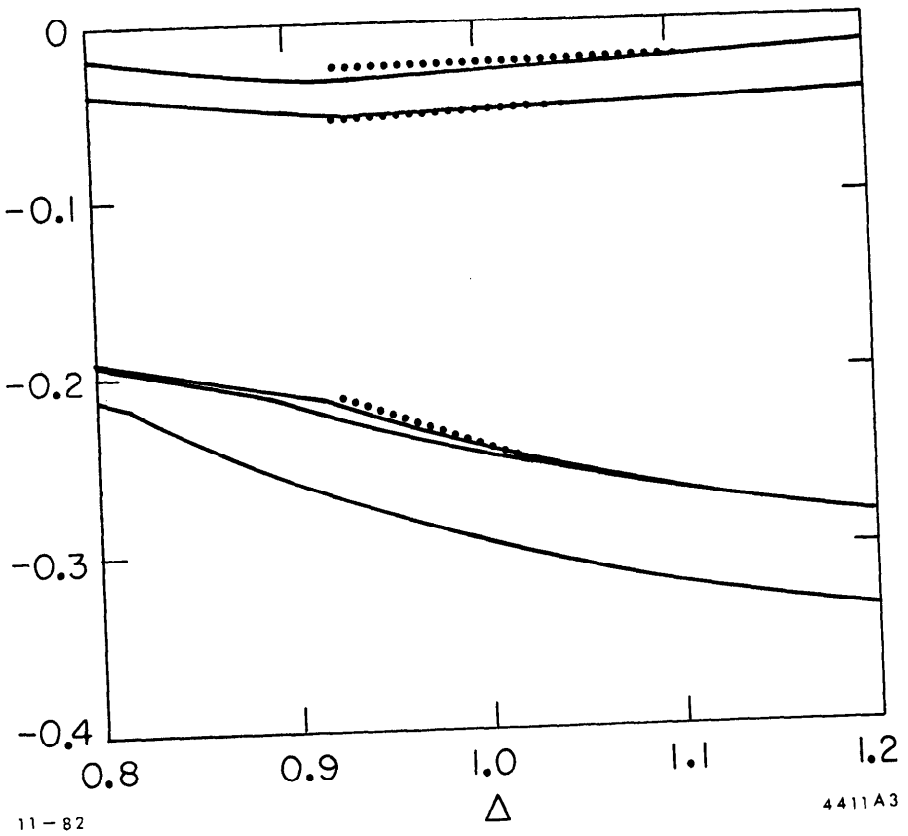

Fig. 3

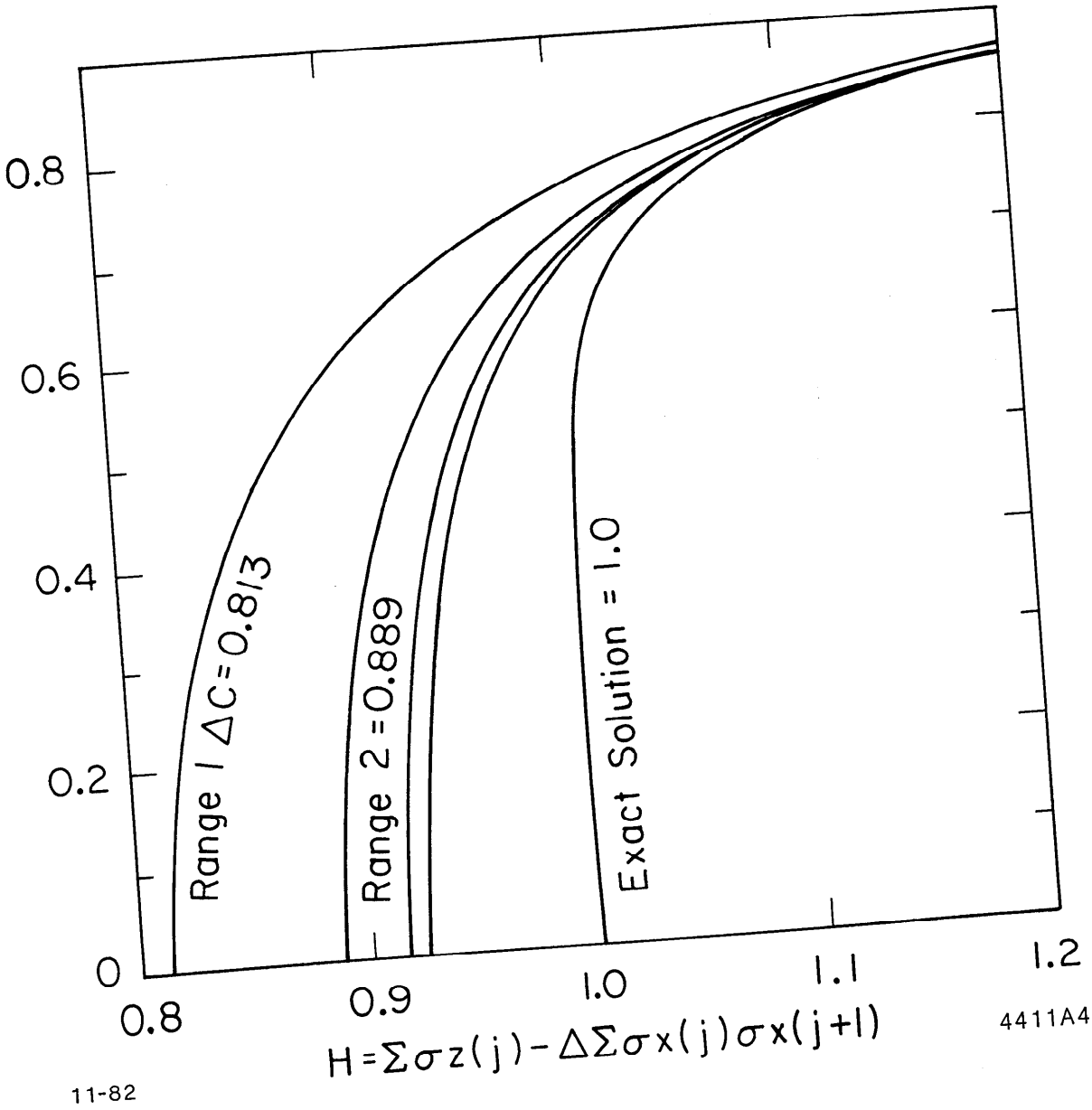
0.8
0.6
0.4
0.2
0
0.8
0.9
1.0
1.1
1.2
Range 1 ΔC=0.8/3
Range 2 =0.889
Exact Solution = 1.0
H=Σσz(j)-ΔΣσx(j)σx(j+1)
4411A4
11-82

Fig. 4